TN 295
.U4

THE LIBRARY OF CONGRESS

IC 8801

Bureau of Mines Information Circular/1979

LIBRARY OF THE U.S.
4
SEP - 5 1979
COPY
EXCHANGE & GIFT DIVISION

Mine Power Systems Research

(In Four Parts)

3. Circuit Protection

UNITED STATES DEPARTMENT OF THE INTERIOR

U.S. Bureau of Mines

Information Circular 8801

Mine Power Systems Research

(In Four Parts)

3. Circuit Protection

Compiled by Staff–Mining Research

UNITED STATES DEPARTMENT OF THE INTERIOR
Cecil D. Andrus, Secretary

BUREAU OF MINES
Lindsay D. Norman, Acting Director

5.C1 1979

This publication has been cataloged as follows:

United States. Bureau of Mines

Mine power systems research (In four parts) : 3. Circuit protection / by Staff–Mining Research. [Washington] : U.S. Dept. of the Interior, Bureau of Mines, 1979.

148 p. : ill. ; 27 cm. (Information circular • Bureau of Mines ; 8801)

Includes bibliographical references.

1. Electricity in mining. 2. Mining machinery • Electric equipment. 3. Short circuits. 4. Electric circuit breakers. 5. Electric power systems • Protection. I. Title. II. Title: Circuit protection. III. Series: United States. Bureau of Mines. Information circular • Bureau of Mines ; 8801.

TN23.U71 no. 8801 622.06173
U.S. Dept. of the Int. Library

CONTENTS

	Page
Abstract	1
Introduction	1
Portable calibrator for dc circuit breakers, by Derek A. Paice	3
Tests results of a mercury-filled current limiting device in dc switching and fault current limiting, by H. B. Hamilton, E. Strangas, and R. L. King	9
Preventive maintenance and reliability testing of molded-case circuit breakers, by E. U. Ibok, M. M. Hassan, and S. S. Venkata	29
Periodic inspection of mine electrical power systems to detect incipient faults, by Y. C. Chou, M. M. Hassan, and E. K. Stanek	49
Batteries and battery-charging safety, by L. A. Morley and J. A. Kiefer.	71
Fail-safe assessment of solid-state protective devices, by S. S. Venkata, W. T. Crawford, and S. V. R. Kolluri	91
An interactive mine power system simulation, by Frederick C. Trutt, Richard A. Rivell, and Lloyd A. Morley	108
Remote energizing-deenergizing of trolley wire, by D. S. Kimmel	131
Portable remote control of trolley circuit breakers, by Harry M. Dushac.	141

MINE POWER SYSTEMS RESEARCH

(In Four Parts)

3. Circuit Protection

Compiled by Staff–Mining Research

ABSTRACT

This Bureau of Mines report describes research on methods of assuring the continued safety of mine electrical power distribution circuits through reliability and quality assessment of the protective devices, innovative inspection techniques for these devices and the circuits themselves, novel applications of trolley line circuit breakers, and computer modeling of distribution systems to determine the proper ratings for cables, power sources, and circuit protective elements. Battery charger safety is included.

INTRODUCTION

In mines, as in other industrial electrical systems, the ultimate line of defense against inadvertent, hazardous overloads and short circuits is the complement of circuit breakers and other circuit protective devices. Certain differences in the philosophy of application of these devices exists, however, in mines compared to other industries. First, the use of a great quantity of portable trailing cable, constantly being moved about in circumstances leading to abrasion, crushing, and damaging tensions and flexure, means that the incidence of wiring faults is high in mines. The circuit breakers, therefore, are subject to much electrical and mechanical wear, requiring frequent replacement or refurbishment.

The components are not optimized for this type of application, and since the quantity of devices procured by mines is not so large that truly special designs are likely to be developed for them, it is necessary to devote special attention to making the best of a compromise situation. This entails close attention to technical details of the protection devices.

In the first paper in this report, techniques are described for the evaluation of circuit breaker reliability, with the ultimate aim of developing preventive maintenance schedules. The second paper considers the theoretical and laboratory assessment of the degree of success achieved in making a particular protective device fail-safe. The techniques are particularly applicable to solid-state devices, which are invading the mines in increasing number.

The paper on a portable calibrator describes a test unit which provides a low-voltage equivalent of fault current to the trip coil of a direct current (dc) circuit breaker while not imposing an actual overload on the trolley line. This facilitates the twice-yearly electrical inspection of overcurrent protection devices required by paragraph 75.1001-1(b) of Title 30 of the Code of Federal Regulations.

The paper discussing batteries and battery chargers describes a charger that incorporates protection against faulty ground connections, excessive battery surface leakage currents, and the effects of carelessly dropping the charger cable into water.

A computer model of a mine power system is discussed next. In planning a mine distribution system, or in contemplating additions to the system, relocating heavy electrical equipment such as continuous miners, or in attempting an analysis of a problem situation, the interactive power system simulation described can save many hours of engineering time and provide high accuracy assessments of the currents, voltages, and power factors at all points in the system. This leads to more accurate specification of substations, cabling, and circuit protection devices.

The periodic inspection techniques discussed in the final paper can provide information on failure trends, giving early warning of incipient hazards in time to make repairs or replacements on the next maintenance shift instead of waiting for the failure to occur. The techniques are considered useful to both mine maintenance personnel and Mine Safety and Health Administration (MSHA) inspectors.

The papers presented in this report are intended for possible immediate application, rather than as a description of Bureau of Mines research programs. Further information is available in the annual and final reports of the various projects or through the technical project officer. Throughout this report, reference to specific companies or trade names is made for information only and does not imply endorsement by the Bureau of Mines.

PORTABLE CALIBRATOR FOR DC CIRCUIT BREAKERS

by

Derek A. Paice[1]

ABSTRACT

A portable calibrator to check the trip setting of direct current (dc) circuit breakers within an accuracy of ±5 pct has been developed and tested. A prototype unit operates from a 300-vdc trolley wire to provide controlled current pulses of 120 msec duration and continuously adjustable from 1,400 to 3,600 amp. These current pulses enable a breaker dc trip current to be determined and subject the contacts to a full current rating. The equipment is simple to use and weighs 86 lb. Connections are made with protected, clamp-on leads, which are separately connected and weigh about 26 lb. An accurate calibration procedure takes less than 5 min to complete.

ACKNOWLEDGMENTS

The work reported was carried out under Bureau of Mines contract No. H0122058, under the guidance of E. Litchfield, the technical project officer. We are also indebted to G. Conroy of the Bureau of Mines for his help during the course of the program.

The Mine Safety and Health Administration (MSHA), Technical Support Group, at Beckley, W. Va., provided valuable suggestions and inputs to the project, and particularly we thank A. B. Massey, who carried out a large number of laboratory and field tests to evaluate the unit.

INTRODUCTION

Coal mine direct current (dc) power systems are generally fed from several dc power substations at suitably spaced intervals, typically 1 mile, throughout the coal mine. The substation output power is fed through circuit breakers that will trip and disconnect the dc power supply when excessive current is being drawn. The calibration of the dc circuit breaker trip setting must be such as to permit normal load currents but cause tripping for low resistance, high current faults. Periodic calibration of the circuit breaker overcurrent trip setting is necessary to insure continued protection and safety of the mine system. Also, onsite adjustment and recalibration become necessary as the mine workings advance and the power system requirements change.

Present techniques for onsite calibration of dc circuit breakers are cumbersome and because of the large amount of power required, potentially

[1]Fellow engineer--Solid State Equipment, Power Electronics Laboratory, Westinghouse Electronics R & D Div., Pittsburgh, Pa.

dangerous. For example, one method uses large intermittently rated power resistors of about 300-v, 3,600-amp rating that must be hauled to the circuit breaker location to perform the test. Another approach uses two locomotives to draw a large current from the breaker, thereby causing it to trip. Neither of these approaches provides a convenient and accurate test of the circuit breaker calibration.

Adequate protection of the electrical system and improved safety can only be achieved when circuit breaker trip settings are properly selected and then periodically checked to make certain that the desired tripping performance is being obtained. The test method and the associated equipment described make the task of checking breaker calibration safer and more convenient. It also provides much more accurate measurement of the trip setting than has previously been available.

CALIBRATOR REQUIREMENTS

Discussions were held with mine operators and electrical inspectors concerning the general requirements for onsite calibration of dc circuit breakers. No specific objections were raised concerning a pulsed approach such as was envisaged, and it was confirmed that existing procedures were not simple to implement.

Information on the probable range of current trip settings was obtained from ITE and also within Westinghouse. Current magnitudes of up to 3,600 amp with durations of up to 120 msec were determined to encompass the range of most mine dc breaker requirements. At the outset, it was recognized that resistance of the equipment output leads would constitute a significant factor in determining the calibrator power rating, and two leads each 10 ft long of 4/0 gage wire have been specified. These leads also contribute significantly (23 pct) to the total equipment weight.

CALIBRATOR DESIGN

There were many candidate approaches for providing the required current pulses, and numerous circuit arrangements were evaluated in sufficient detail to permit accurate trade-offs to be made. The finally selected approach is shown in schematic form in figure 1. A high-frequency thyristor inverter operating over the range of about 1,600 to 2,800 Hz provides a sinusoidal low-voltage, high-current output, which is then rectified and passed through the circuit breaker trip coil. The inverter is automatically stopped and started by means of solid-state devices that respond to low power logic signals. In operation the calibrator draws a momentary current of about 200 amp from the trolley wire 300-v source to supply the maximum output pulse level of 3,600 amp. The amplitude of the current pulse through the breaker is regulated by a closed-loop technique that adjusts the current pulse to match the demanded value independently of lead and contact resistance variations. A 0.33-mohm shunt in series with the test leads provides a current feedback signal and also a means for reading the output current. The amplitude of current pulse is recorded and held for 10 sec by a meter on the equipment front panel.

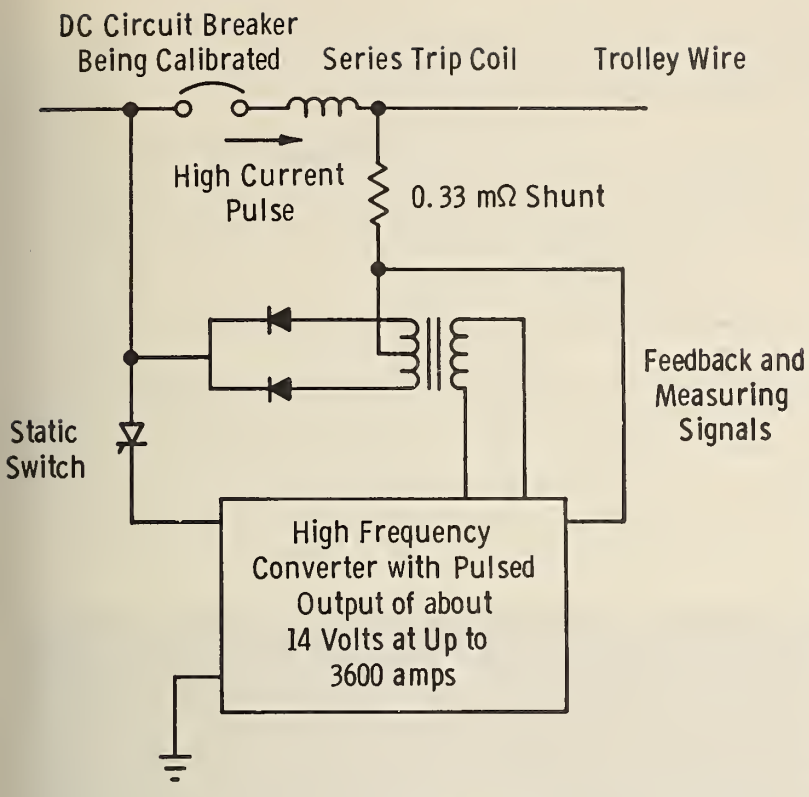

FIGURE 1. - Schematic arrangement of portable calibrator circuit.

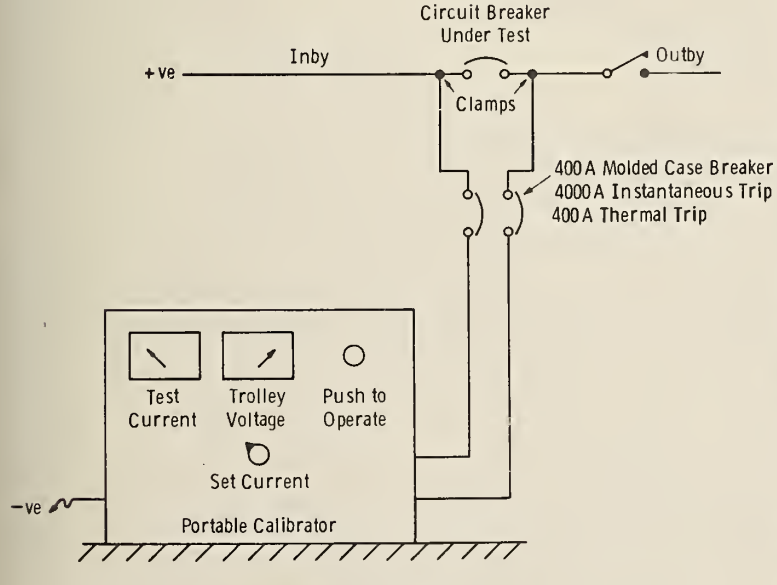

FIGURE 2. - Operating the portable calibrator.

When the circuit breaker under test is tripped by the calibrator current pulse, the breaker contacts are automatically subjected to the 300-v trolley wire voltage, thus the breaker contacts are subjected to both current and voltage stress.

USE OF THE PORTABLE CIRCUIT BREAKER CALIBRATOR

The equipment and connecting leads are taken to the site of the circuit breaker under test and for safety the aluminum case of the equipment should be grounded. The disconnect outby the circuit breaker is opened, and then the calibrator output leads are connected across the breaker under test as shown in figure 2.

The value of current pulse is set approximately by the calibrated dial on the calibrator front panel, and normally one would set-it just below the required trip current for the first test. The red pushbutton on the front panel can now be activated and a controlled current pulse will be passed through the circuit breaker under test.

The value of current pulse is recorded by the meter on the front panel; it may be slightly different from that set by the calibrated knob and, if necessary, it can be readjusted or modified for further tests. Assuming that the calibrator

pulse exceeds the circuit breaker trip level, the breaker will trip. This test, which verifies that the circuit breaker will trip at a certain level of current, is expected to be the normal manner of operation.

Alternatively, the actual current that the circuit breaker trips at can be verified by setting up as in figure 2, but with the current amplitude set at minimum. Successive adjustments can vary the amplitude to determine the actual value of trip current.

TESTS WITH THE PORTABLE CALIBRATOR

Figure 3 shows the calibrator undergoing laboratory tests in conjunction with a circuit breaker series trip coil and using a fused trolley nip connection. In these initial tests, the calibrator was set to provide only a 30-msec pulse. Although laboratory tests with a series trip coil were satisfactory, inmine tests showed that longer duration pulses were necessary to get satisfactory breaker operation. The reason for this is that although the

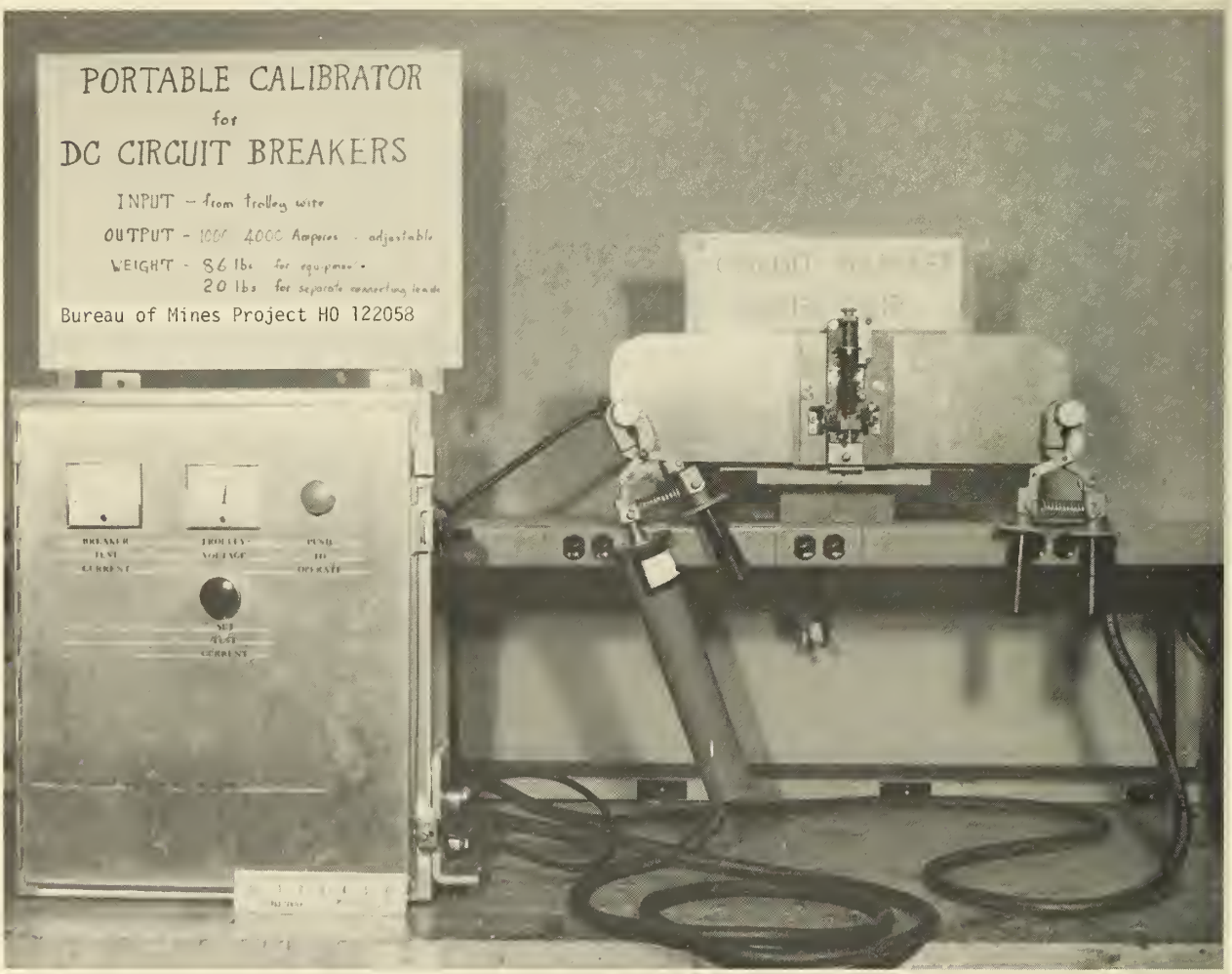
PORTABLE CALIBRATOR
for
DC CIRCUIT BREAKERS
INPUT - from trolley wire
OUTPUT - 1000 4000 Amperes - adjustable
WEIGHT - 86 lbs for equipment
20 lbs for separate connecting leads
Bureau of Mines Project HO 122058

FIGURE 3. - Portable calibrator on test.

Curve 713958-A

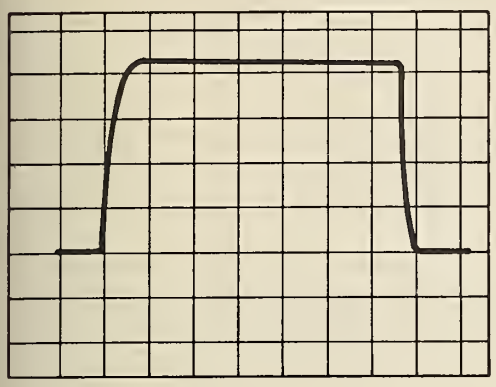

3350 Amperes

780 amperes/div.
20 milliseconds/div.

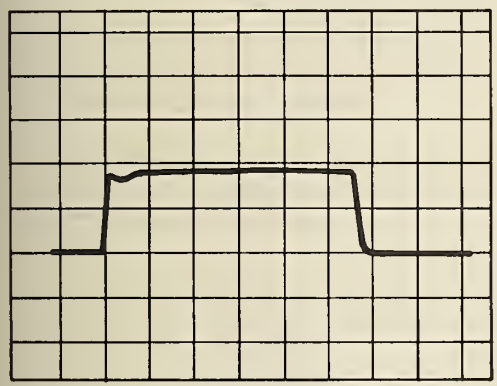

1400 Amperes

780 amperes/div.
20 milliseconds/div.

FIGURE 4. - Current pulses from circuit breaker calibrator (redrawn from oscilloscope trace).

series trip coil can be operated satisfactorily in 30 msec, its operation must be sustained for longer than this to enable other delays in the breaker to be overcome. By using a 120-msec pulse width for the test current, excellent agreement was found between the trip current determined by a continuous dc load and that determined by the calibrator.

Some examples of the current pulse waveforms obtained from the calibrator are shown in figure 4. The current is observed to be well regulated with only a small amount of high-frequency ripple current present.

Further laboratory tests were carried out with the help of A. B. Massey of MSHA at the Electrical Testing Project at Beckley, W. Va. The test breaker was an ITE type KSC with a 2,000-amp rating. A rectifier power source was available rated at 300 vdc and 500 kw. The tests were reported as follows:

Test 1--Check Effects of Pulse Width

Trip level--2,475 amp with 120-msec pulse

2,450 amp with 80-msec pulse

The results of test 1 are practically identical. Therefore, it is concluded that a pulse width of 120 msec is more than adequate to determine the breaker dc trip current level.

Test 2--Compare Calibrator With Steady dc

For this test a 12-sec rated load bank was available which gave 1,680 amp cold and 1,600 amp hot. After considerable adjustment and readjustment which took well over 1 hr to complete, it was determined that with steady dc the breaker was set to trip at 1,700 amp. Using the portable calibrator it took less than 3 min to establish that the trip setting was 1,750 amp.

These results show good agreement between the continuous dc and pulse calibrator readings. Also, the difficulty of using resistive load banks for calibration was highlighted.

CONCLUSIONS

The results show that a portable calibrator using high-power solid-state devices can provide a simple, accurate, and safe means for calibrating dc circuit breakers.

The prototype was designed for nominally 300-v positive trolley systems with currents up to 3,600 amp; however, the design technique could readily be applied to other system ratings. Complete equipment design information is available in the Bureau of Mines project report.

TESTS RESULTS OF A MERCURY-FILLED CURRENT LIMITING DEVICE IN DC SWITCHING AND FAULT CURRENT LIMITING

by

H. B. Hamilton,[1] E. Strangas,[2] and R. L. King[3]

ABSTRACT

Advantage is taken of the marked change in conductivity of a filament of mercury, when it changes from the liquid to vapor state, to form a current limiting device (CLD). The CLD can be used as a component of a heavy current switching system or of a fault current magnitude limiting system. Since change of state is accomplished in the millisecond time frame, the resulting high rate of change of current can produce rather severe surge voltages. This paper details theoretical studies, laboratory tests, and field tests oriented toward understanding and control of these surge voltages. Results of tests to limit fault current magnitude are presented and the parameters of necessary fault detection instrumentation are detailed. Additionally, instrumentation techniques used to determine mechanical stresses in the CLD and time-stress results are discussed.

This is a followup paper to "A New Concept in Arcless Switching of Heavy Current DC Systems" by H. B. Hamilton and T. Ramos presented at the 1975 Mid-west Power Symposium.

INTRODUCTION

It was desired to develop a direct current (dc) switching system, suitable for either complete interruption or for fault current magnitude limiting prior to fault interruption. Ideally, the switching should be accomplished in an enclosure (vapor tight) for safety reasons because the switching might be accomplished in a gaseous, explosive atmosphere.

The physical phenomena associated with dc switching are as follows (refer to fig. 1):

$$V = L \frac{di}{dt} + Ri + e_{arc} \tag{1}$$

where V = driving voltage,

L, R = circuit series inductance and resistance,

i = current,

r = switch shunt resistor,

and e_{arc} = arc voltage.

---

[1]Professor of electrical engineering, University of Pittsburgh, Pittsburgh, Pa.
[2]Graduate student researcher, University of Pittsburgh, Pittsburgh, Pa.
[3]Electrical engineer, Pittsburgh Mining and Safety Research Center, Bureau of Mines, Pittsburgh, Pa.

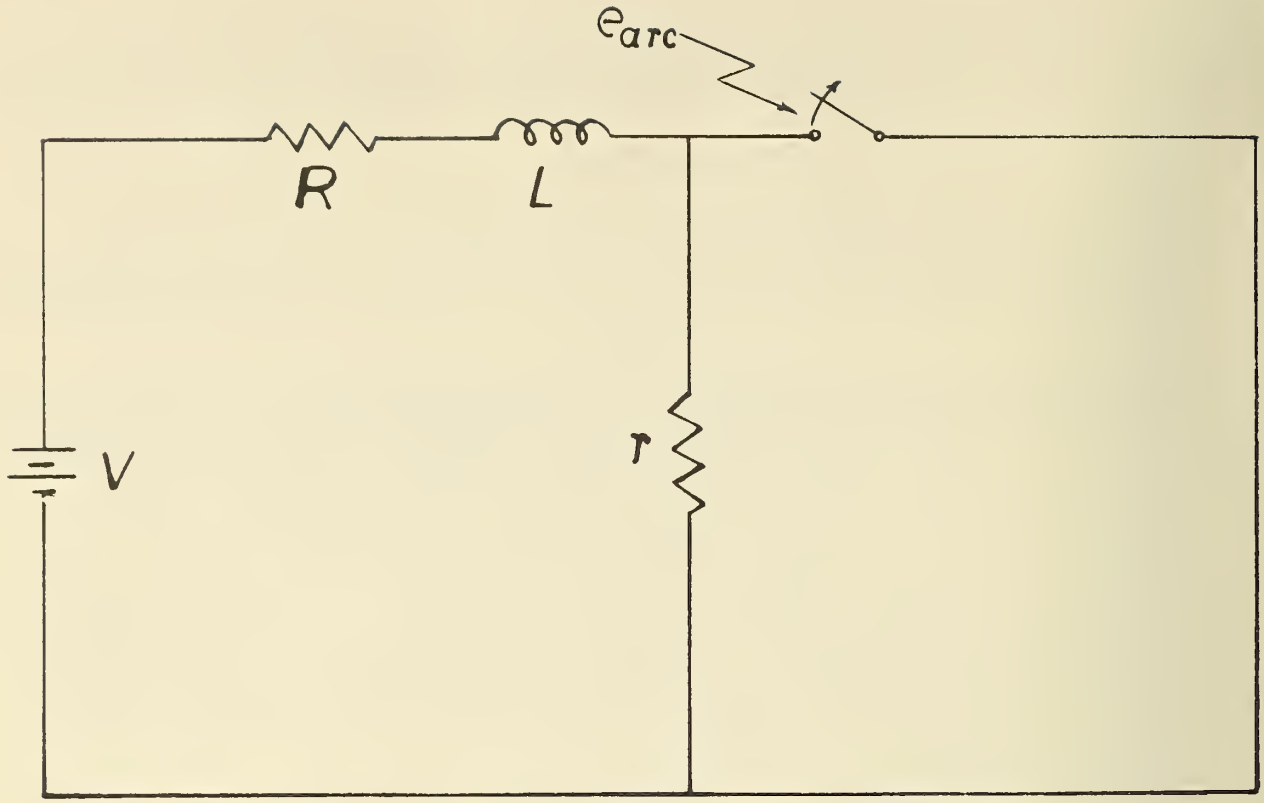

FIGURE 1. - Physical phenomena associated with dc switching.

Denoting the voltage associated with inductance, accounting for change in circuit current, as Δe, we have,

$$\Delta e = L \frac{di}{dt} = (V - Ri) - e_{arc} \qquad (2)$$

(refer to fig. 2). If Δe is negative, that is, $e_{arc} > (v - Ri)$, (the arc voltage curve above the load line) the current is driven toward extinction; if Δe is positive, that is $e_{arc} < (V - Ri)$, the current will increase until a $\Delta e = 0$ point is reached and arc equilibrium exists. For arc equilibrium circuit, the lower the value of r, the more the skew on the arc characteristic, the higher the value of Δe and the easier it is to commutate the current into r. However, the lower the value of r, the greater the value of I_s (short circuit current), and we are now faced with completing the circuit interruption of a series circuit with resistance, R + r. Higher values of r lose the advantages above but make final circuit interruption easier. Fixed value shunting resistance switching entails a compromise or trade off of the above factors.

In an effort to achieve a time dependent nonlinear resistance, r, which has low resistance, for easy commutation at t = 0, and a high resistance for easy total interruption, the authors have evaluated the use of change of state devices utilizing high conductivity liquid or solid metals which then change resistance by orders of magnitude when subjected to high current densities. Such a device is designated as a current limiting device, CLD.

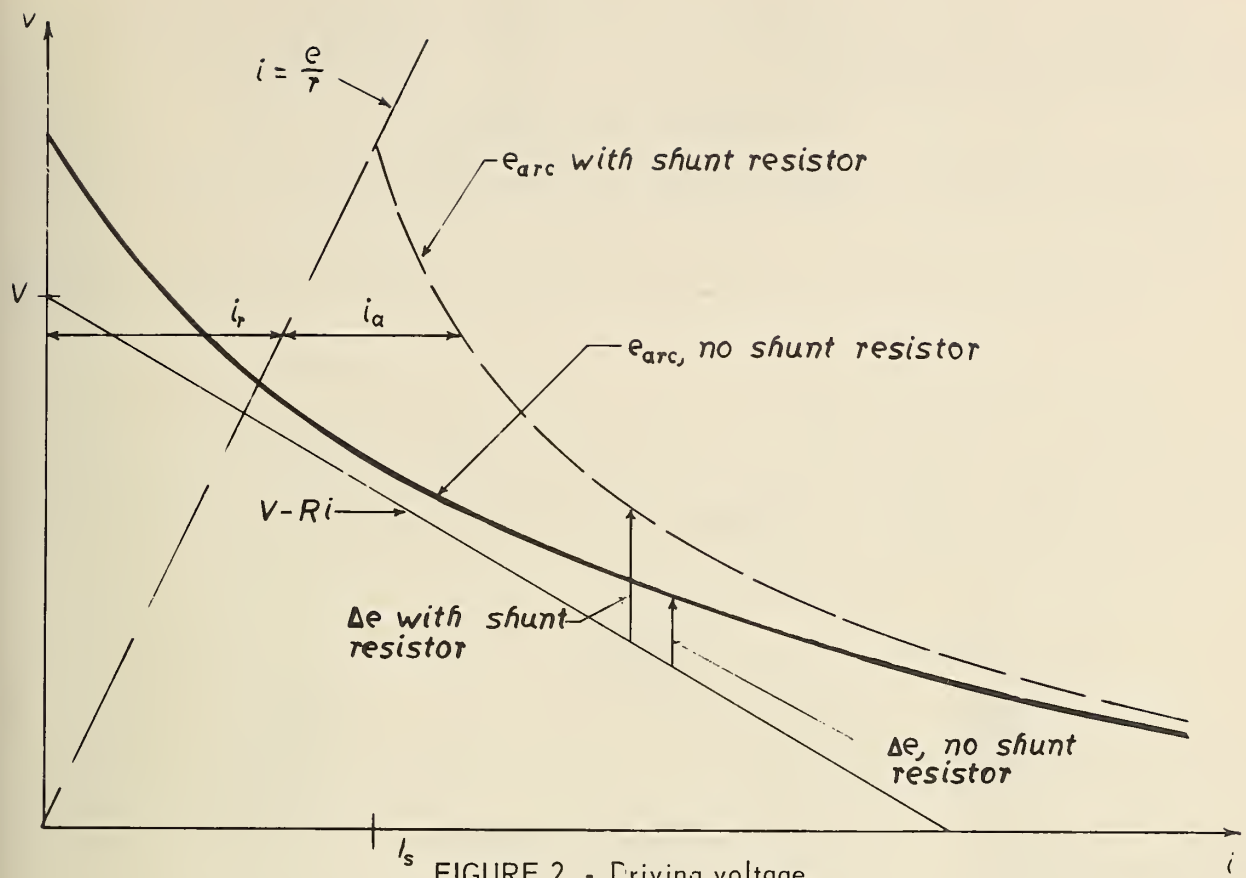

FIGURE 2. - Driving voltage.

CLD THEORY

The simplified version of a CLD is as shown in figure 3. The vapor chamber is one or more small bore filaments of a metal such as Na, K, Hg, etc. When the current is commutated from the switch (by opening) into the CLD, the high current density forms a vapor bubble which expands with explosive force leaving the bore filled with metallic vapor under an equilibrium pressure established by the bellows. The vaporized metal has a much greater resistivity than the solid or liquid form and this accomplishes the desired change of resistance with time, which permits easy, quick circuit interruption.

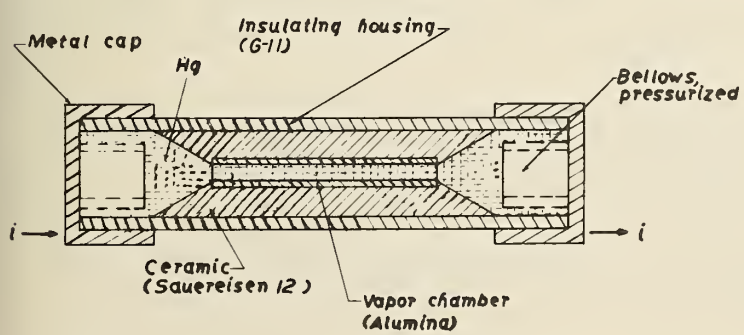

FIGURE 3. - Simplified version of a current limiting device (CLD).

When the circuit interruption is complete, the vaporized metal rapidly liquefies and the pressurized bellows forces the CLD into a reset status, ready for the next switching cycle.

After evaluating and considering parametric effects, ease of handling, fabrication, corrosion problems, etc., it was concluded that, for dc service at industrial levels, that is, 300 to 600 vdc, Hg pressurized at 1 or 3 atm was a satisfactory compromise.

CLD DESIGN RELATIONSHIPS

Theoretical analysis and test results have provided the following relationships:

1. For arc equilibrium, the voltage gradient across the arc should be 100 v/cm or greater.

2. $$\int_{t_1}^{t_2} i(t)^2 dt = KR^4q^2, \tag{3}$$

where t_1 = time i(t) is commutated into the CLD,

t_2 = time of change of state,

R = radius of bore in centimeters,

q = number of parallel bores,

and K = 51.03×10^6 for Hg at 1 atm.

3. The conductivity, Σ, after vaporization (change of state) is approximately 100 ohm-cm.

4. The power dissipated per unit of wall area within the bore

$$\frac{P}{A_w} = \frac{V^2R\Sigma}{\ell 2} \text{ w/cm}, \tag{4}$$

where ℓ = bore length,

and A_w = wall area of a bore.

The number of parallel bores is selected (for a given current magnitude) to limit R (radius) and to control P/A_w, and to establish an upper limit to the "cold" resistance of the CLD.

It should be noted that the "cold" resistance of the CLD multiplied by the current at $t = t_1$ must be less than the arc voltage developed by the switch which commutates the current into the CLD.

A successful switching system for switching currents up to 1,000 amp at 300 v and 500 amp at 600 v has been developed using vacuum switches as the switching devices.

THE SWITCHING SYSTEM

The switching system utilizing the CLD and vacuum switches takes advantage of the inherent "current chop" ability of vacuum switches with tungsten electrodes. Vacuum switches are widely used on alternating current (ac) circuits as circuit interruption devices. The tendency of switches equipped with tungsten electrodes to abruptly chop the current before natural zero has resulted in this type of electrode being replaced, in the majority of applications, by switches equipped with copper-bismuth electrodes. However, this ability to chop current at the 10- to 15-amp level is ideal for the switch system used on dc.

The basic system, used for load switching, is as shown in figure 4.

VS1 is tripped when switching is desired. This commutates the load current into CLD, which vaporizes, and with proper design, drops the load current to a value below 10 amp (the current chop capability of VS2). Nearly full source voltage appears across the CLD. The presence of this voltage, as

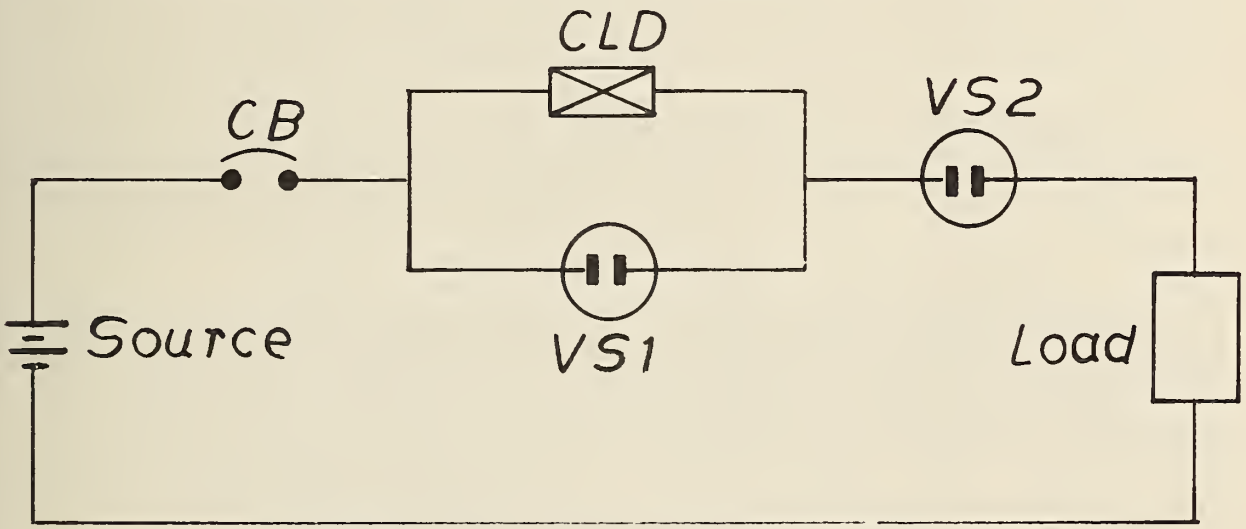

FIGURE 4. - Basic system used for load switching.

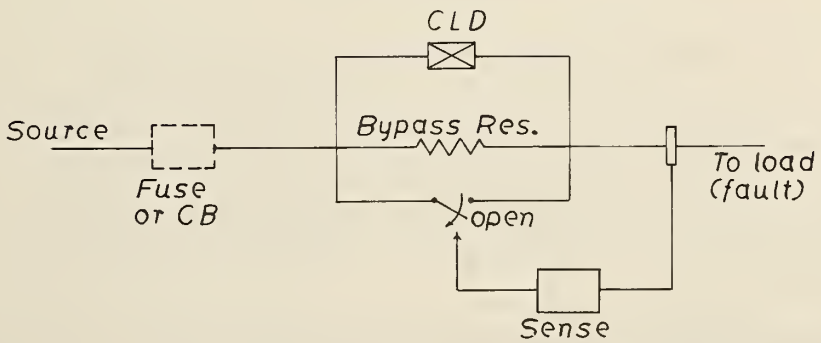

FIGURE 5. - Fuse or circuit breaker with fault current limiter.

detection of rapidly decreasing current, is used to gate a thyristor which in turn opens VS2, completing the switching process. In figure 4, faults would be interrupted by the source circuit breaker (cb). Figure 5 depicts one scheme for handling fault interruption.

Vacuum switches are much cheaper than circuit breakers. The switching scheme shown eliminates energy absorption by the switching contacts. The energy of switching is actually absorbed by the CLD, which of course has a finite operating life. However, it is a simple device and should be relatively inexpensive to manufacture.

FAULT CURRENT LIMITING

Vacuum switches have the inherent limitation that they develop relatively low arc voltage, on the order of 20 to 30 v. For fault switching, if the fault current has relatively high magnitude at $t = t_1$, the required arc voltage may exceed that developed by vacuum switches and another type of high-speed switch may be required. One configuration being evaluated is an exploding bridge wire detonator (designed for multiple operations). This type of mechanism triggers in 1 μsec after command and propagates a shock wave moving at 5,000 to 10,000 m/sec which would actuate a piston, moving oil immersed contacts--yielding a high arc voltage and opening in less than 1 msec.

On dc systems, fault current rate of use is on the order of 2,500 to 10,000 amp/msec, so quick detection, decision, and switching are imperative.

Figure 5 shows a fuse, or circuit breaker (cb), with fault current limiter.

The sensing circuitry reacts to a combination of current level and rate of rise of current to detect a fault condition. It opens the switch, commutating the current to the CLD (low resistance) which changes state (high resistance), commutating the current into the bypass resistor which is sized to limit the current at a value desired and which will trip the circuit open either by the fuse or circuit breaker. The main idea is to limit the peak fault current and to then lower its level to a predetermined value such that excessive damage and/or fires do not result from the fault.

TEST RESULTS

Stress Strain Measurements on the CLD

When the fault current is commutated to the CLD, a bubble of metal vapor is formed in the bore(s). This bubble expands with great speed and expels the liquid mercury from the bore, leaving it filled with a metallic vapor. This accomplishes the desired rapid change of resistance; however, it raises a question pertaining to the effect of the "explosion" on the structural integrity of the CLD.

To determine the actual stresses experienced by the CLD during switching, two units were equipped with strain gages. Four strain gages were placed in

perpendicular-pair array to measure hoop and axial strain along the principal axis. Initially, a Tektronix[4] strain gage amplifier was used in conjunction with a storage oscilloscope to "capture" the transient stress peaks. This method was found to be unacceptable because the oscilloscope failed to have a rapid enough writing speed to display the transient stresses.

To remedy this situation a Biomation 610B transient recorder was connected to the analog output of the strain gage amplifier. The Biomation transient recorder records analog amplitude versus time in 256 discrete digital points. A reconstructed analog signal is then provided for viewing on an oscilloscope. The recorder has a frequency response of 2.5 MHz and the capability of varying the sample interval from 0.1 μsec to 50 msec.

The first unit tested was a two parallel bore unit with a G-11 material housing and two bellows for pressurization at 3 atmospheres. The relevant properties of G-11 are--

1. Axial compressive strength, 20,000 psi;
2. tensile strength, 20,000 psi;
3. Young's modulus, 1.5×10^3

and 4. Poisson ratio, assumed to be 0.3.

Results of two of the strain tests conducted on the G-11 unit are given in table 1, and the corresponding cathode ray tube oscilloscope (CRT) displays of the strains are shown in figures 6 and 7.

TABLE 1. - Strain measurements, 300 v, 1,238 amp

Operation	Type stress	1st peak strain	Rise time to peak, μsec	2d peak strain	3d peak strain	Frequency of oscillation, Hz
87	Hoop.....	36,842	20	6,315	2,105	5,000
92	Axial....	34,210	24	5,263	3,158	5,000

NOTE.--Strain is in microstrains.

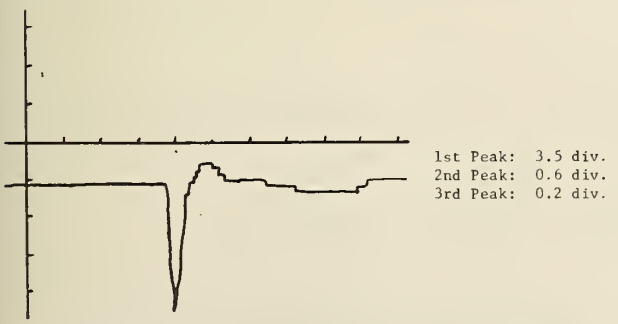

FIGURE 6. - Hoop strain, unit 14 (operation 87).

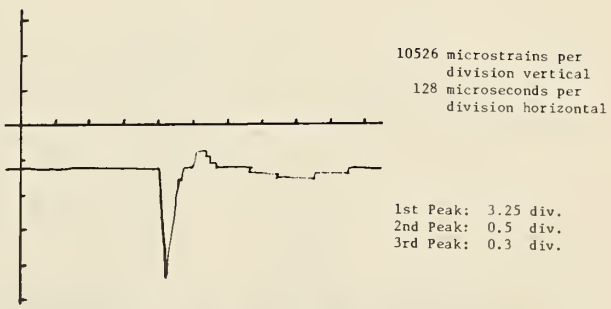
10526 microstrains per division vertical
128 microseconds per division horizontal
1st Peak: 3.25 div.
2nd Peak: 0.5 div.
3rd Peak: 0.3 div.

FIGURE 7. - Axial strain, unit 14 (operation 92).

[4]Use of trade names is for identification purposes only and does not imply endorsement by the Bureau of Mines.

From the given information on G-11 and the measured hoop and axial strains, the corresponding hoop and axial stresses can be calculated from the following formulas:

$$\text{Hoop stress} = \frac{(\varepsilon_h + \gamma\varepsilon_a)}{1 - \gamma^2} \text{ psi},$$

and

$$\text{Axial stress} = E\,\frac{(\varepsilon_a + \gamma\varepsilon_h)}{1 - \gamma^2} \text{ psi},$$

where ε_h, ε_a = hoop and axial strain, respectively,

E = Young's modulus,

and γ = Poisson ratio.

The calculated stress is then as shown in table 2.

TABLE 2. - Stress peaks, unit from table 1

	Hoop stress, psi	Axial stress, psi
1st peak.....	77,650	61,783
2d peak.....	13,011	11,800
3d peak.....	5,030	6,245

The second unit tested has a Ryton R-4 housing and only one bellows. The relevant properties of R-4 are--

1. Compressive strength, 16,000 psi;

2. tensile strength, 8,500 psi;

3. Young's modulus, 1.7×10^6 psi;

and 4. Poisson ratio assumed to be 0.3.

The results of two strain tests are given in table 3 and the corresponding CRT displays of the strains are shown in figures 8 and 9.

TABLE 3. - Strain measurements, 210 v, 620 amp

Operation	Type stress	1st peak strain	Rise time to peak, μsec	2d peak strain	Time between peaks, μsec
2	Axial.....	18,000	32	13,000	410
5	Hoop.....	15,000	26	11,200	730

NOTE.--Strain is in units of microstrain.

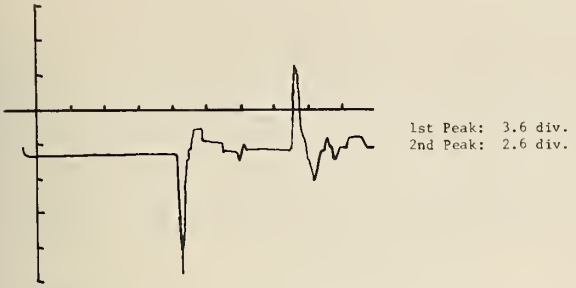

FIGURE 8. - Axial strain, unit 15 (operation 2).

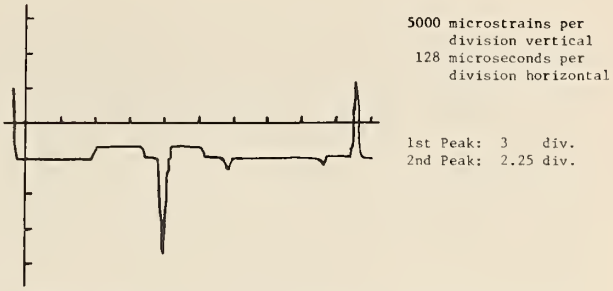

FIGURE 9. - Hoop strain, unit 15 (operation 5).

Once again, the corresponding stresses can be calculated and the results are given in table 4.

TABLE 4. - Stress peaks, unit from table 3

	Hoop stress, psi	Axial stress, psi
1st peak.....	38,100	42,000
2d peak.....	28,200	30,560

Comparing the results of the G-11 unit with the strains of the R-4, it can be seen that the two bellows of the G-11 unit had a rather heavy stress in one direction only; that is, the first peak and rapidly damped oscillations. However, the single bellows unit, R-4 housing, had relatively lower peak stresses in both directions and a "reverberation" effect seems to have occurred.

We do not have sufficient data to determine if the different stress response is due to size, material, or the number of bellows. However, from this test we were able to quantitatively measure transient stresses on the order of 30 usec rise times and to conclude that the structured adhesive used can withstand transient stresses in excess of the steady state withstand specification required of the same material.

Laboratory Surge Test Results

The transition from liquid to vapor state, when the CLD operates, is quite rapid, with transition time of the order of 0.5 to 1.5 msec. The resulting high rate of change of current causes high induced circuit voltages, unless surge suppressing devices are available for absorbing the energy stored in the inductance of the circuit.

In order to evaluate the capability of the various devices with potential usefulness as surge suppressors, a series of tests were conducted on reduced size laboratory machines and full-scale field tests. The experimental results obtained were compared with results of computer simulations based on models of the devices and the circuits in which they were used.

Surge suppression devices tested in the laboratory included energy absorbing capacitors, free wheeling diodes, and varistors ($i - KE^n$).

In the initial laboratory tests the CLD was used to interrupt the current flowing from a shunt-connected dc generator into a series motor, (simulating a dc traction system). The objective of these tests was to obtain data about the operation of the CLD in realistic (no synthetic) test circuits and to draw conclusions about its performance and about the nature and magnitude of the transients associated with its application.

It is generally difficult to accomplish full load operation (rated voltage and current) of large machines in a laboratory, owing to the limited power capability of the supply system. This difficulty can be partially overcome with the use of a system of machines connected as a motor and generator, both electrically and mechanically (a pump-back system). This means that electric power flows from the generator to the motor, and through the common shaft, as mechanical power, back to the generator. The friction, windage, and joule losses are supplied by a third machine, or supply, which need not be as large as the other two. Figure 10 shows the configuration used for laboratory tests.

KEY

I_1, I_2	= vacuum switches
MA	= magnetic amplifier
OS_1, OS_2	= overvoltage suppressors
S_1, S_2	= series field of motor
G	= 230 V, 24.5 amp, 1750 rpm shunt motor
m	= 230 V, 28.4 amp, 1750 rpm series motor
M	= backup contact

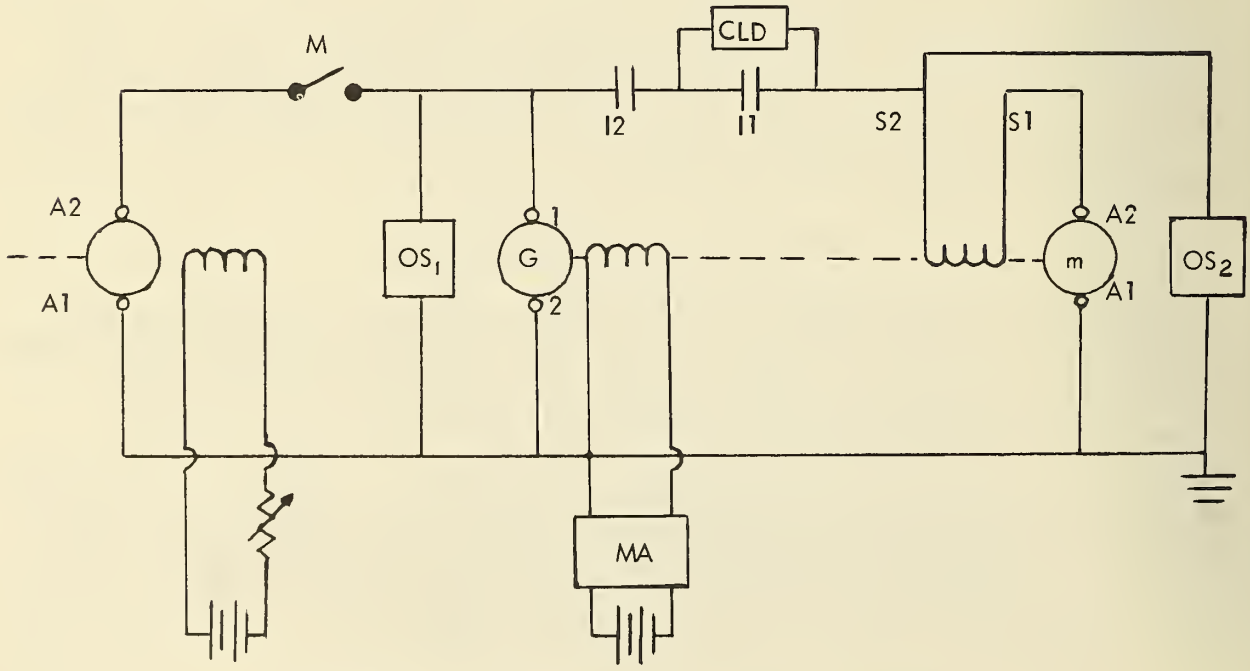

FIGURE 10. - Circuit used for pump-back testing.

Operation without surge suppression yielded a strong negative voltage spike at the motor terminals, and a positive overvoltage at the generator (see fig. 11). Different methods were employed to suppress these overvoltages. A free wheeling diode across the motor terminals proved adequate to suppress the

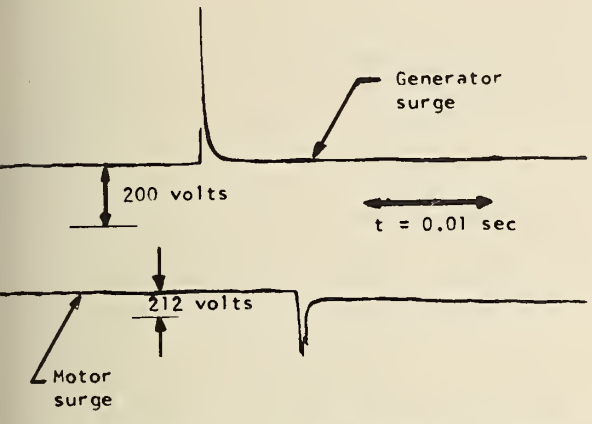

FIGURE 11. - Overvoltages, no surge suppressors.

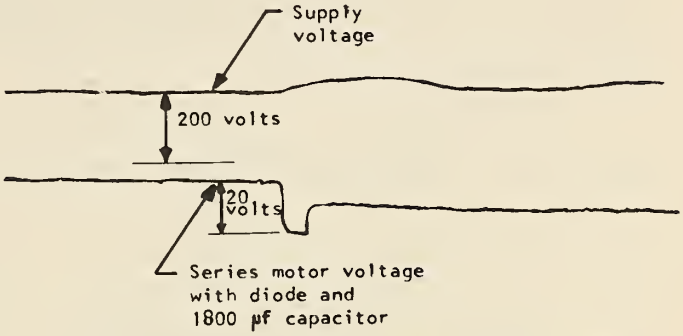

FIGURE 12. - Motor and generator voltage with 1,800 μf parallel to the generator and a free wheeling diode in parallel with the motor.

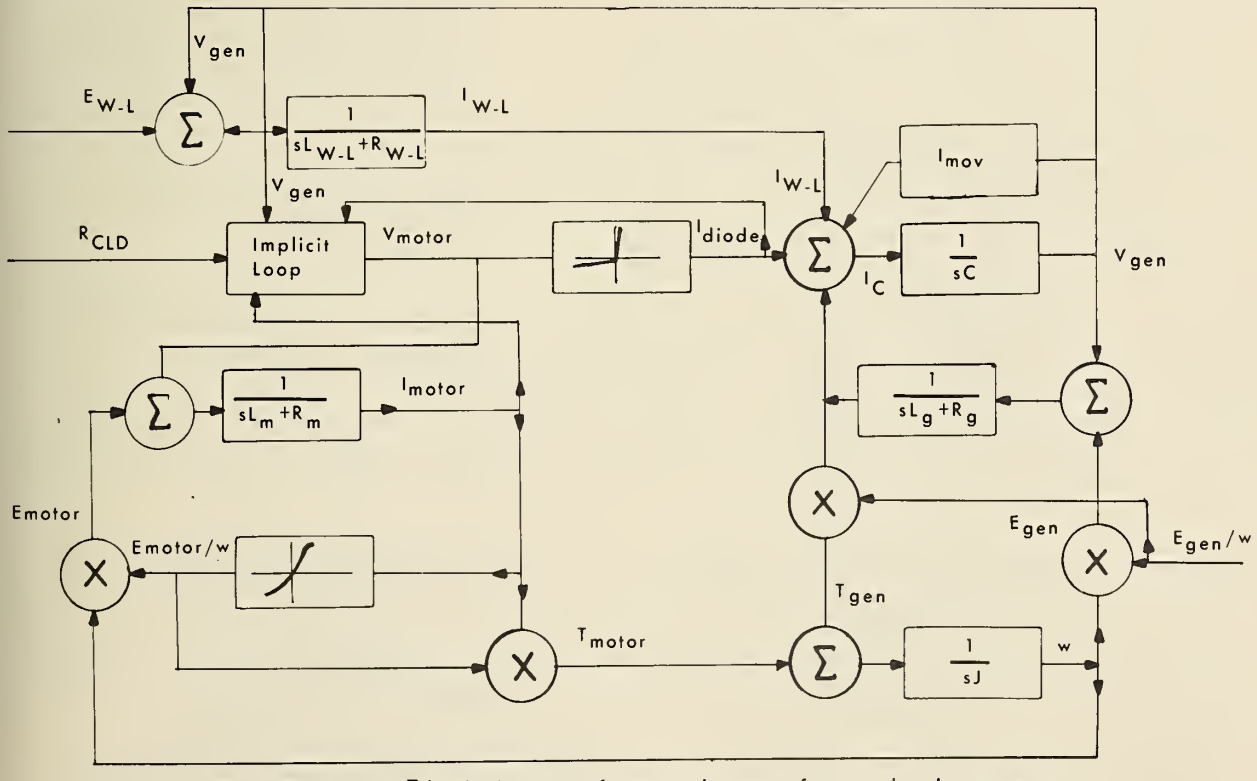

FIGURE 13. - Block diagram for simulation of pump-back system.

negative voltage spike. The voltage will drop to zero (actually the negative of the diode forward voltage drop) and as time passed, would become positive but at a value much lower than the rated voltage of the motor (see fig. 12). This figure also shows the results of capacitance in controlling the generator overvoltages, using a specific value of capacitance.

It appeared desirable, for future application, to develop a computer model of the pump-back loading system, with its nonlinearities and any of the various nonlinear surge suppression schemes that might be used or considered for potential usage. Such a model and program were written and enabled evaluation of various schemes.

The program was written in CSMP[5] and is defined by the block diagram of figure 13. The transient equations of the dc machines were used and friction and inertia of the rotating parts are included.

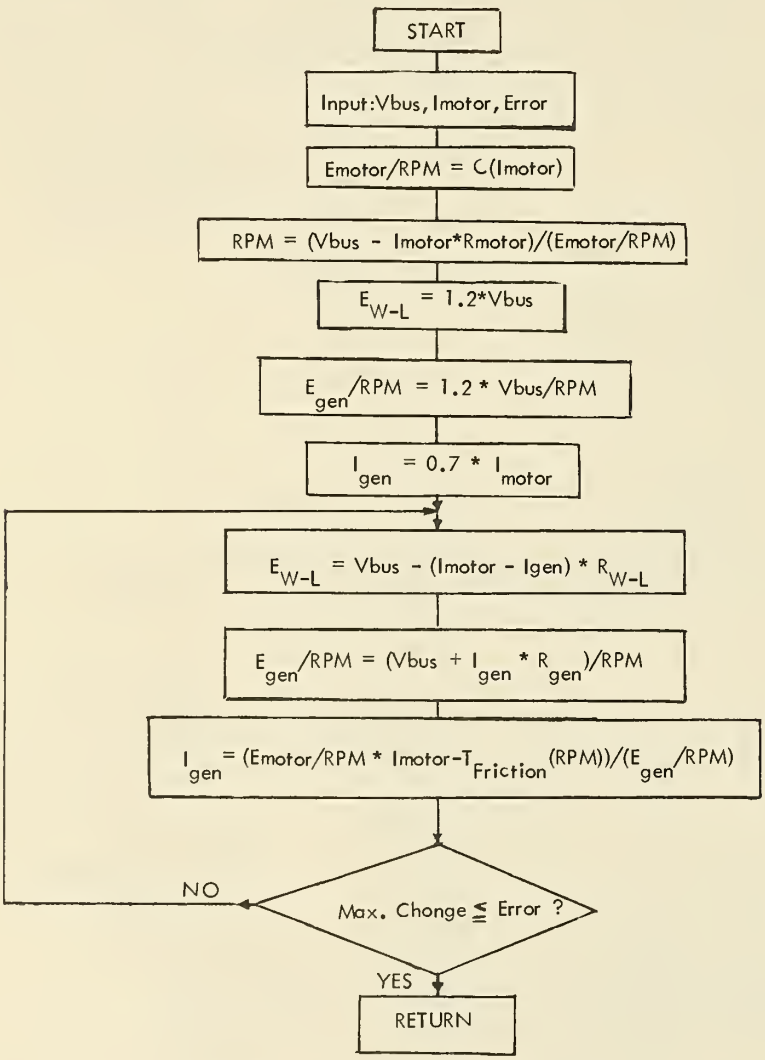

FIGURE 14. - Flow chart for subroutine that calculates steady-state parameters of pump-back system.

The integration method utilized was the Fourth Order Runge-Kutta with variable integration step.

The steady-state parameters were calculated with simple Gauss iterative scheme, a flow chart of which appears in figure 14. Other supporting subprograms were also used. They were--

1. The calculation of the current of the diode across the motor;

2. a linear interpolation for the voltage versus current of the motor;

3. the friction torque as a function of revolutions per minute;

4. the current of the varistor versus voltage.

[5] Continuous system modeling program.

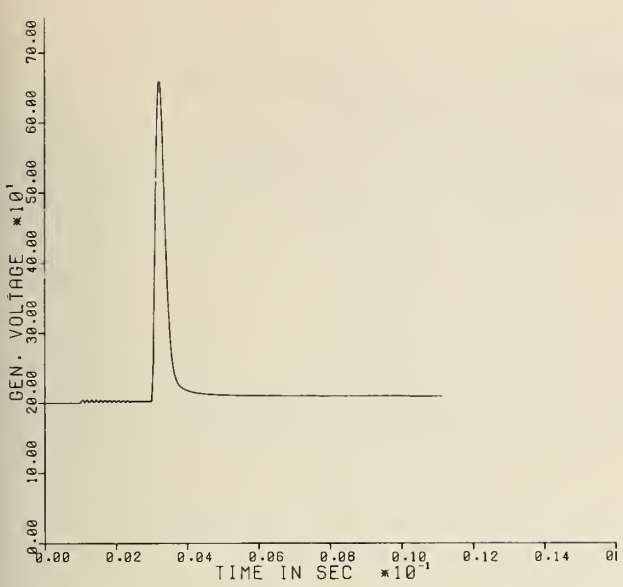

FIGURE 15. - Generator voltage, 200-v, 24-amp operation, no suppressors.

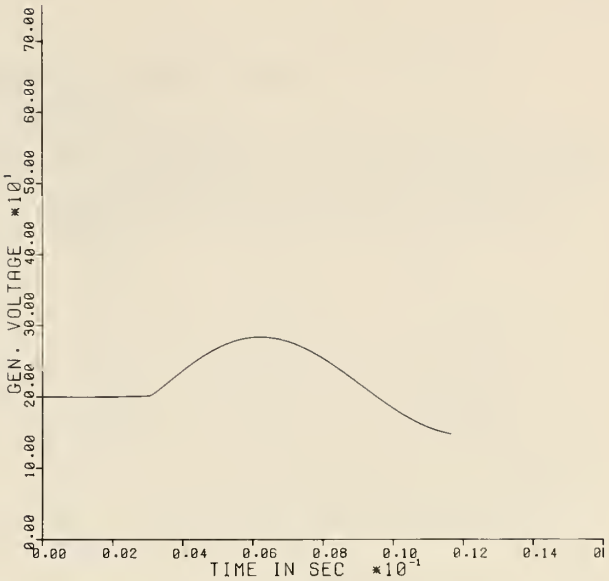

FIGURE 16. - Generator voltage, 200-v, 24-amp operation, 525 μf at the generator.

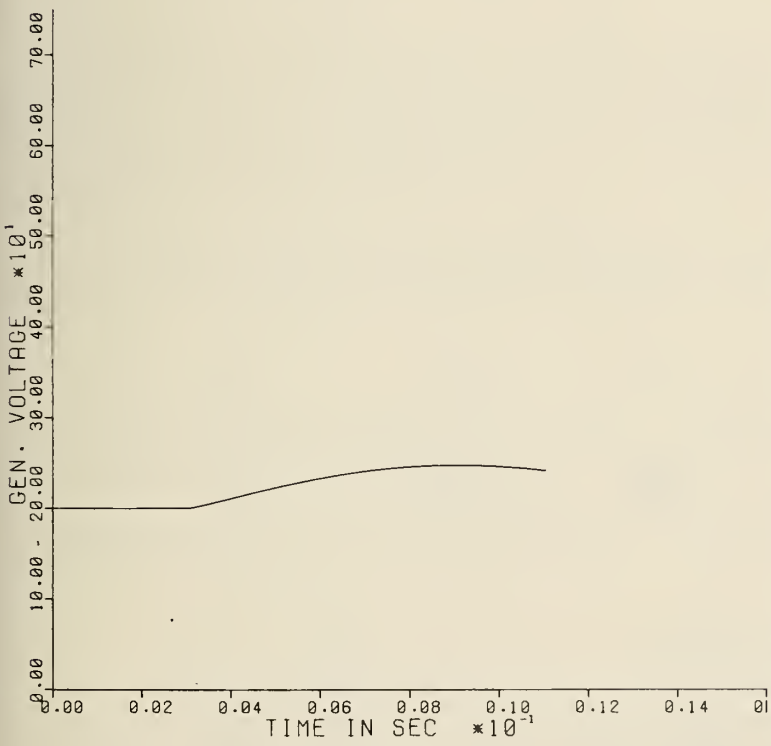

FIGURE 17. - Generator voltage, 200-v, 24-amp operation, 3,600 μf at the generator.

The program was run for a variety of surge suppressing schemes and voltage and current levels. Figures 15, 16, and 17 show the generator overvoltages when the motor, running at 200 v, 24 amp, was switched, both with and without the use of suppressors, and for 525 and 2,600 μf, as examples. These results agree quite well with the test results as shown in table 5. Figure 18 shows generator voltage for the condition when the motor is loaded to 212 v, 26.5 amp before switching. Overvoltages without a suppressor and with a suitable metal oxide varistor are plotted. A small capacitor is placed parallel to the varistor for the purpose of absorbing the initial current of the generator armature coil.

TABLE 5. - Overvoltages at the generator of the pump-back system operating at 200 v and 24 amp

Added capacitance, μf	Measured generator voltage	Calculated generator voltage	Computer results[1]
0	660	-	664
40	450	459	457
100	365	382	375
525	275	285	282
900	269	265	264
1,800	243	246	246
3,600	232	233	232

[1]Continuous system modeling program.

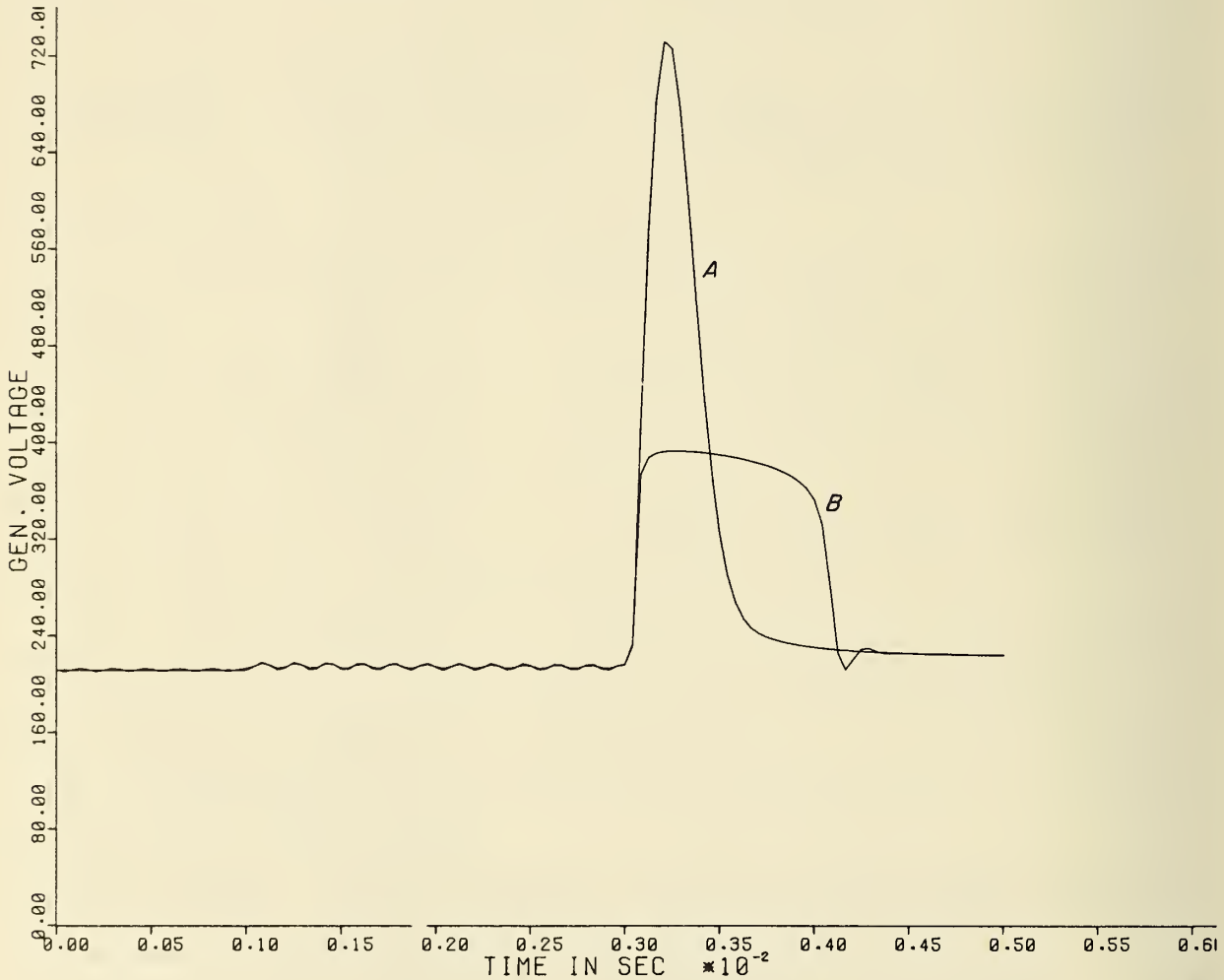

FIGURE 18. - Generator voltage of the pump-back system. Operation at 212 v, 26.5 amp: *A*, Without varistor; *B*, with varistor.

Field Tests

The final stage of this project, the field tests, was conducted at the experimental facilities of the Bureau of Mines at Bruceton, Pa. The apparatus used consisted of a locomotive running on a track, powered through trolley wire from a 300-v, 1,000-amp, 3-phase, full wave rectifier. Figure 19 shows schematically the electric circuit.

The locomotive had two identical dc series motors rated 300 v, horsepower rating unknown, each drawing about 100 amp at empty locomotive load. Various load conditions could be achieved by operating the locomotive up or down a grade and by applying the brakes while accelerating.

Two series of tests were conducted. The first involved the interruption of load current of the locomotive, while it was running under various load conditions. In the second, the CLD was used to limit currents.

Interruption of Load Current

The surge suppression scheme, using capacitors and varistors, as shown in figure 20, was utilized for surge control.

The CLD that was used for the interruption of the motor current was designed for 300 v, 200 amp with a cold resistance of 0.152 and 2 msec time to vaporize. It had two alumina bores of 1 mm internal diameter, 4.6 cm long, cast in Sauereisen 12 and contained in a housing of G-11. The mercury was pressurized at 1 atm with argon.

The connection of the cable coming from the power supply to the trolley wire was interrupted and the switching scheme was inserted as shown in figure 21.

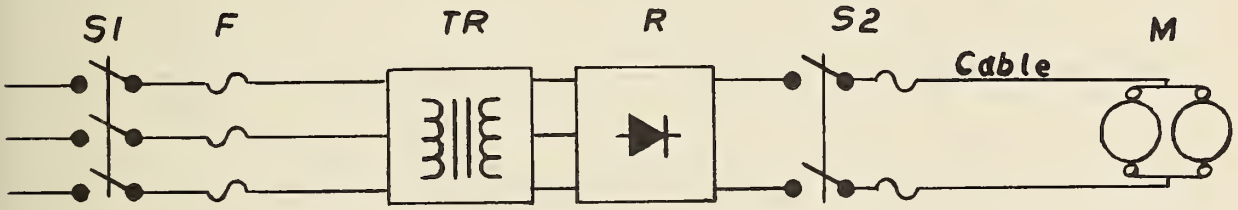

KEY

S1 = load break switch
S2 = fused disconnect switch
F = 150 amp, 5.5 kV fuses
TR = 315 kVA, 3Ø, 60 Hz transformer
2,300 - 222
R = 300 kW, 3Ø full wave rectifier
M = locomotive motors

FIGURE 19. - Electric circuit in the Bureau of Mines facilities at Bruceton.

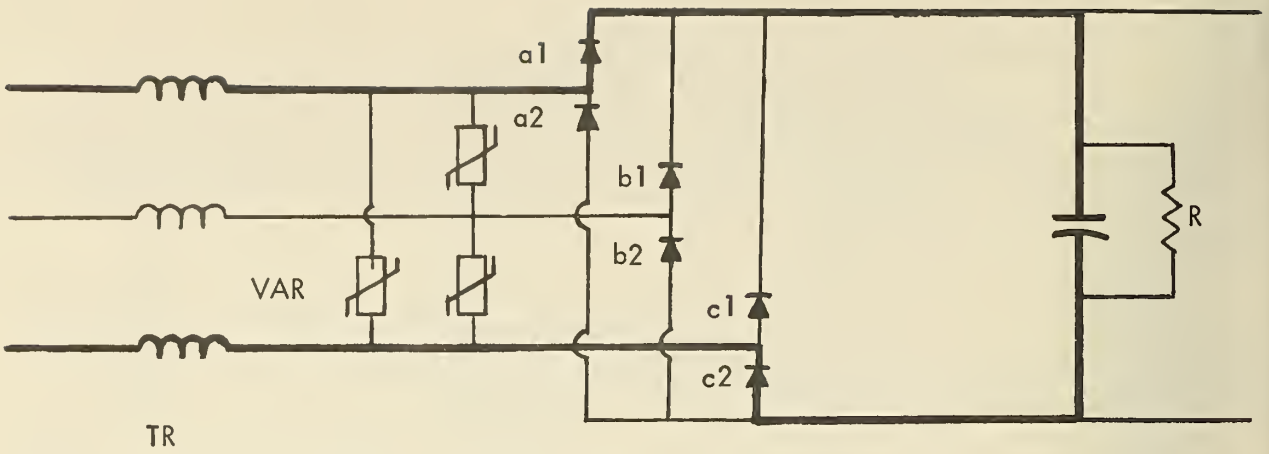

KEY

TR = transformer inductances
VAR = varistors connected between phases
R = bleeding resistor

FIGURE 20. - Overvoltage suppressing scheme for short-circuited rectifier. Heavy line shows the flow of current during the overvoltage.

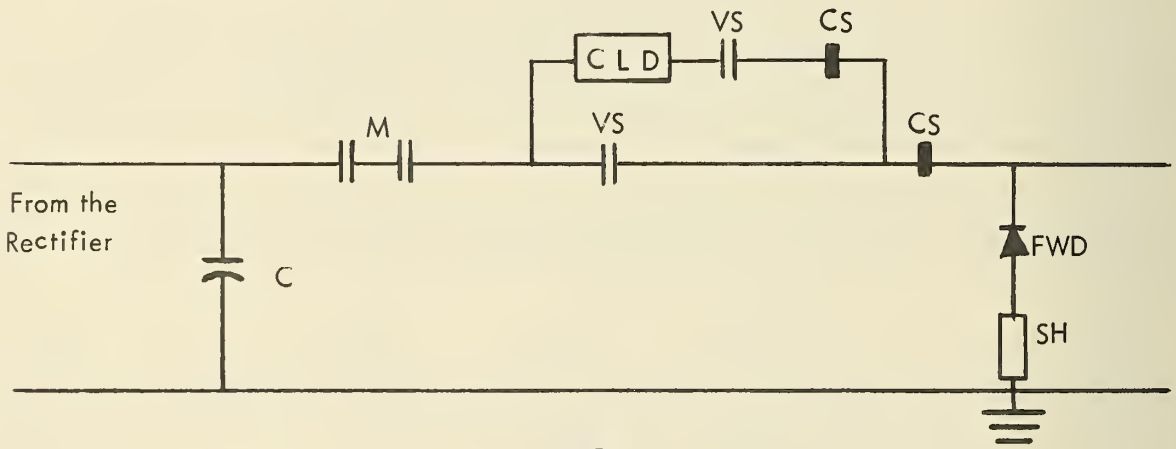

KEY

M = backup switch
VS = vacuum switch
CS = current sensor
FWD = free wheeling diode
SH = current shunt for free wheeling diode current

FIGURE 21. - Electrical connections of the CLD for field tests.

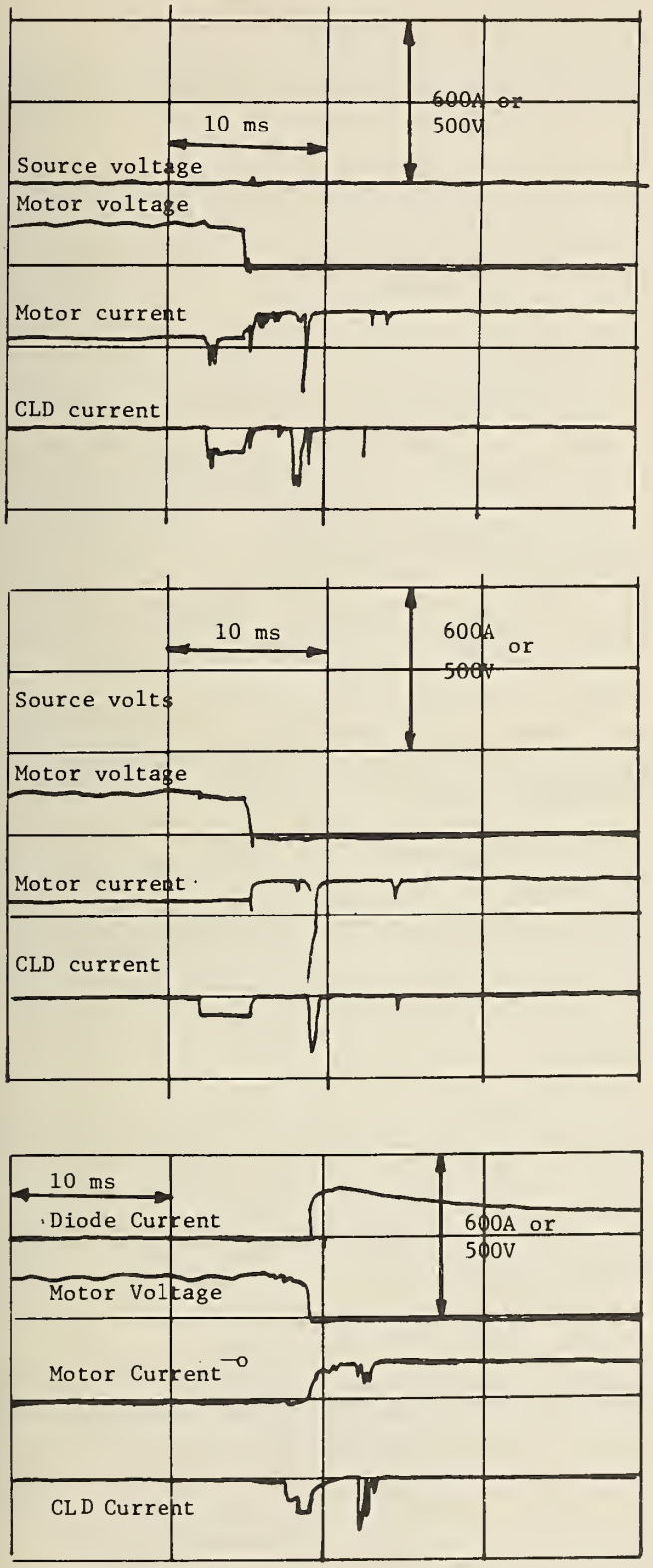

FIGURE 22. - Field test results.

Tests were conducted for various values of the current drawn from the motors. Operating times for the CLD was approximately 3 msec. Figure 22 depicts voltages and currents when the load current was switched using the CLD. In each case successful interruptions resulted, although arc restrikes are apparent in each test. In the results at the bottom of figure 22, it can be seen that not all of the motor current was transferred from the paralleled vacuum switch to the CLD. Examination after the test indicated that one of the two parallel bores was blocked by contamination, causing a doubled value of cold resistance of the CLD and the increased resistance times the total current to be commutated was in excess of the arc voltage that could be developed by the vacuum switch. Hence, total current transfer was not accomplished in that test.

Arc extinction and restrike and accompanying 1-msec current pulses resulted, it is believed, from an excessively low voltage gradient designed into the system (the length of 4.6 cm was too long, being selected on the basis of minimum conductivity of the arc, with no margin for tolerance, on the long side, during fabrication).

Another possible contributing factor in the "noise," restrike, imperfect current transfer problem noted may well have been an other than normal vacuum switch, damaged in previous tests by virtue of faulty switching procedure.

The voltage of the rectifier side of the interrupter did not increase above 15 pct of the rated voltage, being effectively

suppressed by the combination of the varistors and the capacitor. The voltage at the locomotive became negative for a very short period, contrary to the calculations and expectations. This effect was attributed to the fact that the track was rusted, and it introduced a relatively high resistance between the ground and the locomotive and thus in the FWD circuit.

The load current proved lower than anticipated (120 to 170 amp, instead of higher than 200 amp). This was the reason for the increase of the time to vaporize of the CLD. For safety, the backup contactor was set to open very quickly, which it did--once before the CLD had changed state.

Short-Circuit Tests

Because of its very short time to operate, the CLD is extremely useful for the limiting of short-circuit currents. A high-speed mechanical switch that would commutate the fault current to the CLD as well as a suitable device that would sense the presence of the short circuit and trigger this commutating switch, were not available at the time of the tests; therefore, the CLD was connected continuously and the fault applied to the circuit. No suppressing schemes were utilized in these tests because of possible adverse masking results that the presence of the suppressors might have on the short-circuit current rate of rise.

The CLD for the short circuit was similar to the one used in the normal load interruption test; the only difference being that it has four parallel bores instead of two; so that it had a larger current capacity.

Based on system plus transformer inductance, the initial rate of rise of the short-circuit current was calculated to be 1.70×10^6 amp/sec. The steady-state short circuit was calculated to be 2,500 amp on the dc side. It was, therefore, impossible to employ one of the available conventional heavy current (1,250 amp) contactors to commutate this current into the CLD before it reached its steady-state value, since the contactor time to open, after the solenoid was deenergized, was on the order of about 100 msecs.

Because of this, the test circuitry was wired as shown in figure 23, with the fault imposed by contactor M. A resistor, R, sized to pass a desired level of limited current, after CLD operation, was placed in parallel with the CLD.

Tests were run with values of R between 0.25 and 0.4 ohm, thus permitting steady-state short-circuit fault currents in the range of 750 to 1,200 amps to flow after the CLD vaporized.

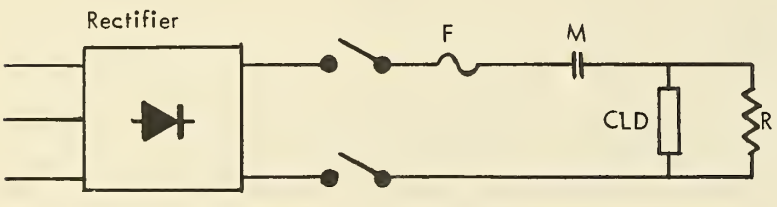

KEY

M = 1,250 amp contactor
R = low valued, parallel resistor
F = 400 amp fuse

FIGURE 23. - Test circuit for current limiting short-circuit field test.

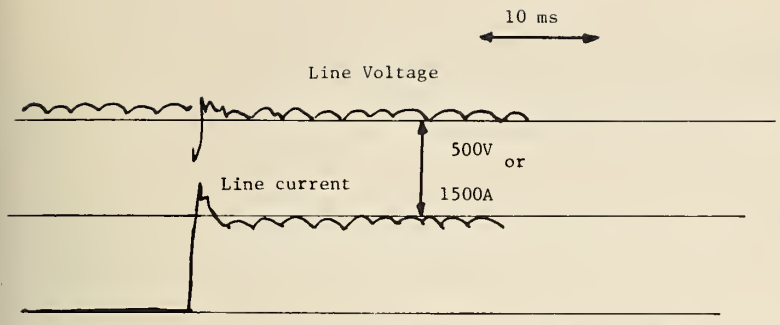

FIGURE 24. - Short-circuit test 1. Parallel resistor: 0.25 ohm. Rate of rise: 2.034×10^6 amp/sec. Steady-state current: 1,031 amp.

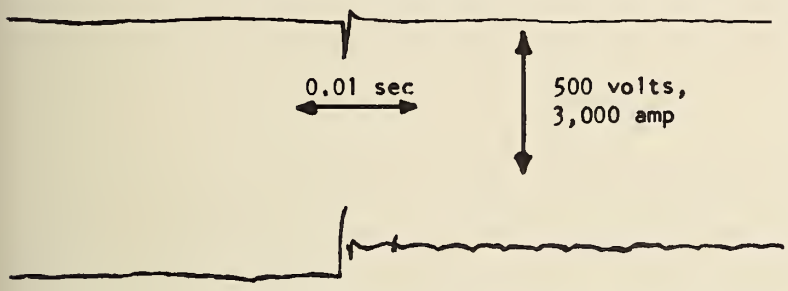

FIGURE 25. - Short-circuit test 6. Parallel resistor: 0.4 ohm. Rate of rise: 2.7×10^6 amp/sec. Steady-state current: 703 amp.

Figure 24 depicts the rectifier current for the case of a parallel resistor of 0.25 ohm. As calculated from the oscillogram, the rate of rise of the short circuit current was 2.03 ka/msec. This represents a circuit inductance of 0.153 mH. The steady-state current was 1,031 amp, which means that an additional resistance of 0.053 ohm existed in the circuit due to cables, shunt resistors, and connections. The 0.7 msec time to vaporize permitted a peak current of 0.7 x 2,030 = 1,421 amp at which time the paralleled resistor, R, permitted a 1,031-amp current to flow.

Figure 25 shows the short-circuit fault of the supply for the case of 0.4 ohm parallel resistance. In figure 25 the supply voltage is also recorded. It dips to about 55 pct of its normal value during the 0.6 msec of the duration of the short circuit, but it comes back as soon as the CLD performs its current limiting function.

CONCLUSIONS

The basic objective of this study was to demonstrate that the CLD could be successfully used for high-speed dc switching and current limiting in a full-size system with motor loads. The anticipated voltage surges, with no suppression devices, did manifest themselves as predicted analytically. Tests on the laboratory system helped to obtain an understanding of the nature of the overvoltages and to develop the method of calculation for what to expect with surge suppression devices.

The overvoltage suppression techniques developed in the laboratory models were successfully applied in the field tests and no significant surges were encountered. A computer program was written to simulate the operation of the CLD and the surge suppressors. The results matched very well with the test results.

The field tests indicate that the CLD can be a very effective device for limiting the short-circuit current level when used as a device injected in

series with the fault and when paralleled with a resistor sized to permit a desired level of sustained fault current (prior to fuse clearing).

ACKNOWLEDGMENT

Work on this project was supported by the U.S. Bureau of Mines under contracts H0357079 and H0366013.

PREVENTIVE MAINTENANCE AND RELIABILITY TESTING OF MOLDED-CASE CIRCUIT BREAKERS

by

E. U. Ibok,[1] M. M. Hassan,[2] and S. S. Venkata[3]

ABSTRACT

In order to guarantee utmost safety in coal mine power systems, molded-case circuit breakers used at distribution level should be reliable. High level of reliability necessitates that the breakers be periodically maintained in an optimal manner. The paper describes techniques for their reliability evaluation and tests for their preventive maintenance.

INTRODUCTION

In most of the electrically operated industries, molded-case circuit breakers are like silent sentinals during normal conditions. They are called upon to operate only during abnormal conditions, such as the occurrence of a short circuit, to isolate the faulted piece of equipment and thus protect the healthy portion of the power system. In the mining industries they are not only required to perform this important function, but they are also operated as a normal switch many times a day. In order for the breakers to perform these requirements of switching and protection with utmost reliability, the preventive maintenance of such devices is highly desirable. There have been many instances of rather phenomenal and costly failures, where later investigations showed that had some minimal preventive maintenance and inspection programs been used, the failures could have been avoided.

The paper describes the techniques for reliability evaluation and preventive maintenance of molded-case circuit breakers used in coal mine distribution systems. A knowledge of the reliability of the breakers will dictate how often these should be maintained.

If these techniques are followed, one can hopefully get an advance warning of an impending breaker failure and replace it before a fault occurs. The ultimate goal in suggesting these techniques is to insure safety in coal mines.

RELIABILITY ASSESSMENT

The reliability assessment of molded-case circuit breakers can be performed in three different ways: Theoretical approach, field test, and

[1]Graduate assistant.
[2]Research associate.
[3]Associate professor.
All of the authors are with the Department of Electrical Engineering, West Virginia University, Morgantown, W. Va.

laboratory test. Before discussing these, the different modes of undesirable operation of circuit breakers are addressed.

Modes of Undesirable Operation

The different modes of undesirable operation of the circuit breakers are as follows:

1. Failure to trip when required to do so.--This particular mode is the one that affects the safety aspect of mine operations. One possible cause of this mode of undesirable operation is welding together of the moving contacts and the stationary contacts.

2. Undesirable tripping.--This mode could be caused by wear out of latching mechanism.

3. Catastrophic failure.--This mode of failure implies that the breaker is of no further use. This mode includes the condition of the breaker not closing when required to do so.

Theoretical Analysis

Definitions

The important terms that will be used in this analysis are defined below:

1. Reliability is the probability of a device performing adequately for the period of time intended under the operating conditions encountered.

2. Hazard rate, $Z(t)$, of a component is the conditional failure rate of the component and is usually expressed in failures per unit time (for example, failures per hour).

3. Failure index, $q(t)$, of a component is the probability of failure of the component within the time t.

4. Reliability index, $r(t)$, of a component is the probability of successful operation of the component within the time t.

5. Mean time to failure, MTTF, of a component is the expected value of time to fail.

$$\text{MTTF} = \int_0^\infty r(t)\, dt.$$

6. Cut-set is a set of components in a given system that interrupts all connections between input and output when removed from the system.

7. Minimal cut-set is a cut-set in which there is no subset of components whose failure alone would cause the failure of the system.

8. Union of minimal cut-sets is all possible combinations of the minimal cut-sets.

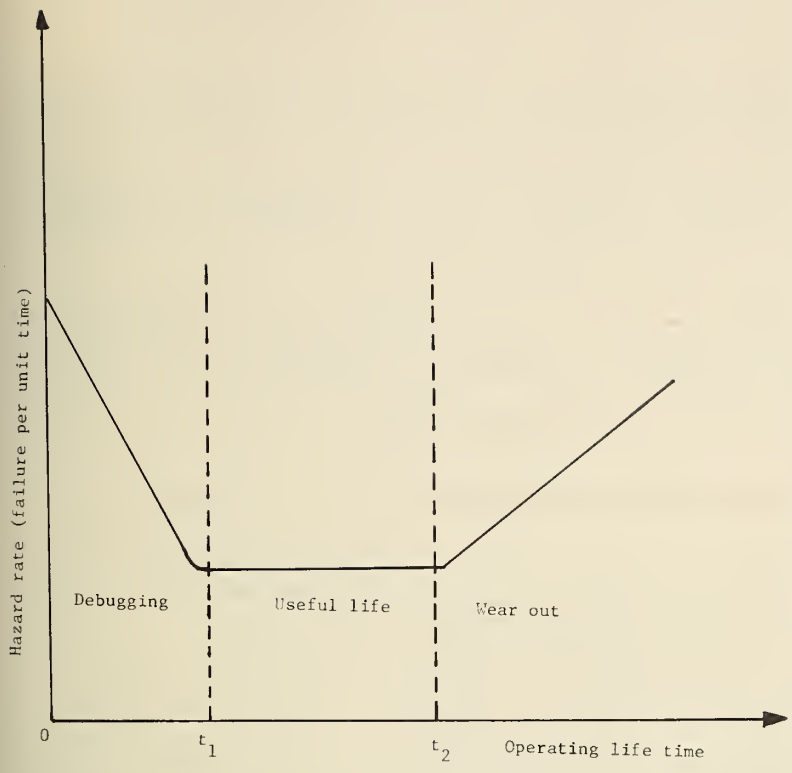

FIGURE 1. - Typical electronic component hazard rate as a function of age.

9. Fault tree is a graphical model that reveals various parallel and sequential combinations of component states that can result in the occurrence of a specified system state known as "top event" in the fault tree.

Mathematical Model

Figure 1 is a typical curve (2, 12)[4] of the time variation of the hazard rate of electronic and mechanical components similar to those found in molded-case circuit breakers. The hazard rate can be constant or can vary with time as depicted by the curve. The curve consists of three segments, debugging period 0 to t_1, useful life t_1 to t_2, and wear out from t_x outwards. The hazard rate is constant within the useful life period. It is during this period, the reliability assessment of the breakers is conducted.

The reasons for the choice of useful life period are as follows:

1. For safety purposes, the reliability of the breakers will be considered from the time it is put into service to the time of its first failure.

2. The failure rate data available for the components pertain to their useful lifespan.

Within the useful life period, the time to failure of the components follow exponential distribution because the hazard rates are constant (2, 4-7, 12, 14-15). Thus mathematically,

$$q(t) = 1 - e^{-\lambda t} \tag{1}$$

and

$$r(t) = e^{-\lambda t} \tag{2}$$

where λ is the constant hazard rate. The mean time to failure is

$$\text{MTTF} = \int_0^\infty e^{-\lambda t}\, dt = 1/\lambda. \tag{3}$$

[4]Underlined numbers in parenthese refer to items in the list of references at the end of this paper.

Application of Mathematical Model to Assessment of Reliability

There are two important approaches among others that could be used to evaluate the reliability of molded-case circuit breaker or any other system. These approaches are block diagram and fault tree analysis. Since the fault tree approach is more superior and systematic than the block diagram approach, the former one is used in this paper to evaluate the reliability of molded-case circuit breakers. This analysis is also confined to the mode 1 failure described earlier--failure to trip when required to do so.

The fault tree approach has had success in the safety and reliability analyses of nuclear reactors and aerospace systems (1, 9).

The main objectives of the fault tree analysis are--

1. To identify systematically all possible modes of occurrence of a given undesired event,

2. To provide a clear picture of the analytical process, and

3. To provide a basis for evaluation of design alternatives.

The basic symbols (1, 9) used in fault tree diagram are as follows:

1. Circle--this symbol represents the primary failure of a component. This type of failure could be caused by design defects.

2. Diamond--the diamond symbol represents the failure of the component due to secondary effects, for example, environmental effects, overstress, etc. It is possible to obtain hazard rates for this type of failure.

3. OR gate--this symbol represents union of two or more events.

4. AND gate--the AND gate describes the logical operation that requires the coexistence of all events to produce the output event.

5. Rectangle--the rectangle represents the output of a logic (AND or OR) gate.

The quantitative reliability of the circuit breaker using the fault tree method involves the following steps:

1. Definition of the top event,

2. Development of the fault tree,

3. Enumeration of minimal cut-sets from the fault tree,

4. Calculation of the failure index of each component from its hazard rate using equation 1, and

5. Calculation of the failure index of the device using the failure indices of the components and the minimal cut-sets of the device.

The components of the circuit breaker are listed in table 1. Figure 2 is the reliability diagram of the circuit breaker. The order and manner in which the components are interconnected in figure 2 depict the signal flow in the circuit breaker. Only those components that contribute to mode 1 failure are shown in figure 3, which shows the fault tree diagram.

TABLE 1. - List of components of molded-case circuit breakers

Number designation	Name of component
1	Input terminal of phase a.
2	Input terminal of phase b.
3	Input terminal of phase c.
4	Undervoltage release (UVR).
5	Bimetallic strip (thermal trip) of phase a.
7	Bimetallic strip (thermal trip) of phase b.
9	Bimetallic strip (thermal trip) of phase c.
6	Magnetic element (magnetic trip) of phase a.
8	Magnetic element (magnetic trip) of phase b.
10	Magnetic element (magentic trip) of phase c.
11	Trip bar.
12	Latch.
13	Spring 1.
14	Spring 2.
15	Contact lever.
16	Moving contact of phase a.
17	Moving contact of phase b.
18	Moving contact of phase c.
19	Arc chutes of phase a.
20	Arc chutes of phase b.
21	Arc chutes of phase c.
22	Output terminal of phase a.
23	Output terminal of phase b.
24	Output terminal of phase c.

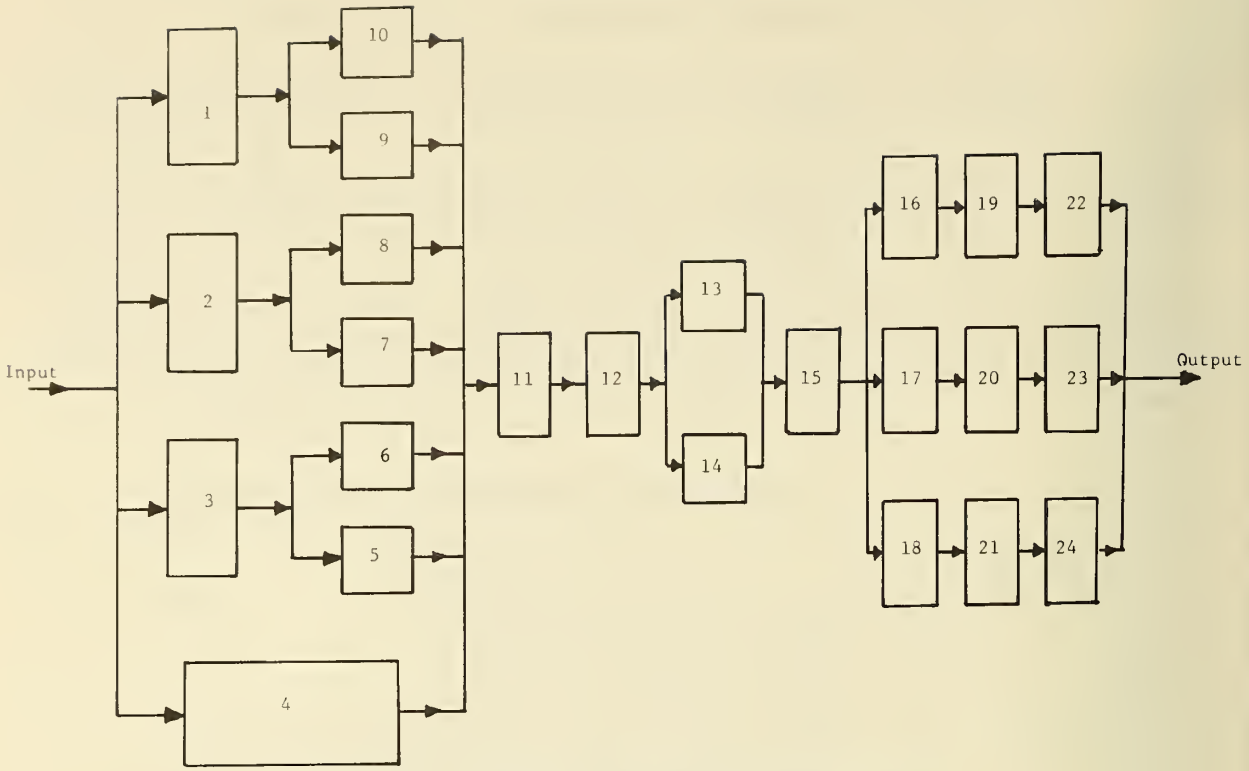

FIGURE 2. - Reliability diagram of circuit breaker.

The circles included in fault tree diagram will not be considered in the analysis because they represent primary failure. The primary failure of components usually occurs in their infancy, as shown in figure 1.

The top event in the fault tree diagram is "moving contacts remain closed when required to open-failure to protect." From the fault tree diagram the minimal cut-sets are 4; 6, 8, 10; 5, 7, 9; 11; 12; 13; and 14. Their description is as follows:

4 Undervoltage release (UVR) jammed in closed position leading to a secondary failure.

6, 8, 10 Secondary failure of the magnetic elements.

5, 7, 9 Secondary failure of the bimetallic strips.

11 Trip bar jammed in a closed position leading to secondary failure.

12 Latch jammed in closed position leading to secondary failure.

13 Spring 1 jammed in closed position leading to secondary failure.

14 Spring 2 jammed in closed position leading to secondary failure.

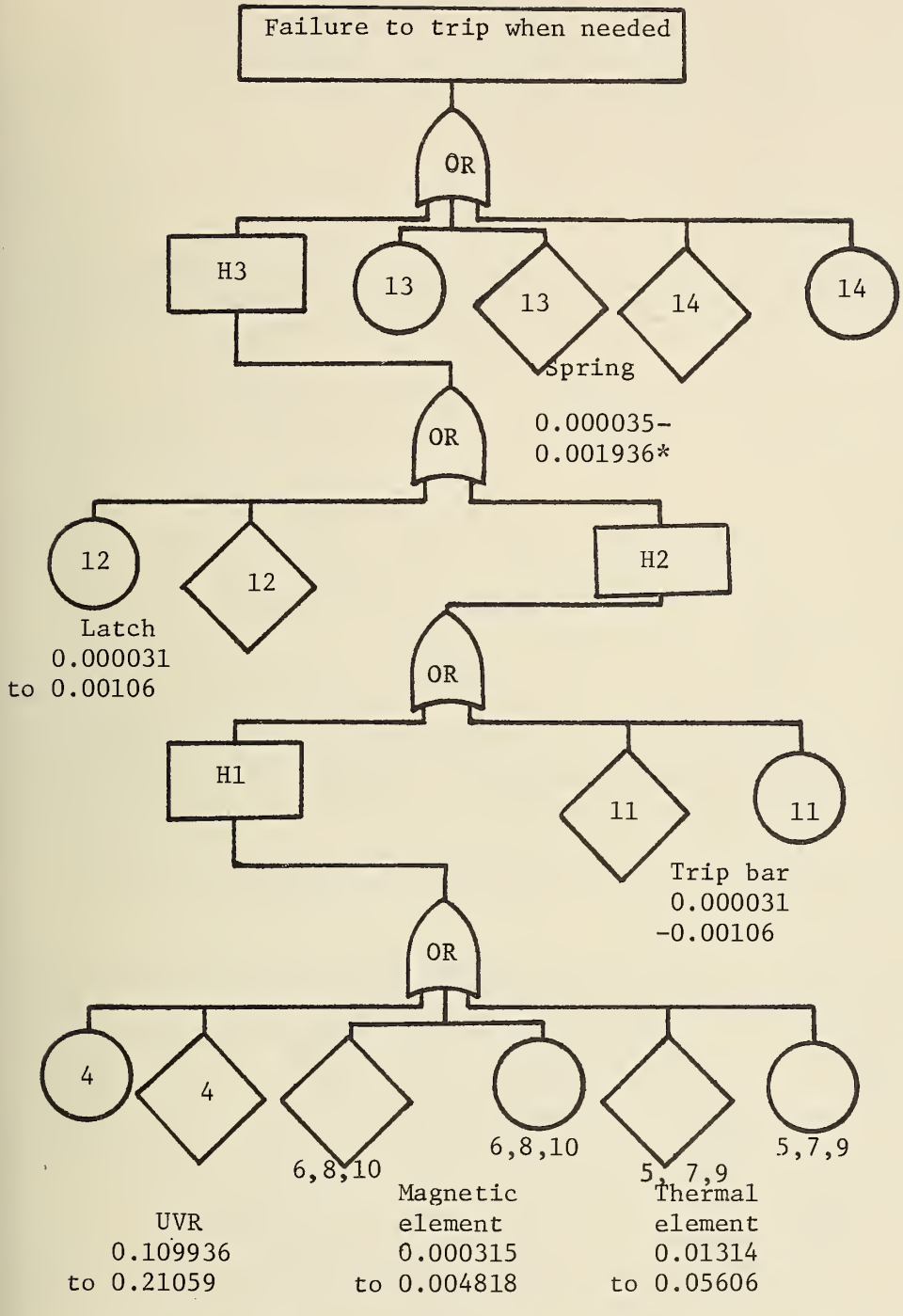

* The range of numbers above indicate hazard rate in failures per year

FIGURE 3. - Fault tree diagram for molded-case circuit breaker—mode 1.

The minimal cut-sets in terms of the failure indices of components are $q_4(t)$, $q_{6,8,10}(t)$, $q_{5,7,9}(t)$, $q_{11}(t)$, $q_{12}(t)$, $q_{13}(t)$, and $q_{14}(t)$. The probability $Q_{CB}(t)$ that the top event in the fault tree diagram (moving contacts remain closed when required to open) is given by the union (U) of the minimal cut-sets. Mathematically this is expressed as (7, 12)

$$Q_{CB}(t) = q_4(t) \cup q_{6,8,10}(t) \cup q_{5,7,9}(t) \cup q_{11}(t) \cup q_{12}(t) \cup q_{13}(t) \cup q_{14}(t), \quad (4)$$

where the sign U stands for the union. It is assumed that the failure of the components is independent. This means that the failure of one component is not caused or affected in any way by another component. Thus

$$Q_{CB}(t) = 1-r_4(t)\, r_{6,8,10}(t)\, r_{5,7,9}(t)\, r_{11}(t)\, r_{12}(t)\, r_{13}(t)\, r_{14}(t). \quad (5)$$

Also the probability $R_{CB}(t)$ that the top event will not occur is given as

$$R_{CB}(t) = 1 - Q_{CB}(t) = r_4(t)\, r_{6,8,10}(t)\, r_{5,7,9}(t)\, r_{11}(t)\, r_{12}(t)\, r_{13}(t)\, r_{14}(t). \quad (6)$$

It might be pointed out here that $Q_{CB}(t)$ and $R_{CB}(t)$ are the failure and reliability indices, respectively, of the circuit breaker.

The values of λ for each component are needed in order to solve equations 5 and 6. These values (4, 10) are given in figure 3. In order to get meaningful results for $R_{CB}(t)$, the common types of faults in a power system which the breaker often experiences have to be considered. These are (1) single phase-to-ground fault and (2) three-phase-to-ground fault.

Solving equation 6 for these two types of fault leads to the results given in table 2 and figure 4.

TABLE 2. - Range and median values of hazard rate and MTTF of circuit breakers

Types of System	Range of hazard rate, failures per year	Median value of hazard rate, failures per year	Range of MTTF, years	Median Value of MTTF, years
1	0.06097-0.31746	0.15528	3.15-16.4	6.44
2	.02458- .128041	.072727	7.81-40.68	13.75

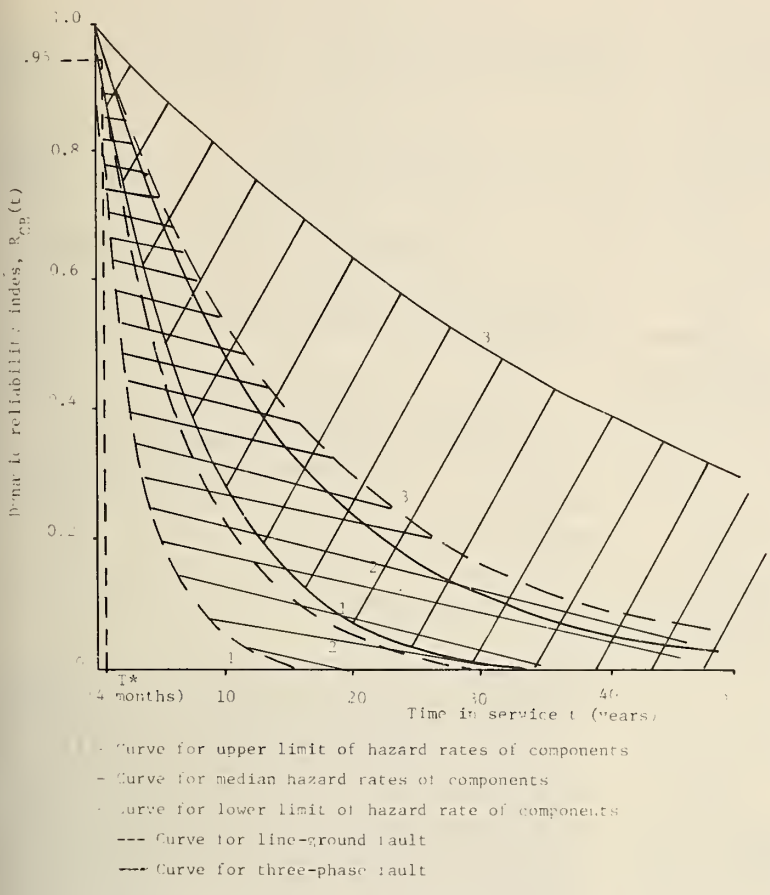

FIGURE 4. - Range of reliability characteristics of molded-case circuit breaker.

Experimental Reliability Analysis

Field Tests

The purpose of the field tests is to monitor the performance of the molded-case circuit breakers under the normal environmental conditions prevailing in the mines. It usually takes a long time for all these protective devices to fail in their normal course of operation. Therefore it is contemplated to monitor the data for sufficient length of time (1 to 3 years), until some of them fail. In this case, partial-test-to-failure method (13) will be used to analyze the data to come up with the hazard rate λ_{CB} of the devices. The hazard rate will then be used to evaluate the reliability index $R_{CB}(t)$ and mean time to failure $(MTTF)_{CB}$ of the devices.

Twenty new three-phase molded case circuit breakers rated 480-v, 130-amp (400-amp frame) have been bought. Ten of these will be installed at various selected locations in Consolidation Coal Co.'s Blacksville No. 2 mine in Blacksville, W. Va. In order to obtain necessary information to evaluate the breaker's reliability performance, each of them will be equipped with a threshold counting device. The device has six counters; five of them designed for the following five discrete current levels: 0 to 60 amp (no load range), 60 to 224 amp (no-load to lower thermal trip limit), 225-400 amp (thermal trip range), 400 to 750 amp (magnetic trip range), and above 750 amp. When the breaker trips successfully at any current level (normal or fault), the appropriate counter will register. The sixth counter registers when the breaker fails to operate when it is supposed to do so. The basic block diagram of the device is given in figure 5. It works in the following manner: The current in each phase is sensed first and rectified. Then the maximum of the three currents is selected and fed into the range discriminating network which in turn operates the appropriate counter depending on the fault current level.

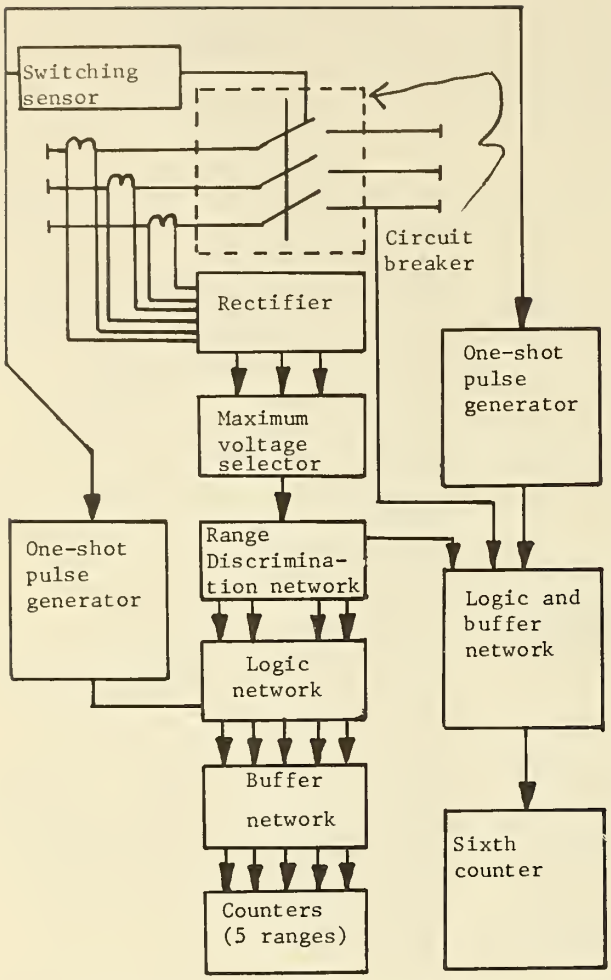

FIGURE 5. - Basic block diagram of threshold counting device for circuit breakers.

In the sixth counter logic network the following items are monitored:

1. Low voltage,

2. Overcurrent,

3. Thermal current level, and

4. The switching of the circuit breaker.

It usually takes about 14 min for the thermal sensing components (bimetal) to initiate tripping when once the current reaches the thermal loading level. Also it takes the circuit breaker 133 msec to completely open its contacts from the time tripping is initiated. All these time delays are taken care of in the logic network.

The prototype of the counting device has been built and tested in the laboratory. Recently it has been installed to monitor its performance inside the mine. The nine other samples will be fabricated later.

The data anticipated from this test are--

1. The total number of counts registered by the first five counters for each breaker. This number is then the total number of operations of a breaker at the time of failure.

2. The number of counts registered by the sixth counter.

3. The total number of circuit breakers that fail catastrophically and are taken out of service.

The sets of data in 2 and 3 above can be analyzed using partial-test-to-failure method if the test is terminated before all the circuit breakers fail. The data in 2 will give the hazard rate λ_d, for degraded operation, while data in 3 will give hazard rate λ_c, for catastrophic failure. Since the partial-test-to-failure method involves, only pertinent mathematical relevant equations are given below:

$$\lambda_d \text{ or } \lambda_c = n/\left(\sum_{i=1}^{n} t_i + (m-n)\ t_n\right), \qquad (7)$$

where t_i = ith ordered degraded operation or failure time,

t_n = time at which test is terminated,

n = number of degraded operations of catastrophic failures at the time test is terminated,

and m = total number of circuit breakers used in the test.

The reliability index pertaining to degraded operation for each circuit breaker is

$$R_{CB}(t) = e^{-\lambda} dt. \qquad (8)$$

Also the reliability index pertaining to catastrophic failure for all the circuit breakers is

$$R_{CB}(t) = e^{-\lambda_c t} \qquad (9)$$

and $$(MTTF)_{CB} = 1/\lambda_c. \qquad (10)$$

In the expressions of equations 8 and 9, it is assumed that the time to degraded operation or catastrophic failure is exponentially distributed.

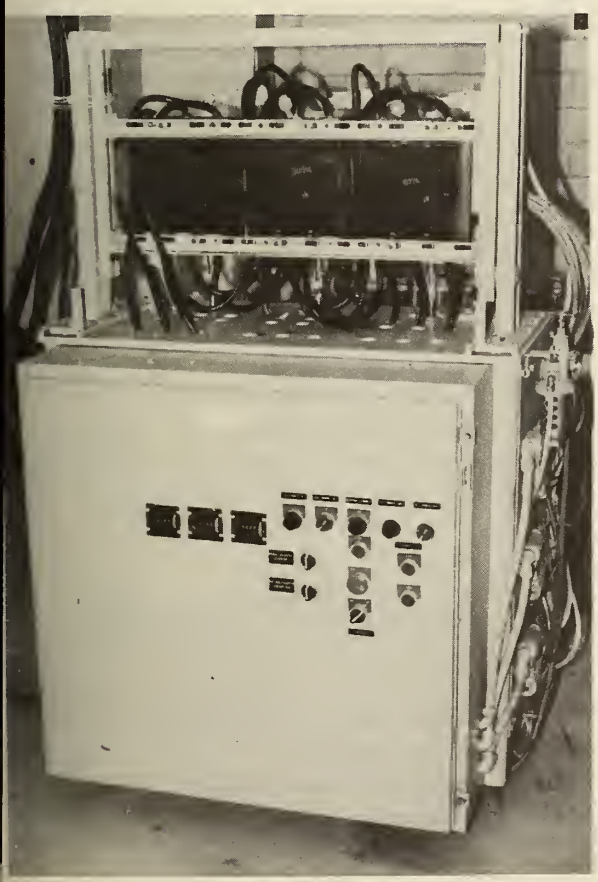

FIGURE 6. - Pneumatic device designed and built to test the 20 breakers.

Laboratory Test

The 10 molded-case circuit breakers to be installed in the mine mentioned above will be exchanged for 10 old ones already in operation in the mine. These 10 old breakers along with 10 new breakers will be subjected to accelerated partial-test-failure at West Virginia University's (WVU) Power Laboratory.

A pneumatic device which has been designed and built will be used to test the 20 breakers mentioned above in the WVU laboratory. Figure 6 shows a picture of the device. It has been designed to perform as follows:

1. Test three circuit breakers automatically.

2. Most of the alternating current (ac) (<1,000 v) and direct current (<500 v) breakers in the 100- to 1,200-amp range can be tested. Due to power limitations in the WVU laboratory, the three circuit breakers will be connected in series and will carry a maximum current of 150 amp at 480 vac. Since the continuous current rating of the particular circuit breaker type under test is 130 amp, 150 amp gives some degree of acceleration in the test.

3. Shut down the testing process in case of any circuit breaker operating in a faulty mode.

4. Identify the circuit breaker that is faulty.

The sequence of operation during the test and the different positions of the circuit breaker handle are shown in figures 7 and 8, respectively.

The following information is expected to be gathered from the laboratory test:

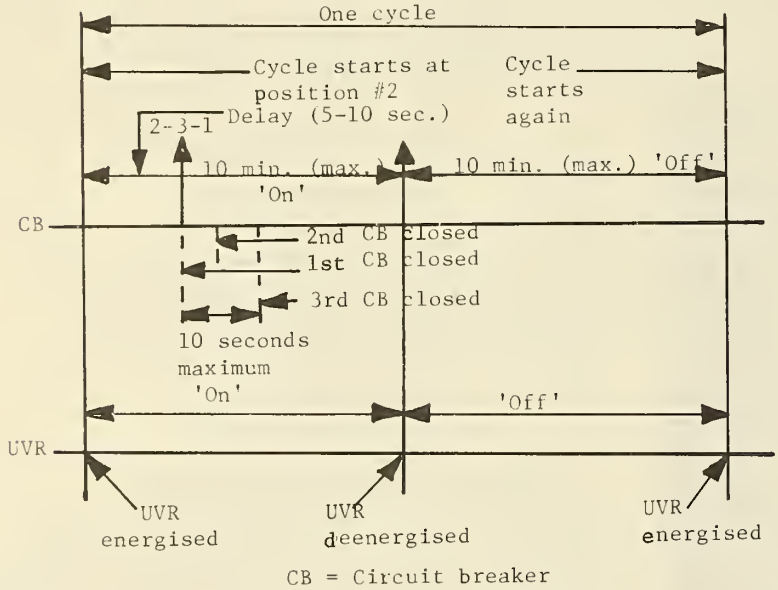

FIGURE 7. - Sequence of operation of molded-case circuit breaker along with UVR.

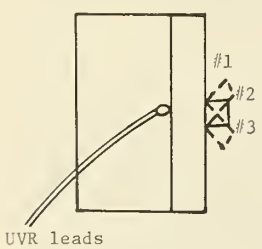

#1: On (closed position) - top
#2: Off (open position) - middle
#3: Reset (reset position)- bottom

FIGURE 8. - Side view of molded-case circuit breaker showing different handle positions.

1. The number of times the circuit breakers operate in a degraded mode in which case the breakers are not taken out of the test. Also the times these degraded operations occur.

2. The number of breakers that fail catastrophically and are taken out of the test. Also the times these catastrophic failures occur.

These data will be analyzed in the same manner as the field test data for the same end results.

Conclusions Related to Reliability Assessment

Considering both types of faults, it can be observed from table 2 that the hazard rate ranges from 0.0246 to 0.3175 failure per year while the mean time to failure is from 3.15 to 40.68 years. From figure 4 it can be concluded that for the circuit breakers to have

greater than 95 pct reliability they may be replaced before they complete a continuous service of 2 years. But the cost of replacing circuit breakers every 2 years would be enormous. It is felt that the breakers could operate properly for a longer period with a reliability greater than 95 pct if suitable periodic maintenance is carried out. The techniques for doing it are the subject of the second part of the paper.

PERIODIC FIELD MAINTENANCE

The importance of field maintenance of circuit breakers has already been discussed. The concept of field testing is very well known and many papers have been written on the subject (3, 11). However, most of the techniques used for field maintenance of low- and medium-voltage breakers tend to neglect one important aspect of breaker operation, that is circuit breaker restriking. As is the case with the mine power systems, the circuit breakers may be called upon to switch large capacitive currents and any restrike of the breaker could give rise to abnormal transients on the system. Besides suggesting a standard test program for field testing of breakers, a circuit description is given that can enable one to have a fairly good idea of interrupting capability of a circuit breaker. It may be noted that since this test is to be carried out as a routine field test it has certain limitations associated with it which have been adequately described. However, it is felt, if the suggested test procedures are followed regularly, the failure of the circuit breakers can be minimized to a great extent.

Typical Test Procedures

The following test procedures should be followed in a comprehensive field testing program.

Mechanical Operation

All the mechanical parts of the breaker should be routinely examined, cleaned, and lubricated. The springs should be checked for proper pressure. Also the main and arcing contacts should be inspected and properly dressed. If they are badly corroded, they should be replaced.

Insulation Resistance Test

This test is carried out using a megger. Insulation resistance should be measured between different phases as well as from current carrying parts of the circuit breaker to ground. Also a test should be made between the line and load terminals with the breaker to open position.

Insulation resistance values of below 1 Mohm are considered unsafe. Care should be taken to disconnect the line and the load conductors from the breaker under test.

Contact Resistance Test

Extensive operation of the circuit breaker under load conditions beyond that for which the circuit breaker was intended, may cause deterioration of the contacts and increase the contact resistance. A simple way of determining this deterioration is by measuring the voltage drop across the closed contacts. Excessive voltage drops across a closed breaker can be an indication of contaminated contacts, or loose connections within the circuit breaker.

It is recommended that this test be made at a low ac or dc voltage at a practical value of current (50 to 100 pct of rated) and the voltage drop across the breaker measured and recorded to be compared against manufacturer's data.

Instantaneous Magnetic Overcurrent Trip Test

In routine tests it is more important to determine that the magnetic overcurrent trip feature is operating and will trip the breaker rather than the exact value at which the instantaneous magnetic feature operates.

Since the instantaneous magnetic trip characteristics of the breaker can be influenced by stray magnetic fields, the test setup must be made in such a way that fields caused by either the test equipment itself, steel enclosures, or the conductors from it to the circuit breaker do not affect the test results.

Test results can also be greatly influenced by the wave shape; therefore, it is desirable to have a sinusoidal output for the test equipment.

For testing the breaker assume that the instantaneous trip is adjusted to some setting, say 600 pct. Under ideal conditions one would adjust the current control of the test set to this value of current and connect it to one pole of the circuit breaker. When the power is switched on the breaker should trip. Invariably this does not happen because the actual current may be different from the set current owing to increased lead or breaker contact resistance. However, if the current is injected at a higher voltage this problem can be overcome.

Alternatively, the current control is set at a point where approximately 70 pct of the expected tripping current will flow when energized. The power is turned on and the current increased till the breaker trips. If the current is increased too slowly, the breaker may trip owing to the time delay element especially if more than one test is run at a high current level. If the current is increased too rapidly an erroneous reading will be obtained because the meter indication lags behind the actual current because of meter damping.

The errors incorporated make these test results useful only for "order of magnitude." Therefore, unless special apparatus is available, field test results for magnetic trip currents may vary from manufacturer's published data.

Overcurrent Trip Tests

A general indication of the proper action of the overcurrent tripping characteristics of the circuit breaker can be verified by selecting a certain percentage of the breaker rating, such as 300 pct, and applying this to a pole of the circuit breaker to determine whether it will cause automatic opening of the breaker. The tripping characteristics at 300 pct of the rated current is an indication of the breaker operation throughout its entire overcurrent trip range. Two test methods are possible:

1. Test connections can be cascaded from load side of one pole to the line side of the next, so that the total current passes through all the trip units in series. This test is more indicative of actual load conditions temperature-wise and will give an excellent indication if the breaker is operating correctly.

2. Each pole of the breaker can be tested separately. The test results will generally be within 10 pct of that of the series tests of all poles. This test may be most desirable if nuisance tripping has been experienced, indicating one pole has a tripping characteristic different from the other poles.

Principles of Synthetic Testing

All the test procedures described above are of a general nature and are almost universally accepted. But none of the above tests give any information about the arc interruption capabilities of the circuit breaker. This test is accomplished using the concept of synthetic testing.

The basic underlying principle of synthetic testing can be explained by reference to figure 9, which represents an oscillogram of the current and voltages obtained during a circuit-breaking operation.

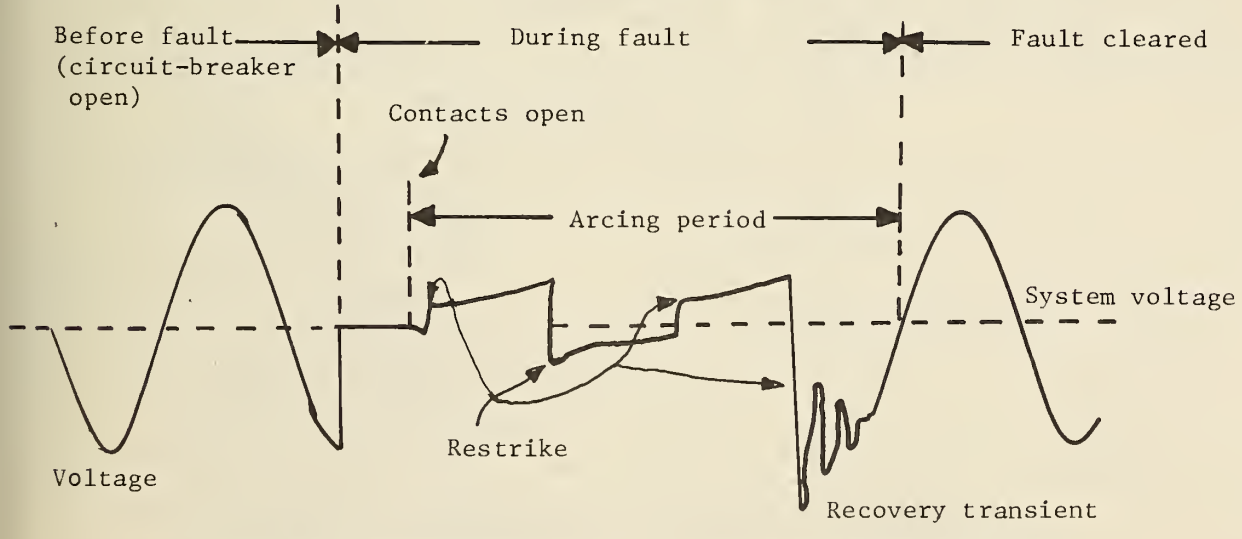

FIGURE 9. - Voltage oscillogram of a circuit breaker clearing a fault.

Here it will be seen that, during the main current flow, a comparatively low voltage appears across the opening circuit breaker, while during the restriking and recovery voltage period it conducts little or no current. It is, therefore, possible to use a comparatively low-voltage source to supply the test current and a low-current source to supply the test voltage. This is the basic underlying principle of synthetic testing. The voltage of the current source should be just enough to counteract the arc voltage across the circuit breaker. The ratio of the test breaker recovery voltage to the voltage of the current source is a measure of the effective gain in the testing power.

One other important advantage of the synthetic test is that it tends to be less destructive because, should the circuit breaker fail to clear the circuit, it has only to deal with the low power of the voltage circuit.

Description of Portable Circuit Breaker Tester

The principles of synthetic testing were incorporated in a portable circuit-breaker tester fabricated at West Virginia University.

The basic arrangement of the test circuit is shown in figure 10: A is the high-current, low-voltage transformer (480/32 v, 25 kva) which is used to supply the short-circuit current. C is one pole of the breaker under test. B is a current transformer used to get a sample of the current to be fed into the control circuit. E is another pole of the breaker under test and is used in series to prevent the recovery voltage from appearing across the current source.

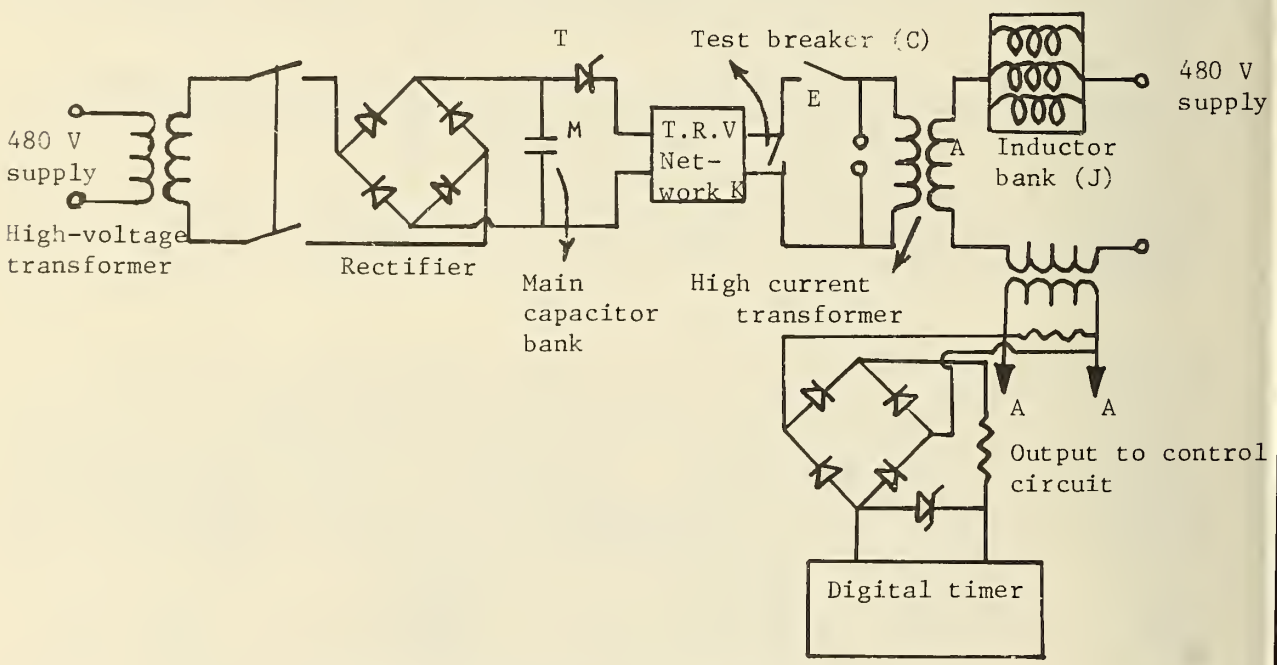

FIGURE 10. - Basic setup of synthetic test circuit.

In case the pole E breaks down before the pole under test, the back up protection is provided by surge arrestor SG.

The transient recovery voltage (TRV) is provided by a precharged capacitor bank M discharged through a TRV shaping network K. Thyristor T is normally off, but is fired at the instant the recovery voltage is to be applied. The synchronization of the voltage and current sources is achieved by a control circuit shown in figure 11. The current signal is fed into a voltage comparator and then a monostable multivibrator and a logic gate. The result is a short pulse each time a current zero occurs. Another part of the circuit gives a long pulse delayed by a preset time after the opening of the circuit breaker. Where both of these pulses are present there is an output pulse from the output AND gate which is used to trigger the thyristor T in the voltage circuit.

The simple circuit used to shape the transient recovery voltage is given in figure 12. The various components are designed to give the required peak and frequency of the recovery voltage.

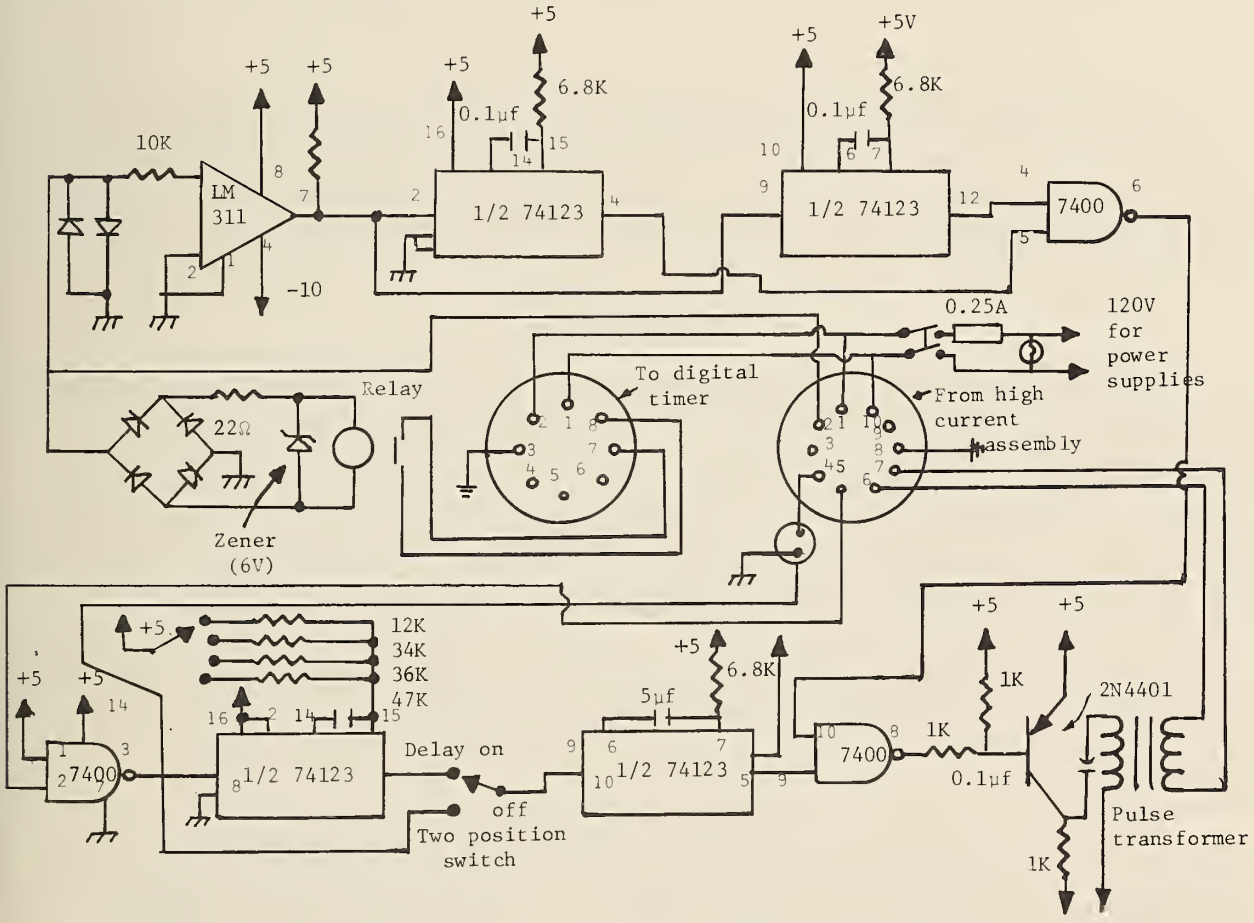

FIGURE 11. - Control circuit assembly for circuit breaker test set.

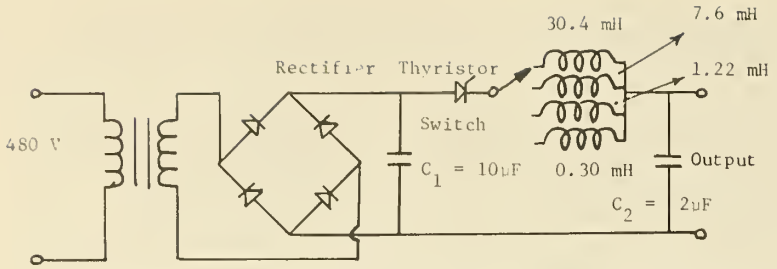

FIGURE 12. - Schematic diagram of transient recovery voltage generating circuit.

The output voltage is given by

$$V_o = V_{in}\left[\frac{C_1}{C_1+C_2}\right]\left[1-\cos\left(\frac{t}{\sqrt{LC}}\right)\right]$$

where V_o = open circuit output voltage,

V_{in} = charging voltage of capacitor C_1,

and $C = C_1/C_1+C_2$.

Capabilities and Limitations of the Test Set

The test set can perform almost all the routine field tests described above. The maximum current available is around 5,000 amp. The current can be varied in steps. A smooth variation however is not possible. The frequency of the transient recovery voltage is variable in four steps of 1,000, 2,000, 5,000 and 10,000 Hz. The operating time of the breaker can be measured from 1 msec to 100 msec.

Preliminary tests have revealed some difficulties with synthetic testing. Since this concept has not been previously used, standards have to be set to determine the optimum time delay between current interruption and the application of the transient recovery voltage to simulate an actual fault condition. These standards can then be used to rate breaker performance and their ability to interrupt fault currents.

CONCLUSIONS

The first part of the paper describes the three different types of techniques for the reliability assessment of molded-case circuit breakers. These are field tests, laboratory tests, and fault tree analysis. Preliminary results based on the application of these three methods to a 400-amp frame, 600-vac, three-phase breaker indicated that its hazard rate is 0.1553 failure per year as can be seen from table 2. This figure when compared with 0.0035 failure per year reported for similar type of breakers used in other industries (8) indicates clearly that the breakers used in the mining industry do not possess a high degree of reliability. This is perhaps due to the added function they perform as switches apart from being protective devices, and also due to the hostile environment in which they operate. These failure rate numbers also emphasize the need for proper maintenance of the breakers in an optimal way.

The second part of the paper describes the tests to be carried out for periodic maintenance of the breakers. The concept of synthetic testing is discussed and a portable circuit breaker test set to carry out these tests is described.

REFERENCES

1. Barlow, R. E., J. B. Fussell, and N. D. Singpurwalla (ed.). Reliability and Fault Tree Analysis. Society for Industrial and Applied Mathematics, Philadelphia, Pa., 1975, pp. 1-33.

2. Billinton, R. Power System Reliability Evaluation. Gordon and Breach Science Publishers, New York, 1970, pp. 1-229.

3. Buck, A. Q. Field Testing of Low-Voltage Breakers. IEEE Conf. Rec., 23d Ann. Conf. in Rubber and Plastic Industry, Akron, Ohio, Apr. 5-6, 1971, p. 97.

4. Earles, D. R. Reliability Growth Prediction During the Initial Design Analysis. Proc. 7th Nat. Symp. on Reliability and Quality Control in Electronics, ASSOC, Philadelphia, Pa., January 1961, pp. 380-388.

5. Ibok, E. U. Reliability Analysis of Undervoltage Release/Relay in Coal Mine Electrical Power Systems. M.S.E.E. Thesis, W. Va. Univ., Morgantown, W. Va., 1975, 92 pp.

6. Ibok, E. U., W. T. Crawford, S. V. R. Kolluri, and S. S. Venkata. Safety and Reliability Assessment of Solid-State Protective Devices Used in Coal Mine Power Systems. Conf. Rec., 11th Ann. Meeting, IEEE, Ind. Appl. Soc., 1976, pp. 85-90.

7. Ibok, E. U., and S. S. Venkata. Reliability and Sensitivity Analyses of Undervoltage Relays Used in Coal Mine Distribution Systems. Proc. 7th Ann. Pittsburgh Conf. on Modeling and Simulation, Instr. Soc. America, v. 7, pt. 1, April 1976, pp. 233-237.

8. Institute of Electrical and Electronic Engineers. Report on Reliability Survey of Industrial Plants, Part I. IEEE Trans. on Industry Applications, v. IA-10, No. 2, New York, March-April 1974, p. 220.

9. Lambert, H. E. Systems Safety Analysis and Fault Tree Analysis. Report for U.S. Atomic Energy Commission (Contract No. W-7405-Eng-48) by Lawrence Livermore Laboratory, Univ. of Calif., Livermore, Calif., 1973, pp. 1-72.

10. Polovko, A. M. Fundamentals of Reliability Theory, Transl. by Scripta Technical, Inc., and ed. by W. H. Pierce. Academic Press, New York, 1968, pp. 1-180 and 373-449.

11. Rumohr, C. G., and E. R. Redlahammer. Field Testing of Low-Voltage Power Circuit Breakers. Trans. AIEE, January 1965, p. 12.

12. Shooman, M. L. Probabilistic Reliability: An Engineering Approach. McGraw-Hill Book Co., Inc., New York, 1968, pp. 1-488.

13. Smith, C. O. Introduction to Reliability in Design. McGraw-Hill Book Co., Inc., New York, 1976, pp. 1-235.

14. Venkata, S. S., E. U. Ibok, W. T. Crawford, and S. V. R. Kolluri. Safety and Reliability Assessment of Protective Equipment Used in Coal Mine Power Systems. Proc. 3d W. Va. Univ. Conf. on Coal Mines Electrotechnol., IEEE, Ind. Appl. Soc., August 1976, pp. 3-1--3-17.

15. Venkata, S. S., E. U. Ibok, and S. V. R. Kolluri. Reliability Assessment of Undervoltage Releases and Molded-Cage Circuit Breakers Used in Coal Mine Power Systems. Conf. Rec., 12th Ann. Meeting, IEEE, Ind. Appl. Soc., 1977, pp. 776-782.

PERIODIC INSPECTION OF MINE ELECTRICAL POWER SYSTEMS TO DETECT INCIPIENT FAULTS

by

Y. C. Chou,[1] M. M. Hassan,[2] and E. K. Stanek[3]

ABSTRACT

All electrical power systems are subject to short circuits at random intervals. The mean time between faults can be lengthened by more conservative design at greater cost. Prohibitive costs and other practical limitations such as space, cable flexibility, etc., make it impractical to completely eliminate faults on electrical power systems. The next best alternative might be to identify equipment that is about to fail and take it out of service. This alternative looks especially desirable in coal mine electrical systems because of the severe ramifications of faults in these systems with respect to safety. A number of promising tests have been identified that may be capable of locating devices with degraded insulation in the field.

The feasibility of using these tests to detect incipient faults is being determined by performing these tests on actual coal mine systems and by performing accelerated life tests in the laboratory. Also, environmental tests have been carried out to determine the relationship between the various insulation and environmental parameters.

INTRODUCTION

A power system is a complicated network of various electrical components, such as cables, transformers, electric machines, circuit breakers, etc. For a system to work continuously and efficiently, each of the components has to be in good operating condition. The failure of any single component can cause interruption of the supply and may involve a lot of downtime and labor in removing and replacing the damaged equipment. It may also give rise to dangerous overvoltages on the system, thereby causing a safety hazard.

The problem of failure becomes more acute in the case of a mine power system because of the hazardous environment existing inside the mine. In many cases the energy released due to the occurrence of a fault because of component failure may be enough to cause a fire, thereby endangering the lives of personnel working inside. Also, the need for a highly reliable power supply is augmented by the fact that the complete operation of the mine, that is, movement of personnel in and out, carriage of coal, and operation of mining equipment, is dependent on electrical service.

[1]Graduate assistant.
[2]Research associate.
[3]Professor of electrical engineering.
All of the authors are with West Virginia University, Morgantown, W. Va.

A survey (7)[1] conducted by the United States Mining Enforcement and Safety Administration on electrical hazards in underground bituminous coal mines reveals the following:

> An investigation of 1,404 injuries related to electricity in underground bituminous coal mines revealed that more the 96 percent of all electrical accidents were caused by (1) arcs resulting in burns, (2) electrically generated heat resulting in burns and scalds, and (3) electrocution and shock. Data analysis indicates that a reduction in electrical accidents is immediately possible by reducing defective splices and insulation breaks and by proper placement of the trolley poles. Sixty-six percent of the mine fires investigated by the Bureau of Mines through 1972 and 21 percent of all methane ignitions can be attributed to electrical ignition sources and inadequate design of electrical equipment used in the mining environment.

Description of Work Carried Out (2)

The initial part of the research effort was devoted to designing test procedures and test equipment for periodic testing of mine power systems. Efforts were also made to acquire commercially available test equipment wherever possible.

By carrying out these tests periodically, one can hopefully monitor and pinpoint the abnormal condition of a piece of electrical equipment prior to the occurrence of a fault. One can thus replace the defective equipment prior to catastrophic failure, thereby enhancing safety to the mine and personnel working in it.

Most of the tests described here are carried out periodically on an unloaded system, with each piece of electrical equipment being tested individually. It was felt that the unloaded tests would be preferable to a continuous monitoring of the system because the loaded condition of the system could mask the minute changes occurring in various parameters due to insulation aging.

The tests that were assembled and will be reviewed in detail are--

1. Insulation resistance measurement.
2. Capacitance and dissipation factor measurement.
3. Harmonic analysis.
4. Power factor versus voltage.
5. Infrared detection.
6. High-voltage direct current (dc) testing.

---

[1] Underlined numbers in parentheses refer to items in the list of references at the end of this paper.

The field research plan was to conduct a series of inmine tests to evaluate the ability of the individual tests to detect insulation problems before they developed into full-scale short circuits.

Three major problems were uncovered that made the straightforward program, as outlined above, impossible. The first problem had to do with the portability of equipment such as high-voltage power supplies, high-current sources, spectrum analyzers, insulation power factor meters, etc. A large investment would be needed to produce miniature, lightweight test equipment for fieldwork before the effectiveness of the tests, that the equipment was to perform, were evaluated.

In addition to the above problems with moving equipment into and out of mines, there was the problem of regular access to the mines. All of the tests under consideration are designed to be performed on unloaded power systems or systems with a dummy load connected. Thus, the times that the tests could be run were largely during maintenance shifts, weekends, etc. These access problems pointed out that any researcher who is not affiliated with a coal company would have difficulty in performing the periodic tests on a regular basis. The two problems outlined above (portability of equipment and regular access to coal mines for periodic testing) were attacked by starting a series of accelerated life tests on cables, motors, and transformers.

The third problem encountered was related to apparent inconsistencies in the data that were being collected. Some of the values that should have been increasing or decreasing monotonically with aging or time were oscillatory. In fact, it was possible to relate these changes to existing atmospheric conditions without the benefit of statistical analysis. With this in mind, it was decided that a method was needed to compensate for environmental changes. Thus, a series of tests were performed in an environmental chamber to determine the relationship between the temperature and relative humidity and the insulation parameters being measured in the various tests.

DESCRIPTION OF TESTS AND TEST EQUIPMENT

Insulation Resistance Measurement

One of the most common tests for insulation is to measure the dc resistance with a megger. There are three common test methods one can use to measure insulation resistance (3).

1. Short-time or spot readings.

2. Time-resistance.

3. Step voltage or multivoltage.

Short-Time or Spot Reading Test

In this test the megger is operated for a short specified time period (60 sec usually is recommended). By taking readings periodically and

recording them, any persistent downward trend is usually fair warning of trouble ahead, even though the readings may be higher than the suggested minimum safe values.

Time-Resistance Method

In this test, successive readings at specific times are taken. This test is based on the absorption effect of good insulation compared with contaminated insulation. It is important to notice that a continual increase in resistance is an indication of good insulation. This test is independent of equipment size.

Step-Voltage Method

In this test, two or more voltages in steps are applied, for example, 100, 250, 500, and 1,000 vdc. A large reduction of insulation resistance at the higher voltages is an indication of an insulation weakness.

Analysis of Insulation Resistance Data

After all the above tests were carried out on different samples of insulation, it was found out that the step-voltage method was the most effective in determining insulation weakness.

Results for a defective dc machine are shown in table 1. As can be seen from table 1, as the applied voltage is increased the insulation resistance decreases appreciably. For example, the insulation resistance of the armature windings to frame is 70 Mohm at 100 v and it is only 40 Mohm at 1,000 volts, a drop of almost 43 pct. Insulation resistance of shunt field windings to armature windings is 200 Mohm at 100 v and it is 120 Mohm at 1,000 v, a drop of 40 pct. This is an indication of insulation weakness. This insulation weakness could also be noted in the other types of tests, which were carried out on the windings of this machine.

TABLE 1. - Insulation resistance measurements on the windings of an old dc machine

Applied voltage, v	Insulation resistance, Mohm				
	A to G	F to G	S to G	F to A	F to S
100	70	100	0	200	150
250	50	90	0	140	90
500	43	85	0	130	85
1,000	40	84	0	120	84

NOTE.--A = armature winding.
F = shunt field winding.
S = series field winding.
G = ground.

It is clear that this dc machine has a short from the series field to the frame. This is not the type of problem that the tests are designed to detect.

Hopefully, the periodic tests will detect problems before they develop into complete short circuits.

A large volume of data on insulation resistance were gathered on other pieces of equipment. All of these devices appear to be sound, with typical values of cables being in the neighborhood of 100 Mohm and above. Minimum values for circuit breakers appear to be about 20 Mohm.

Based on a large volume of data, in the step voltage test, a drop of 30 pct or more of insulation resistance at higher voltage is an indication of insulation weakness.

As will be shown later, the insulation readings should be corrected to a base temperature such as 20° C using temperature correction factors for various kinds of insulation.

Capacitance and Dissipation Factor

When an ac voltage is impressed across sound insulation, the current will very nearly lead the voltage by 90°. Thus, the power factor will be very low and nearly equal to zero.

The dissipation factor is defined as the cotangent of the power angle ($= \text{Cot } \theta = \frac{\text{Cos } \theta}{\text{Sin } \theta} \simeq \text{Cos } \theta$ for θ near 90°). As insulation deteriorates because of aging or excessive mechanical of electrical stresses, large leakage currents may develop that will tend to increase the dissipation factor of the insulating systems.

A capacitance and dissipation factor bridge manufactured by the Biddle Co. has been used to measure the capacitance and dissipation factor of electrical insulating materials. This bridge puts out a voltage of 32 v at 100 Hz across the sample under test. While the main advantage of the bridge is its lightweight and resulting portability, the disadvantage is that it does not allow measurements at variable voltage or frequency.

Analysis of Capacitance and Dissipation Factor Data

The capacitance and dissipation factor were measured for a variety of equipment. Table 2 shows a shorted winding (series field to frame) as well as apparently sound insulation between various windings and the frame is an old dc machine. It should be noted that not only was one winding shorted to frame but also, all of the dissipation factors were significantly higher than in sound machines.

TABLE 2. - Capacitance and dissipation factor measurement of old dc machine windings

Connection	Capacitance, pf	Dissipation factor, pct	Calculated power factor, pct
A to G.....	2,243.5	21.65	21.16
F to G.....	1,050.8	19.50	19.14
S to G.....	Short	Short	Short
A to F.....	1,055.6	19.39	19.03

NOTE.--A = armature winding; F = shunt field winding; S = series field; G = ground.

Harmonic Analysis

When insulation deteriorates, a small initial current flows that is rich in harmonics because of electrical discharge across voids (corona and tiny arcs). This causes chemical changes to take place in the insulating material, producing substances which have largely nonlinear resistance. These nonlinearities produce harmonics. A similar process occurs when a liquid, such as insulating oil of a transformer, breaks down.

This suggests a new method for predicting electrical insulation failure in power systems, since deterioration of the insulation can be detected by the presence of audio frequency harmonics in the charging current waveform. The waveform can be analyzed by using a spectrum analyzer.

A spectrum analyzer is a swept receiver that provides a CRT display of signal amplitude versus frequency. It shows how energy is distributed as a function of frequency, displaying the Fourier components of a given waveform.

The test set up for the spectrum analysis test is given in figure 1.

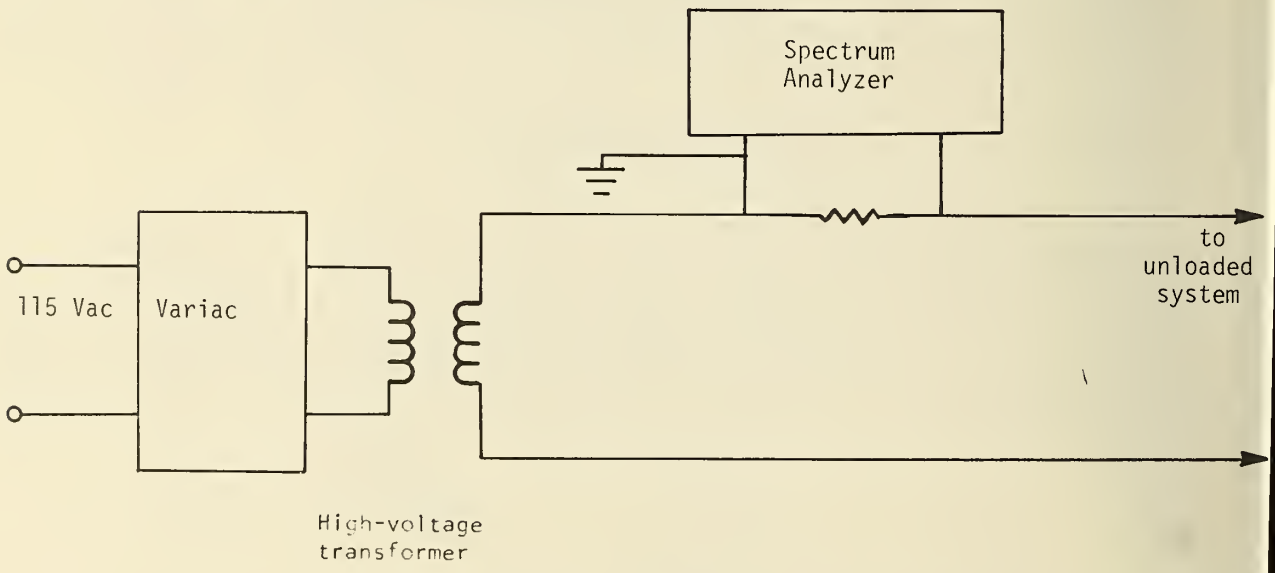

FIGURE 1. - Schematic diagram for harmonic tests.

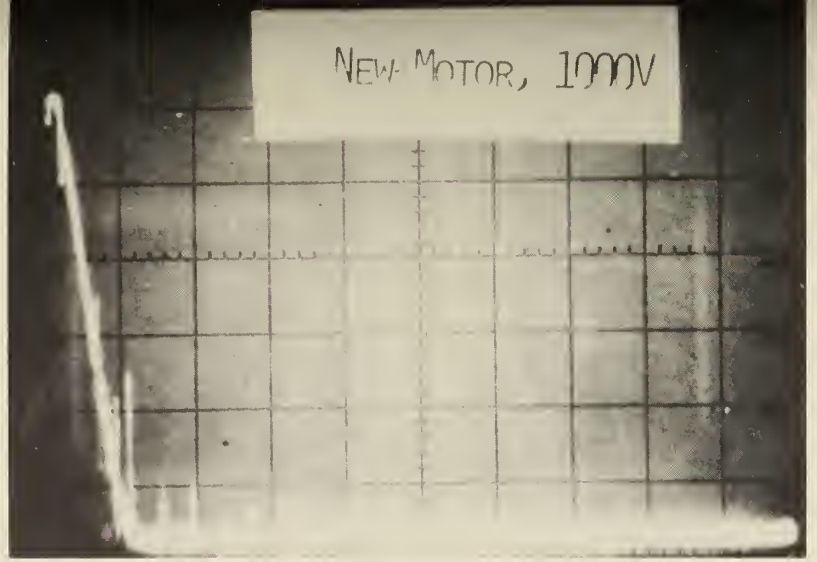

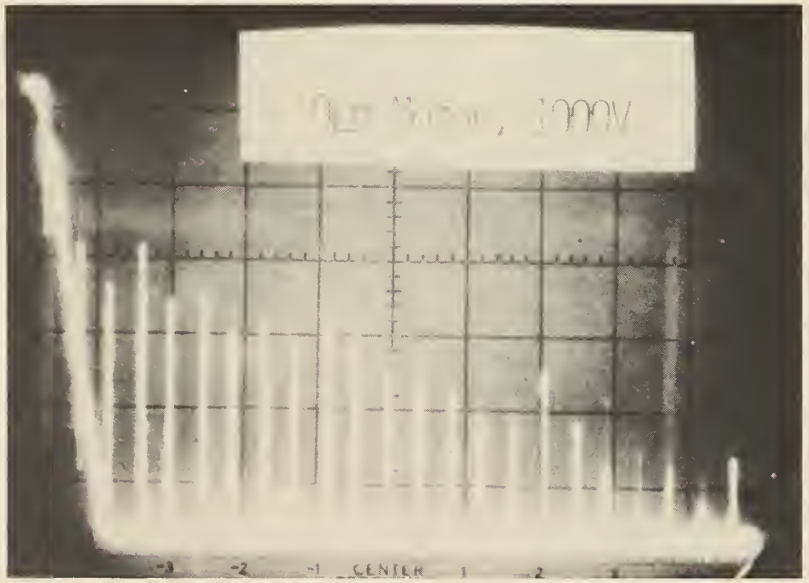

FIGURE 2. - Spectrum analyzer displays for different kinds of motors.

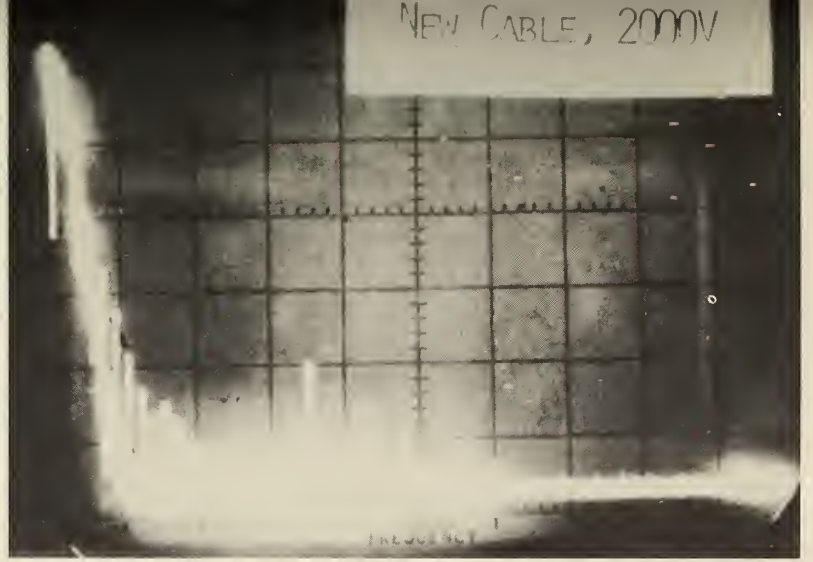

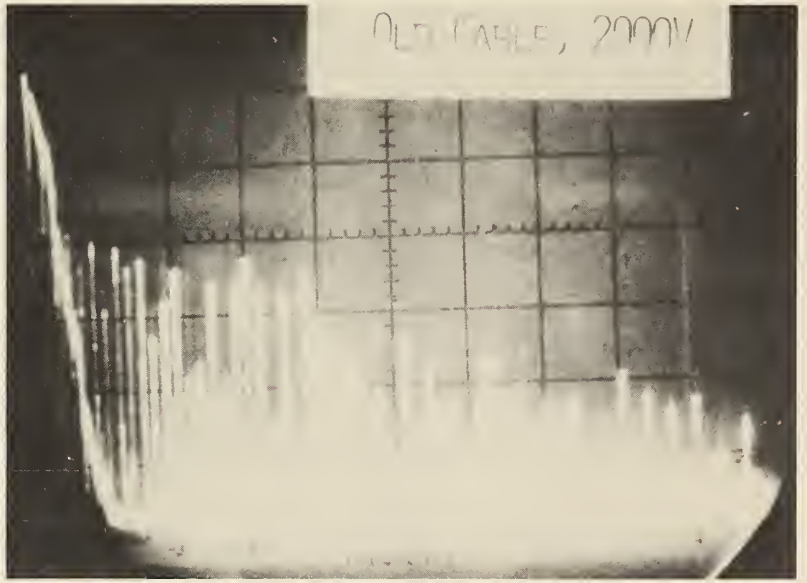

FIGURE 3. - Spectrum analyzer displays for different kinds of cables.

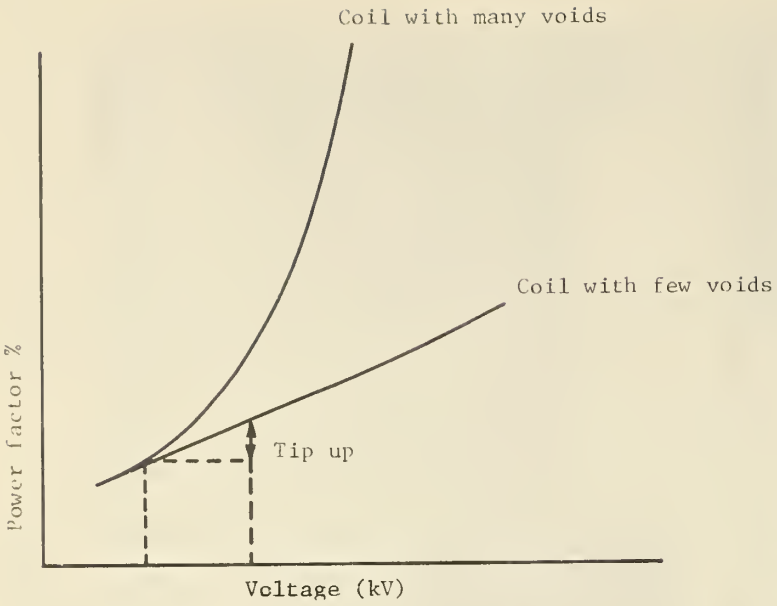

FIGURE 4. - Curves showing tip up of power factor versus voltage.

Trend With Aging

Figures 2 and 3 give the spectrum analysis display for various pieces of equipment. The tests for the motors were made at 1,000 v, while for the cables the test voltage was 2,000 v. The frequency range was 0 to 100 kHZ. As one can see from the displays, in the older insulation there is a higher content of harmonics present. For the older cable and motor components, frequencies up to 100 kHz were present; for the new motor and cable, the highest frequency present was around 30 kHz and 50 kHz, respectively.

Power Factor Versus Voltage

A perfect insulator will have a power factor (or dissipation factor) versus voltage curve that is a straight line. Voids inside the structure contain entrapped air that tends to ionize as the voltage per mil thickness approaches the breakdown point. This type of ionization inside the structure causes an extra loss which makes the dielectric loss higher than the square of the applied voltage (as in the linear case) so that the charging current appears to depart from Ohm's Law. The power factor versus voltage curve, therefore, rises with increasing voltage in the form of a parabola. As the quantity of ionized voids increases, power factor will rise, and this provides a measure of the soundness of the internal insulation. The rise in the curve has been termed "tip up" (4). Figure 4 shows a typical power factor versus voltage curve showing a tip up.

It is difficult to measure power factors of insulation systems using the conventional method of measuring power, current, and voltage because the power levels are very low. Thus, alternative methods had to be designed to measure power factors of insulation systems. One such method is described below.

Electronic Power Factor Measurement

An electronic circuit has been designed to measure power factor on an unloaded system as a function of applied voltage. The circuit diagram is given in figure 5. The power factor circuit basically measures power factor angle by detecting the zero crossing of the current and voltage, and by proper wave shaping, producing a pulse width equal to the time between zero crossings. For a sound insulation the power factor angle is around 88° to 89°. In order

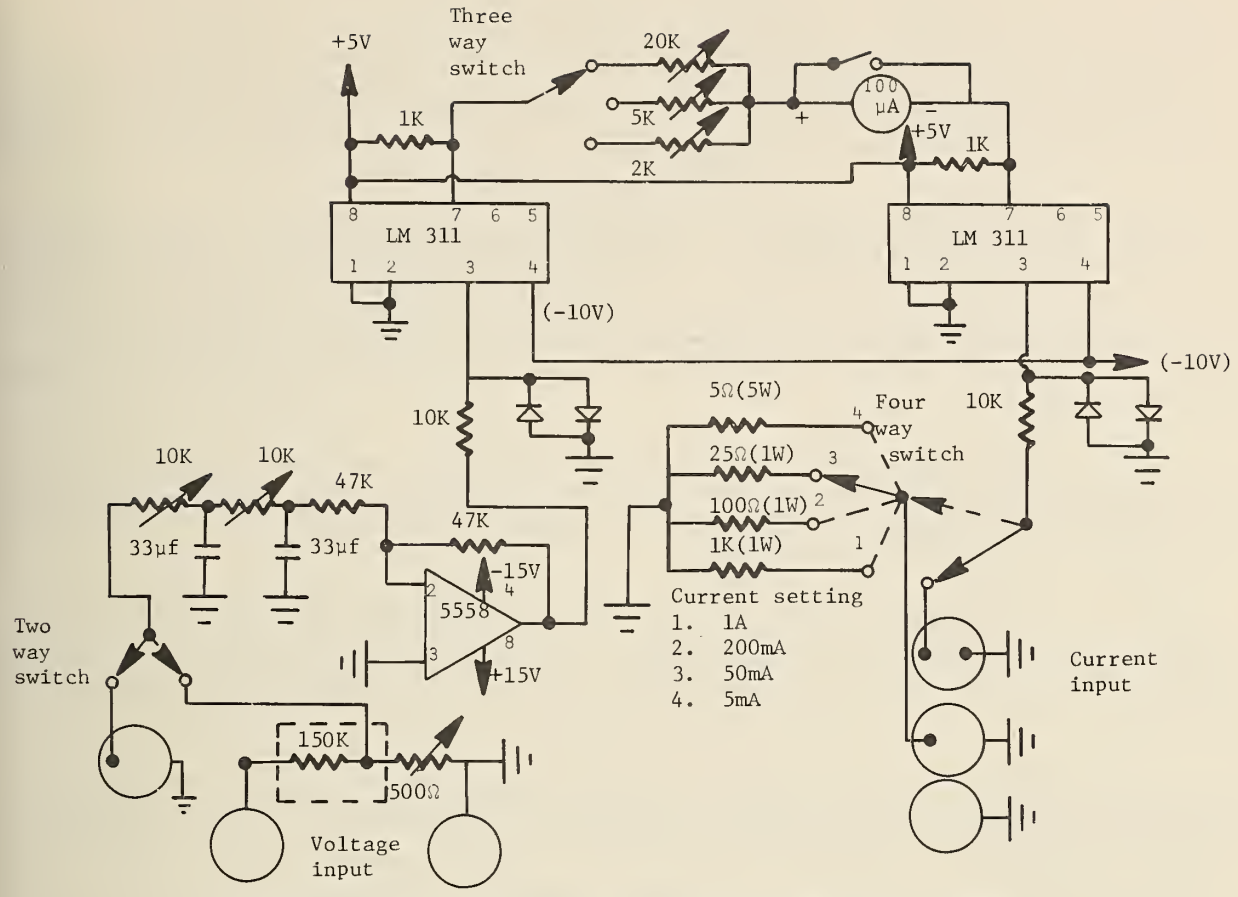

FIGURE 5. - Circuit diagram for electronic power factor meter.

to make the circuit more sensitive, the input voltage is shifted by 90° so that the circuit produces very narrow (in width) pulses. The pulses are rectified by the diode circuit and fed to a dc microammeter. The dc microammeter reads the average value of current which is proportional to the width and hence to the phase angle, as shown below:

$$I_{dc} = \frac{\frac{V_{max}}{R} t}{T}, \qquad (1)$$

where I_{dc} = the ammeter reading in amperes,

R = the resistance in series with the dc microammeter in ohms,

V_{max} = the peak value of the pulse and is constant for the particular circuit in volts,

t = the width of pulses in seconds,

and T = the period of the pulses and in this case, T = 1/60 sec; thus,

$$t = \frac{I_{dc}TR}{V_{max}}, \quad \theta = \frac{t\ 360}{T}, \text{ and power factor, p. f.} = \cos\theta \qquad (2)$$

Knowing I_{dc}, V_{max}, and T, the scale can be calibrated in terms of power factor.

Infrared Detection

All bodies radiate energy in the electromagnetic spectrum unless the body is at absolute zero temperature. A very small part of this spectrum is seen as visible light which is a mixture of energy at different wavelengths in the very narrow visible band. On either side of this band of visible radiation is the ultraviolet extending on from the blue and the infrared extending on from the red side.

Any hot body emits energy both in the visible as well as infrared regions. The greater the temperature of the body, the greater is the energy radiated in the visible regions of the spectrum. At lower temperatures most of the energy is radiated in the infrared region.

For all practical purposes one can assume that a body radiates infrared energy in proportion to its temperature. If one can measure the energy radiated, the temperature can be determined by suitable calibration which can relate the two.

The objective of this test is to detect abnormal hot spots in electrical equipment by measuring the amount of infrared energy radiated with the help of a suitable infrared scanner.

The hot spots may originate in different equipment because of different reasons. In case of a cable it may be because of broken strands of conductor or excessive leakage in insulation; in a rotating machine, it may be due to defective coils; or in a transformer, it may be due to excessive leakage flux. In any case, hot spots can cause failure if allowed to persist.

Temperature Rise in a Cable Due to Change in Series Resistance

The change in series resistance could be due to broken strands. The calculations below show that the hot spot formed in the cable when carrying load current could be significant enough to be detected easily by any sensitive infrared detector. Some of the data in these calculations have been assumed but are well within the acceptable range. Assume a 4/0 cable, with a normal series resistance of 6.3×10^{-5} ohm/ft for each conductor and a full load current of 200 amp. Using the basic principles of heat transfer, for an ambient temperature of 20° C the temperature rise along the cable is calculated as 33.6° C. For a local increase in series resistance to 1.5 times its original value, similar analysis predicts a local temperature rise of 39.3° C. Thus the hot spot has a temperature of 5.7° C above the remainder of the cable, which can be detected easily.

Description of Test Setup

To carry out this test, a sensitive infrared detector (Model PRT 11 manufactured by Barnes Engineering) was procured. The device has temperature scales of 200° C absolute and ±10° C differential. The temperature sensitivity is 0.4° C, which is sufficient for the range of measurements needed.

This test was carried out on actual mine systems as well as old cables in the laboratory. Difficulties encountered in carrying out this test on loaded mine power systems are enumerated below.

1. Some of the cables are spooled for some portion of their lengths. Also, in many places cables are bunched together, making testing of individual cables very difficult.

2. The most loaded portions of the systems are near the face of the mine. But since there is a lot of activity in that region (to and from movement of shuttle cars, etc.), there is hardly any time available for making measurements.

Although nothing concrete can be done about the first problem, ways were designed to circumvent the second. The most feasible was to connect a dummy load to the system. Initially it was thought to use a resistive or inductive load, but the idea was rejected because of the excessive size of the load. A simpler procedure was designed which is shown in figure 6.

One of the ends of the cable is short circuited. A low voltage is applied at the other end to circulate the full load current. It is necessary to use a three-phase auto transformer and a wye-delta transformer to regulate the current. Since the transformer secondary voltage has to be just enough to supply the full-load voltage drop in the cable, the size is tremendously reduced. Calculations were performed to determine the voltage and current ratings of the transformers for the sizes of cable found in a mine system assuming that the maximum length of cable to be tested was 500 ft and available supply voltage was 480 v, which is the case in most mine systems.

The calculations revealed that the smallest commonly found cable size (AWG 1/0) determined that the maximum transformer secondary voltage should be 12 v. Similarly, the largest size cable commonly found (500 MCM) set the maximum secondary current rating at 290 amp. Then the ratings of the three single-phase transformers used were calculated at 2 kva/phase. In addition, the calculated voltage and current set the rating of the three-phase auto-transformer as 0 to 480 v at 10 amp.

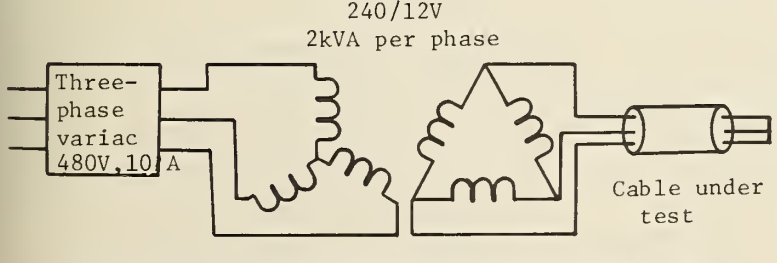

FIGURE 6. - High-current circuit for infrared test.

High-Voltage DC Testing

It may be rather strange to use dc for evaluating the insulation of ac systems, but dc is preferable to alternating current (ac) for the following reasons (1):

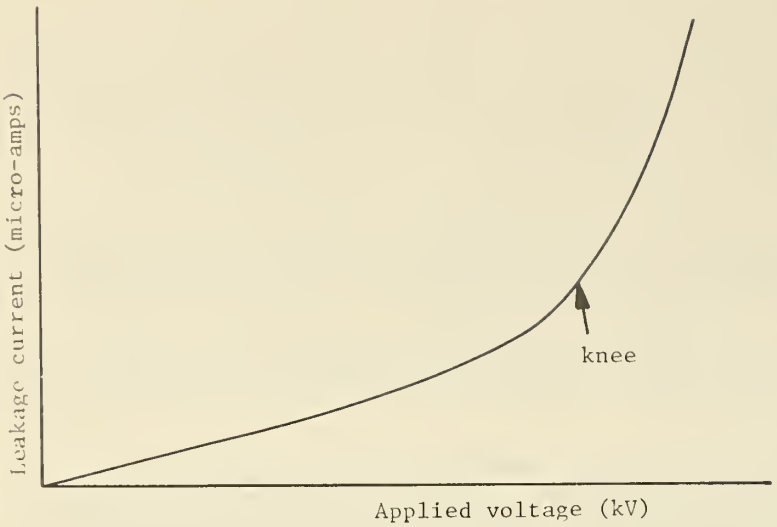

FIGURE 7. - Typical leakage current characteristics of insulation in a degraded state.

1. Elimination of capacitive charging currents.

2. Small size of dc test sets and their resulting portability.

3. Experience has shown that dc is less damaging to the insulation than ac.

The different test procedures are given below.

Leakage Current Characteristics (8)

The steady-state leakage current is measured as a function of voltage applied between conductors and ground.

For practical reasons, the applied voltage is increased in finite steps during the leakage current test. Consequently, with each increase of voltage some time must be allowed to establish a steady-state current. A typical value of voltage step is 500 v to 1,000 v and of time is 1 to 2 min.

The curve I = f (V) (fig. 7) is used in different ways for predicting the breakdown voltages. In all cases where polar materials, such as water and certain types of contaminants, are present or a deteriorated insulation is being tested, the leakage current characteristics will have more or less a pronounced knee after which the current increases more rapidly with increase in voltage. This led to the hope that an asymptote may be found to indicate the value of voltage at which the current would increase to infinity. This voltage would then be looked upon as the breakdown level.

It was found that the leakage current showed a marked dependency on the humidity and temperature at the test site. Thus, factors had to be developed to correct the measured values of the leakage current to some base value of temperature and humidity. This is discussed in more detail later in this paper.

Absorption Current Characteristics

There are three components of current resulting from the application of direct voltage to dielectric. They are as follows:

1. Geometric capacitance current.
2. Absorption current.
3. Conduction current.

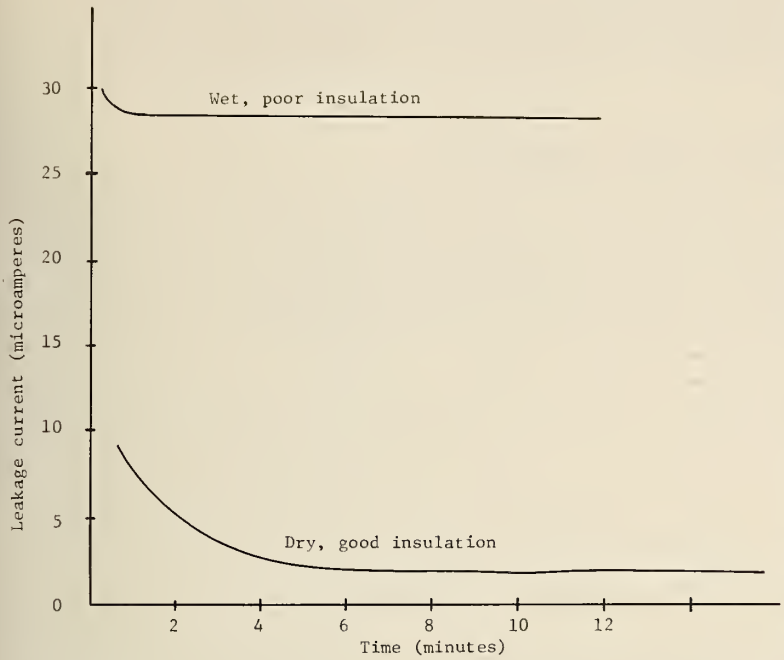

FIGURE 8. - Typical absorption current characteristics of insulation systems.

The capacitance and the absorption currents are time dependent, the conduction current is relatively constant. Although the capacitance current has a very short time constant (a few microseconds depending upon capacitance), the absorption current has a relatively large time constant.

In this test a constant dc voltage (say 1,000 v) is applied to the insulation and the 1-min leakage current recorded. The current is recorded again after 10 min and the ratio $\frac{I_1}{I_{10}}$ is calculated. This is known as the polarization index. Here I_1 is current 1-min after the application of voltage and I_{10} is the steady current after 10 min. For a good insulation the polarization index should be greater than 1. A lower polarization index indicates a contaminated insulation and could contribute to future breakdown. Typical absorption current characteristics are shown in figure 8.

LABORATORY AND FIELD TESTING PROGRAM

Accelerated Life Testing

All the experiments described above must be performed on insulation systems to verify their ability to detect the incipient failure of the insulation. This is being done in an actual mine environment, but there are some problems associated with this method of verification. The two most important of these are--

1. The verification time for each test must be of the same relative time duration as the life expectancy of insulation (many months to several years).

2. The experiment does not have good control of variables.

A good example of what is meant by the second item is an experience with infrared tests. One set of measurements made on a trailing cable were very interesting because there were several hot spots on the cable, usually near splices, that seemed to be good candidates for incipient faults. However, before the next set of measurements were made, the cable was mechanically damaged and taken out of service. Thus, the first good chance to predict a fault was lost.

The proposed way to overcome both problems listed above is through a set of experiments that will be referred to as accelerated life tests. These are well known to engineers and scientists interested in properties of materials and insulation breakdown.

Design of the Experiment

The tests would ideally be performed on full-scale samples of mine electrical equipment, such as motors rated 10 to 200 hp, cables several hundred feet long, etc. The actual tests were performed on fractional horsepower motors, cable samples about 10 ft long, and 1/2-kva transformers. In fact, the actual tests were performed on six each of the following devices:

1. Transformers rated 0.5 kva, 480/240 to 240/120 v, single-phase 60 Hz, with class B insulation.

2. Motors rated 1/2 hp, 115 v, 60 Hz, split-phase 8.4 amp, with class A insulation.

3. Cables of size 2 (AWG), rated 2,000 v, 3 conductor, type G-GC, 90° C insulation.

It was decided to use these items basically to reduce the cost of the experiments and allow them to be performed within the West Virginia University (WVU) laboratory current capacity. The aging was done by elevating the temperature of the devices via high circulating currents. In each case the amount of current was adjusted to provide a stable device temperature that would shorten the insulation life to approximately 500 hr. Thus, at the end of about 40 to 50 hr of heat treatment a series of tests could be made and data recorded. About 10 to 12 such sets of test data plus a set of initial data before any aging had been done were gathered.

Based on published data on insulation life at various temperatures, the calculated temperatures needed to decrease the insulation life to 500 hr are 200° C for the transformers, 150° C for the motors, and 150° C for the cable samples. These were obtained by using combinations of variable autotransformers and fixed ratio transformers from the 230-v laboratory supply to circulate currents which produce the desired temperatures based on heat transfer and radiation.

Conclusions Related to Accelerated Life Testing

The test data were obtained under different environmental conditions. Thus, they had to be corrected to a base temperature and humidity.

It was found that the dissipation factor test best showed the aging effect on the insulation. Figure 9 shows the typical dissipation factor versus aging curve. The dashed curve shows the actual data obtained, while the solid curve shows the data after making corrections for temperature and humidity.

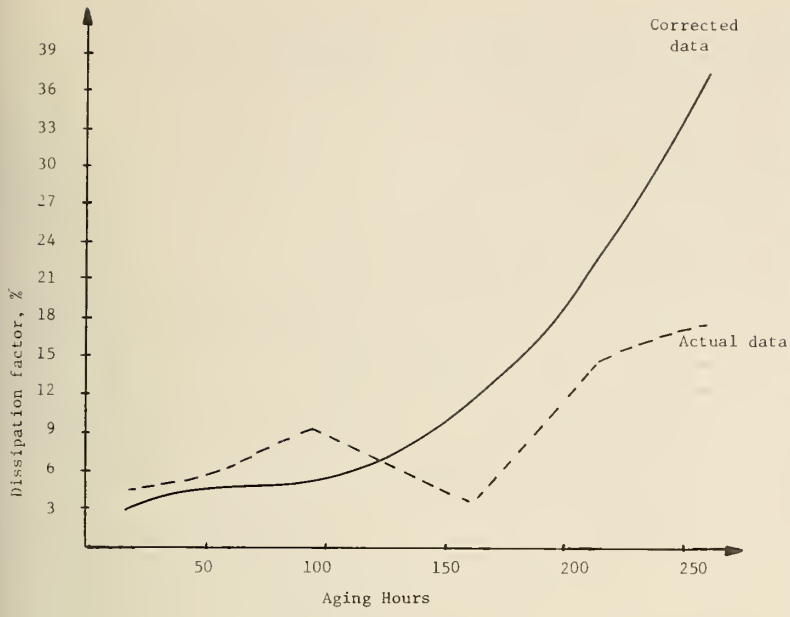

FIGURE 9. - Dissipation factor versus aging hours for a transformer.

It was also found that the high-voltage tests such as high-voltage direct current (HVDC) and high-voltage alternating current (HVAC) are a serious factor in shortening the life of the insulation. In fact one sample of each device was held out of all high potential tests. These devices showed longer life than the others, which were subjected to high-voltage tests.

Environmental Tests

During some of the previous laboratory tests it was found that some test parameters showed marked dependence on the environmental conditions, for example, humidity and temperature. This was quite undesirable since these changes in the parameters could mask the changes due to actual insulation deterioration. An attempt was made to determine the exact relationship between the various measured parameters and temperature and humidity by laboratory testing. Little success was obtained because one didn't have any control over the environment within the laboratory and any changes occurring were due to natural causes.

Large-scale testing was carried out using the U.S. Bureau of Mines environmental chamber facilities at Bruceton, Pa. Subsequently, some more tests were performed in the environmental chamber borrowed from the Bureau. Due to the limitation of testing space and ease of transportation, only small lengths of cable, small transformers and motors were tested.

Description of Equipment Tested

The following is a description of various equipments which were tested:

1. Cable 1, 3-phase, type-G, flat, size AWG 1, 12 ft long.

2. Cable 2, 3-phase, type-G, flat, AWG w, 22 ft long.

3. Cable 3, 3-phase, type G-GC, round, AWG 2/0, 24 ft long.

4. Cable 4, 3-phase, type-G, flat, AWG 2, 20 ft long. (This cable had one splice in it).

5. Transformer 1, 460 v/230-115, 1-ϕ, 1-kva.

6. Transformer 2, 230 v/115 v, 1-ϕ, 1.5-kva.

7. Motor, GE dc motor, 1/2 hp, 115 v, compound-wound.

Tests Carried Out

The following tests were carried out:

1. Insulation resistance measurements using a megger.

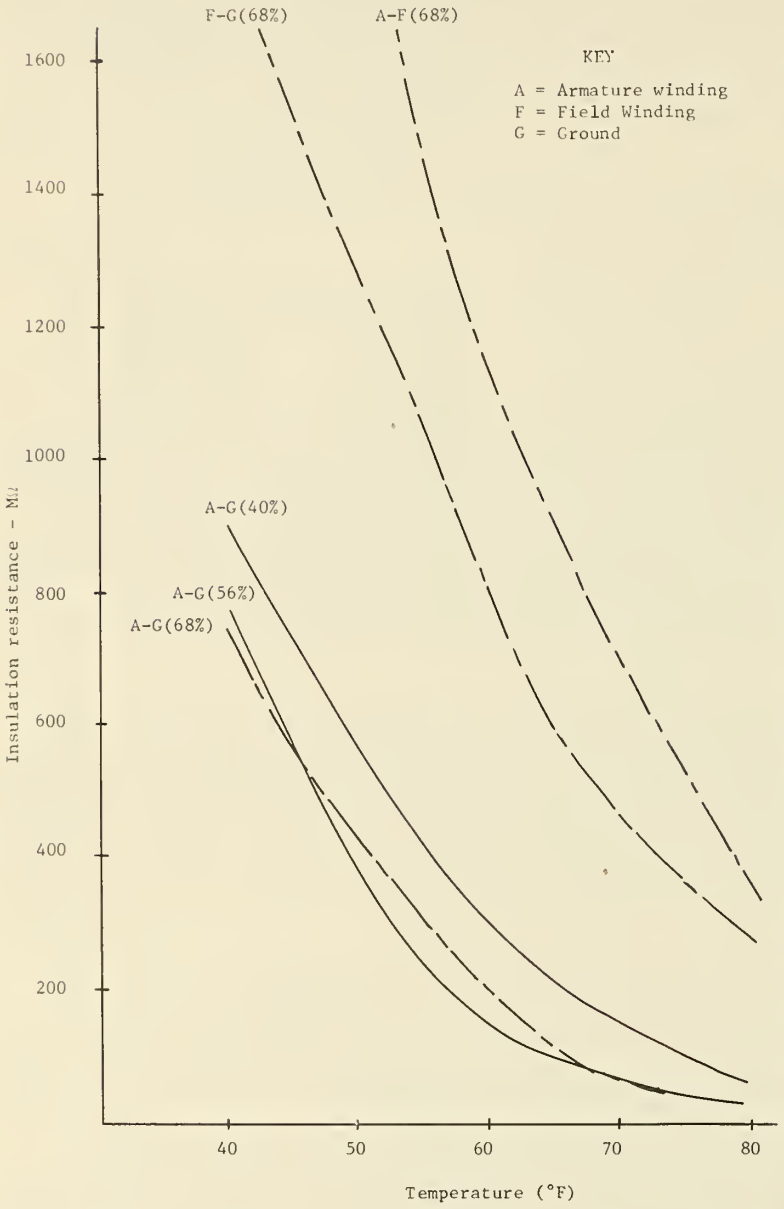

FIGURE 10. - Insulation resistance of motor versus temperature. Tests were made at 1,000 v (numbers in parentheses refer to relative humidity values).

2. Capacitance and dissipation factor measurements.

3. High-voltage dc tests.

4. Spectrum analysis.

Test Results

The volume of the data gathered was so huge that it will not be possible to list all the results here. The statistical analysis system (SAS) software package which is available in West Virgina University's 360/370 computer system was used to analyze the data. To express the relationship in a two-dimensional curve, the analyses were performed in two ways, one was done with constant humidity and the other with constant temperature. Three models--linear, polynominal, and exponential--were tried. Some of the typical results obtained are as follows:

Insulation Resistance Versus Temperature for Motors

The plot of insulation resistance versus temperature for different connections is shown in figure 10. As can clearly be seen, the insulation resistance decreases with an increase in temperature. At higher values of

temperature the change in resistance becomes smaller. This suggested the use of an exponential model to express the relationship. The model tried was

$$R_t = R_o e^{-\alpha t},$$

where R_t is the insulation resistance at temperature t (in degrees Fahrenheit),

R_o is the resistance at temperature 0° F,

and α is a coefficient to be determined by regression analysis.

The results of the statistical analysis are shown in table 3. Excellent correlation was obtained with α values ranging from 0.048 to 0.077.

TABLE 3. - Results of statistical analysis of insulation resistance data for motors and transformers

Sample	Connection	Humidity, pct	Relationship, Mohm	Correlation coefficient, pct
Motor.....	A-G..	40	$R_t = 14{,}367.84\ e^{-0.0674T}$	99.5
		56	$R_t = 16{,}627.25\ e^{-0.0773T}$	99.9
		68	$R_t = 16{,}313.85\ e^{-0.07537T}$	99.5
Do.....	F-G..	68	$R_t = 13{,}095\ e^{-0.0477T}$	99.5
Do.....	A-F..	68	$R_t = 38{,}816\ e^{-0.0586T}$	99.9
Transformer 1...	X-G..	68	$R_t = 9{,}283\ e^{-0.041T}$	98
	H-G..	68	$R_t = 8{,}619\ e^{-0.039T}$	99
	X-H..	68	$R_t = 13{,}907\ e^{-0.037T}$	99.99
Transformer 2...	X-G..	68	$R_t = 21{,}929\ e^{-0.049T}$	99
	X-H..	68	$R_t = 22{,}624\ e^{-0.0460T}$	99

NOTE.--A = armature winding.
F = field winding.
G = ground.
X = low-voltage winding.
H = high-voltage winding.

Dissipation Factor Versus Temperature for Cables

The effect of temperature on dissipation factor is shown in figure 11. As can be seen from the figure, cables 1, 2, and 3 show similar characteristics while cable 4 shows somewhat different behavior. This could possibly be attributed to the presence of a splice in the cable. Two different models were tested for representing the effect of temperature:

Linear model $D_t = D_o + \alpha t$

and Nonlinear model $D_t = D_o + \beta t + \gamma t^2$,

where D_t is the dissipation factor at temperature t (in degrees Fahrenheit),

D_o is the dissipation factor at temperature 0° F,

and α, β and γ are the coefficients.

Although the nonlinear model showed an excellent correlation (the values being around 99 pct), the coefficients β and γ showed no consistency. β ranged from -0.052 to +0.033, and γ, from -0.0001 to +0.0009. Thus, this model was rejected.

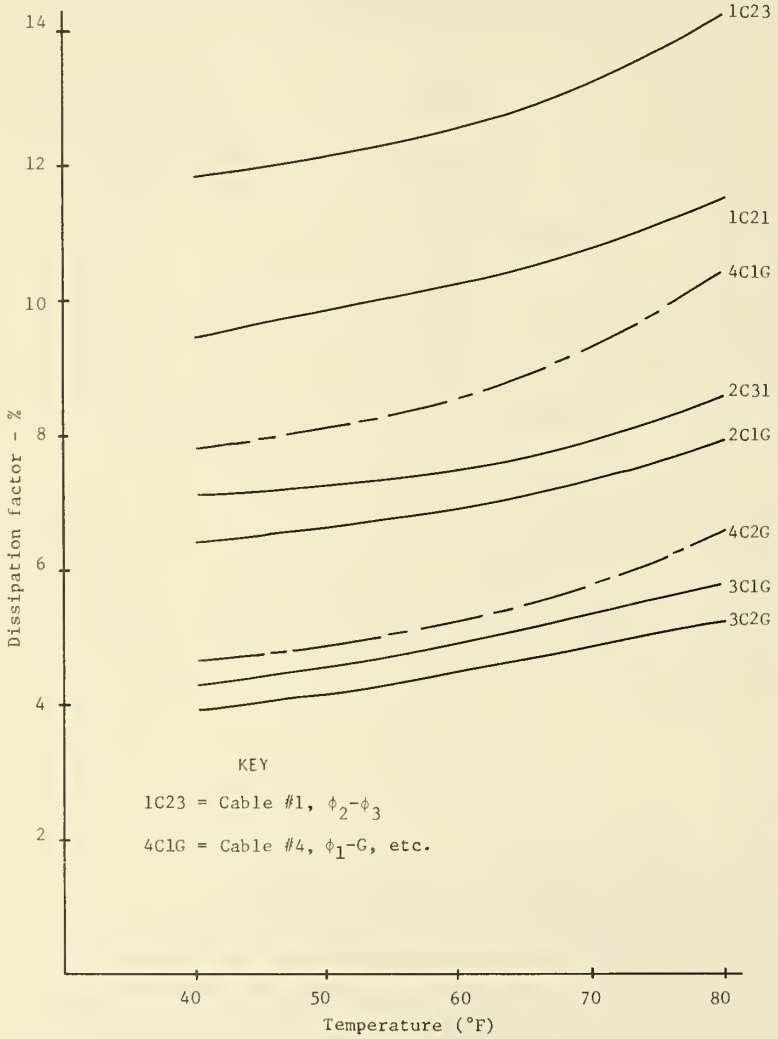

FIGURE 11. - Plot of dissipation factor of cables versus temperature at 40 pct relative humidity.

On the other hand, the linear model showed lesser correlation (around 97 pct), but the values of α showed better consistency. The values varied between 0.03 and 0.06, with a most probable value around 0.035. For cable 4 the value was much higher (around 0.065).

Conclusions Related to Environmental Tests

Based on a purely statistical analysis, factors have been developed to correct the various measured insulation parameters for different kinds of insulation to fixed base values of temperature and humidity. This will allow better comparison of data to evaluate the aging of insulation. However, the results (excepting cables) are based on testing of small-scale models and their application to actual size equipment should be verified.

Field Tests

There are several pieces of equipment that

have proven to be useful in laboratory testing. However, the final goal of this research is to establish these test procedures as a useful tool in detecting incipient faults in coal mine electrical systems by a periodic field testing program. This program has not progressed as expected owing to several reasons, the most important being inaccessibility of coal mines at regular intervals.

The field testing program was started in two mines. It had to be discontinued at one because of a policy decision made by the mine superintendent. Some useful results were obtained from test data gathered at the other mine, but again the tests had to be discontinued owing to the coal strike and related problems.

Analysis of Test Data

The results presented here were obtained in a series of field tests over a 6-month period. The approximate time period between each series of tests was 6 to 8 weeks.

Figure 12 represents the insulation resistance and figure 13 the dissipation factor data for a continuous miner cable. The cable size was 4/0 and length was approximately 500 ft. After the third series of tests, the insulation resistance dropped off considerably, and the dissipation factor showed a reverse trend. The general conclusion reached as the result of the measurements was that the cable was in very bad shape. All the insulation resistance values were well below the minimum required. In some cases the dissipation factors were so high that they were beyond the range of the meter. The prediction was made that the cable would fail shortly.

It was learned later that 2 weeks after this series of tests, this particular cable was taken out of service because of defective insulation. This is an indication that it is possible to predict cable failure by the techniques described.

Conclusions Related to Field Testing

As pointed out earlier, one of the major difficulties encountered with the field testing program was the inaccessibility of the coal mines at regular intervals. However, some other problems were encountered, which are enumerated below:

1. It was observed that most of the smaller size cables change position so often that it is very difficult to keep track of their location. In some cases, longer lengths of cables are cut into small lengths to distribute power to loads over relatively short distances. This poses a major difficulty in the field testing program since the aim was to make a series of measurements at intervals of about 8 weeks on the same piece of cable and to determine whether the changes occurring in the insulation parameters could be related to the remaining life of the insulation.

2. In order to have a chance to try out some of the more bulky test equipment, the problem of portability has to be solved.

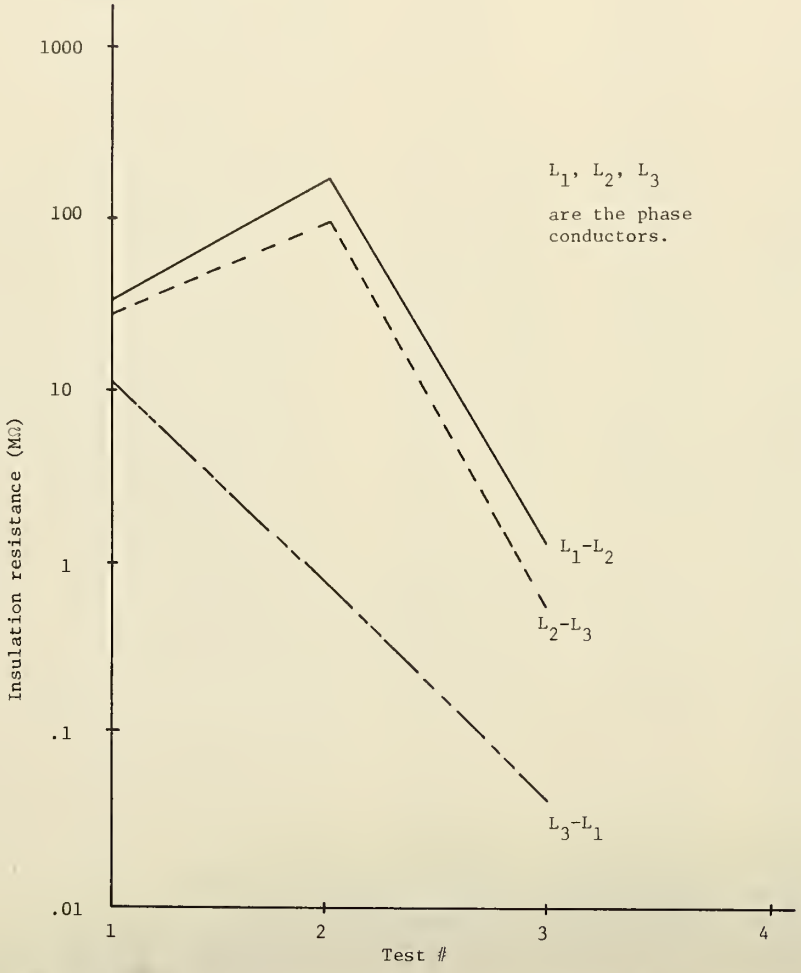

FIGURE 12. - Insulation resistance data for the bad miner cable taken out of service after third series of tests.

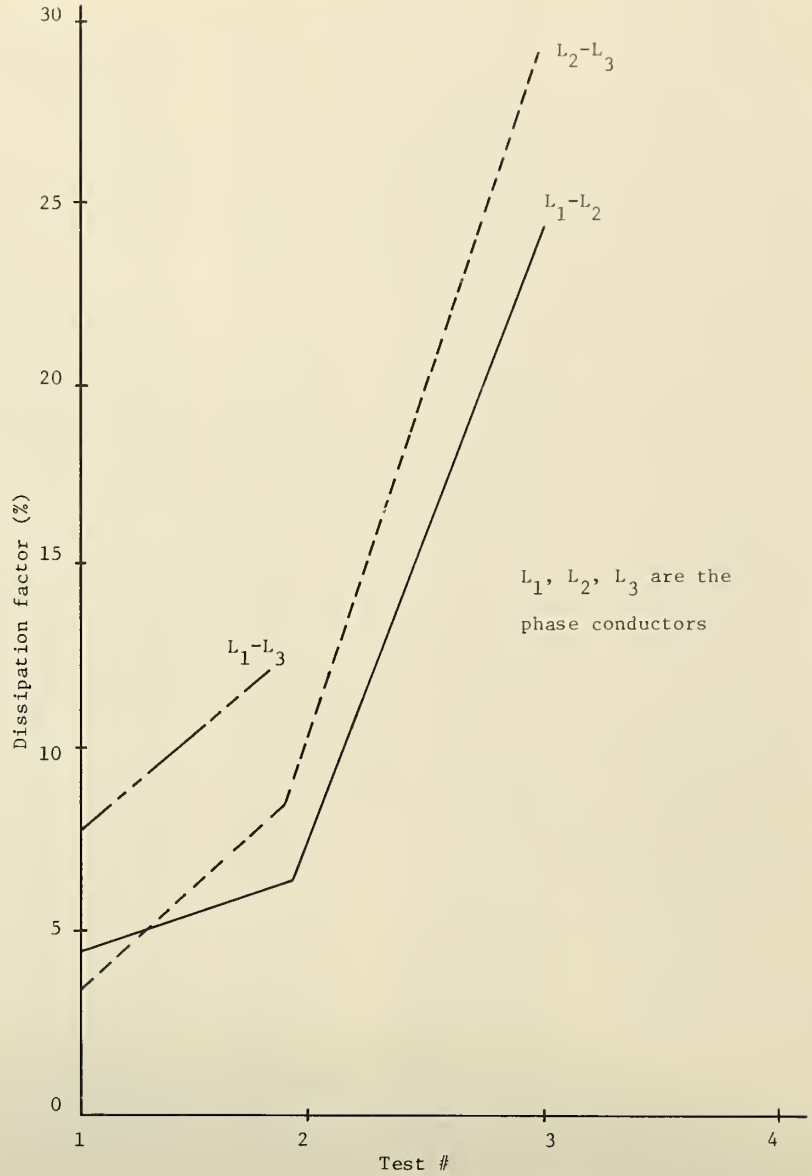

FIGURE 13. - Dissipation factor data for the bad miner cable.

3. A detailed plan of field tests has to be assembled before the beginning of each set of field tests to insure that the collected data are meaningful.

4. In order to do the exact analysis, the environmental conditions in the mines have to be recorded.

OVERALL CONCLUSIONS AND RECOMMENDATIONS

Generally speaking, this research, the periodic inspection of mine power systems, is a large and a long-term program. Although many test procedures have been identified and evaluated, more effort has to be concentrated on performing field tests in mines.

It is suggested that any further work in this area should be concentrated on the following:

1. Find the relationship between insulation behavior and environmental conditions for different insulation classes no matter what the size of the equipment.

2. Prove the results of the environmental tests are independent of the age of the equipment. In other words, prove that the variations in the insulation parameters due to the variation of environmental conditions is always the same for the same insulation class in spite of the difference of the equipment age.

3. Get the cooperation of mine operators in order to obtain the whole history of mine equipment without any unnoticed replacement by mine operators.

4. Get field data on two or more mines in order to arrive at more definite conclusions on the usefulness of various tests.

5. Collect the data on environmental conditions in mines simultaneously when the field test is being conducted.

REFERENCES

1. Bhimani, B. V., and C. M. Foust. Predicting Insulation Failures With Direct Voltages. AIEE Trans., December 1957, p. 1120.

2. Chou, Y. C. Periodic Inspection of Mine Power Systems. M.S. Thesis, W. Va. Univ., Morgantown, W. Va., 1977, 79 pp.

3. Crudts, E. B. Insulation Testing by DC Method. James G. Biddle Co., Plymouth Meeting, Pa., Tech. Pub. 22T1, 1971.

4. Findly, D. A., R. G. Brearly, and C. C. Louttit. Evaluation of the Internal Insulation of Generator Coils Based on Power-Factor Measurements. AIEE Trans., June 1959, p. 268.

5. Hassan, M. M. Periodic Testing of Mine Power Systems To Detect Incipient Faults. M.S. Thesis, W. Va. Univ., Morgantown, W. Va., 1976, 114 pp.

6. Hassan, M. M., H. Shamash, and E. K. Stanek. Periodic Testing of Mine Power Systems To Detect Incipient Faults. IEEE Conf. Proc., Ind. Appl. Soc., October 1976, p. 446.

7. Mason, W. A. Electrical Hazards in Underground Bituminous Coal Mines. MESA Inf. Rept. 1018, 1975, 5 pp.

8. Odok, A. M., and T. M. Soelaiman. Improved DC High Potential Testing of Insulation Systems in Low and Medium Voltage DC Equipment. AIEE Trans., September 1959, p. 186.

BATTERIES AND BATTERY-CHARGING SAFETY

by

L. A. Morley,[1] and J. A. Kiefer[2]

ABSTRACT

This paper reviews the major hazards inherent with underground coal mine battery utilization. Recommendations are made to significantly improve personnel safety in this important area, including minimum ventilation flow rates, charger station placements, battery surface leakage and faults, and safety design for mine chargers.

INTRODUCTION

General

The battery-powered vehicle has become an important part of many underground coal mine haulage schemes, and several factors are responsible for the recent increase in popularity. The trend in industry today is towards conveyor belts for coal transport and rail systems for personnel and supply movement. Mines, which employ alternating current (ac) face equipment and direct current (dc) trolley lines, can be subjected to problems such as nuisance tripping of ac circuit breakers from stray dc ground currents. These currents, which often result from poor track bonding, ineffective trolley-line insulators, or inadequate dc to ac ground-system isolation, are eliminated when batteries are used to power locomotives.

Regardless of the intermediate and main-line haulage methods, many operations have found it profitable to utilize articulated ram-dump haulers (Ramcars), tractor-trailer units, or scoops (front-end loader tractor units). When employed for face haulage, they eliminate the headaches involved with shuttle car trailing cables. In small conventional mines, the operator can be spared the cost of a loading machine and a separate machine for cleanup and supply haulage. For moderate to large production operations, the extreme mobility of the tractor-trailers and scoops has made them invaluable ancillary equipment for cleanup and supply in practically all longwall and many continuous operations.

The batteries themselves have been considerably improved. A prominent manufacturer reports a 70-pct increase in ampere-hours per cubic foot (amp-hr/ft^3) and a 39-pct increase in watt-hours per pound (whr/lb) over earlier models (1).[3] In addition, improvements in plate and grid design have increased the average service life of motive power batteries.

---

[1]Associate professor of mining engineering.
[2]Graduate assistant in mining.
Both authors are with the Pennsylvania State University, University Park, Pa.
[3]Underlined numbers in parentheses refer to items in the list of references at the end of this paper.

Statement of the Problem

Storage batteries have a relatively good underground safety record. However, the increased use of batteries has recently resulted in several fatalities and minor injuries (4). When comparing the number of these accidents against all electrical mishaps for the same period, the percentage of battery incidents is significantly high. This is indeed serious considering that battery utilization is just a small portion of underground mine electrical usage throughout the United States.

Hazards related to batteries fall into three broad categories:

1. Batteries emit hydrogen, an explosive gas, while charging;

2. batteries and battery chargers are capable of delivering a fatal electric shock; and

3. batteries are a potential fire hazard.

In addition, a number of less catastrophic hazards may be encountered, including acid burns from spilled electrolyte, pinched fingers from careless handling, and so forth.

Under the Interior Department's Bureau of Mines Grant G0155003, the Mine Electrical Research Group at Penn State University has been performing research into this vital area of mine electrical safety. This paper is basically a summary of the effort. The following paragraphs will cover the battery hazards of ventilation, surface leakage, and faults as well as battery-charging hazards. Afterwards, a design for a safe battery charger will be discussed. Recommendations to improve battery safety will be presented throughout the paper.

BACKGROUND

Lead-Acid Batteries

Two types of storage batteris have been employed in underground traction applications. The nickel-iron or Edison cell is an alkaline-type cell. The plates for this battery are constructed of nickel oxide and iron, immersed in an electrolyte of potassium hydroxide and lithium hydroxide. Edison cells were once popular in the mining industry because of their high reliability and minimum maintenance characteristics. Lead-acid batteries have replaced the Edison cell because of their high energy per unit volume and high-power capability.

The basics of lead-acid batteries is not within the scope of this paper. However, some fundamentals are necessary to emphasize certain battery and battery-charging safety aspects.

The lead-acid cell utilizes a lead-peroxide (PbO_2) positive plate and a sponge lead (Pb) negative plate. These plates are suspended in a solution of

dilute sulfuric acid (H_2SO_4). When a large portion of the PbO_2 and Pb is in the form of $PbSO_4$ and H_2O (the discharged state), the battery is in need of charge. Charging a battery consists of supplying electricity to convert $PbSO_4$ and H_2O back into PbO_2, Pb, and H_2SO_4.

The number of times a lead-acid battery can be recharged is a function of--

1. The discharge level of the battery during its working cycle,

2. the method used to charge the battery, and

3. the quality of battery maintenance.

Each of these parameters is independent of the others, and they will be considered separately.

Battery manufacturers recommend that lead-acid batteries not be discharged below 80 pct of their capacity. Because it is difficult to determine the extent of battery discharge until the battery is dead, it suffices to say that a battery should be recharged when the machine it is powering begins to show signs of sluggishness, if not before.

The rate at which charge is restored to the lead-acid battery is an important consideration in getting the maximum number of charge cycles and maximum life out of the battery.

Some of the electricity supplied to a cell being charged is used to break the water down into its constituents, hydrogen and oxygen, which is called "gassing." It is at this level that increasing quantities of current become available for electrolysis because of the higher state of charge in the cell.

A certain amount of gassing is a necessary consequence of a good charge; this explains why water must periodically be added to batteries. However, excessive gassing causes damage to the plates, excessive water consumption, and excessive hydrogen evolution. For this reason, the amount of charging current must be regulated as the battery charges. Large amounts of H_2 and O_2 released during excessive gassing cannot be detected by charger personnel. However, this condition is sometimes accompanied by amounts of H_2SO_4 released into the mine atmosphere, which is easily identified.

Chargers

Most mining batteries today are charged underground from the ac distribution or utilization system, using a transformer-rectifier combination. Silicon rectifiers are generally considered to be the industry standard. Transformers, whether single- or three-phase, generally have isolated secondaries.

There are several methods which are commonly used to control the rate of charge. Each one is designed to initiate the charge at a fairly high current and then taper the rate off as the battery charge is restored. Charge-rate control devices can be divided into two basic groups, either active or passive.

The most popular passive system uses modified constant potential or taper charging, where some value of ballast resistance is placed in series with the battery. This resistance limits initial charge current and give a relatively flat current versus time curve throughout the charging cycle. The advantage of this method is its simplicity. Its disadvantages include the fact that the ballast resistor dissipates a rather large amount of energy, and the charge rate does not coincide with what is considered optimal for lead-acid batteries. A variation of the above system uses a timer to switch additional resistance in series with the battery, thereby reducing the rate of charge at some point in the charge cycle.

A common characteristic to all active systems is that information concerning the battery-charge level is used to control the charging current. This information is obtained through the use of a voltage sampling feedback system.

The simplest active system is another modification of the taper method previously mentioned; here, a voltage-controlled relay switches additional resistance in series with the battery at a cell voltage of 2.37 v. This system, as with all active systems, must have different voltage thresholds for batteries with different numbers of cells.

A relatively new active method uses silicon-controlled rectifier (SCR) in place of the silicon diodes. The SCR can be either full-wave or half-wave, and the firing angle is determined by a feedback circuit that senses battery voltage and/or current. The SCR system, as well as the other active system, has an advantage over passive systems in that charge rate can be more accurately controlled using feedback principles.

Charge termination is achieved by several methods. Passive chargers generally use a timer, as do some active systems. The cell voltage or its rate of change can also be used to determine when the battery is fully charged.

Maintenance

Proper battery maintenance is a very significant consideration in the determination of battery life. Battery manufacturers should provide a maintenance program with their batteries that includes the following information:

1. Specific gravity levels. One characteristic of the lead-acid battery is that electrolyte specific gravity is a function of the state of battery charge. Manufacturers should provide plots of electrolyte specific gravity versus discharge depth for their particular batteries.

2. Equalizing schedules. Equalizing is the process by which all the cells in a battery are brought to the same voltage. All lead-acid batteries require periodic equalization; however, excessive equalization causes unnecessary battery deterioration.

The following discussion is a guideline for a good battery maintenance program (3). The program involves three groups of activities, those that should be performed during each charge period (daily), those that should be

performed weekly, and those that should be performed approximately once every 3 months. Accurate records should be kept of all maintenance activities for each battery. Records provide a convenient way to monitor individual battery performance, thus exposing deteriorating battery conditions before the battery becomes a safety hazard or the source of costly downtime.

Daily battery-maintenance activities should include the monitoring of one of the battery cells (called the pilot cell), and any battery cell can be used as the pilot. The following cell characteristics should be recorded during each charge: Specific gravity before and after charging, electrolyte temperature before and after charging, and the water level in the cell. If any of the pilot parameters fall outside those specified as acceptable by the manufacturer, all of the cells should be checked and corrective action should be taken. Other daily maintenance activities should include checking the battery for physical defects such as cracked cell plugs and insuring that the charger output voltage is correct.

The weekly maintenance program includes checking all battery cells for proper water level and cleaning the battery tops if corrosion is present. It should be noted that the water consumption of a good battery is generally equally distributed among the individual cells.

At every 3 months, it is a good practice to take a complete set of cell-voltage and specific gravity readings at the end of an equalizing charge. These parameters should meet manufacturers' specifications; if not, corrective action should be taken.

The success or failure of a battery-powered mine transportation system is largely a function of the operator's ability to get maximum life from the batteries. It is also a function of the relative safety factor involved in battery usage.

BATTERY HAZARDS

Ventilation

As was mentioned previously, a consequence of battery charging is the liberation of hydrogen gas near the charge cycle end. Modern battery chargers, however, are designed to prevent excessive gassing in the latter phases of charge. This is usually accomplished by a relay in the charger that automatically drops the charge rate to a very low value when a certain cell voltage is reached. Although this eliminates much of the gassing, it is impossible to properly charge a battery without producing some gas.

For this reason, some method is required to dilute the explosive gas and render it harmless. The traditional method is by forced ventilation of the charging room. Another possibility is the use of catalytic battery caps to remove hydrogen at the source. The concern is to always keep the concentration of hydrogen below its lower explosive level of 4 pct. Because of the catastrophic nature of underground explosions, Federal regulations limit the permissible concentration of H_2 in coal mine atmospheres to 0.8 vol-pct which

provides a safety factor of 5. This is analogous to the maximum allowable methane concentration of one-fifth its lower explosive level, and seems reasonable.

By assuming a typical charge characteristic, manufacturers have made it possible to estimate hydrogen evolution from the number of cells and rated ampere-hour capacity. Table 1 lists such formulas from three different manufacturers. As shown in the table, the H_2 evolution calculated from these equations is fairly consistent, ranging from 0.0024 to 0.0028 ft^3/cell amp-hr. These figures are applicable to the latter stages of the charge cycle (at cell voltages of 2.37 v and greater).

TABLE 1. - Formulas to estimate hydrogen evolution

Formula number	Formula	Rate of H_2 evolution per cell amp-hr, ft^3/hr
1	(Number of cells) (rated amp-hr capacity) (0.0024) = cubic feet of H_2 liberated in last 3 hr of charge.	0.0008
2	(5) $\left(\frac{\text{amp-hr}}{100}\right)$ (number of cells) (0.016) = cubic feet of H_2 liberated in last 3 hr of charge.	.0008
3	(Number of cells) (amp-hr) (0.002948) = cubic feet of H_2 liberated in last 4 hr of charge.	.0007

In the course of this study, visits to typical underground charging installations were performed. Using various apparatus, measurements were made to determine hydrogen concentrations and ventilation flow rates. The prime objective of these trips was to evaluate the ventilation schemes at the charging stations, included was an assessment of the formulas in table 1. The following paragraphs discuss the results; complete documentation can be found in reference 5. In general for the mines visited, actual hydrogen concentrations were within the legal limits. In analyzing these concentrations and charging-room airflow rates with calculations using the table 1 formulas and dilution requirements, the results compared favorably.

Separate Split of Fresh Air

Present regulations stipulate a separate split of fresh air for underground charging stations. While this is a good safety precaution, there are certain cases where it may not be necessary.

Some mines use battery equipment for face haulage and require very large battery-charging stations that are capable of generating considerable volumes of gas. Yet, the majority of mines use only a few battery vehicles, mostly for supply haulage, and in these mines charging stations may only have a capacity for one tractor at any given time.

Consider the following hypothetical example. Suppose a mine was designed with 20- by 5-ft entries. A charging station with one battery charger is located in a panel intake entry, where the average air velocity is 400 ft/min. The resulting airflow is 40,000 ft^3/min.

Assume the station was designed to charge scoop tractors powered by 765-amp-hr, 64-cell batteries. During the gassing phase of the charge (the last 3 hr), the battery would evolve (using table 1, formula 2):

$$(5)\left(\frac{765 \text{ amp-hr}}{100}\right)(64 \text{ cells})\ (0.016) = 39 \text{ ft}^3\text{/hr gas.}$$

The total volume percentage of hydrogen contained in the air inby the charging station can be calculated assuming perfect mixing of the two gases. This assumption is not unreasonable considering the following. H_2 is a very mobile gas; hydrogen's extreme mobility results from its low molecular mass. With the velocities normally encountered in a mine intake airway, the air is flowing in the turbulent regime, a definite aid to dilution. Given the properties of the gases involved, the turbulent nature of the airflow, and allowing an enormous safety factor, the hazard of a hydrogen explosion would be negligible. With this example,

$$39 \text{ ft}^3\text{/hr} \div 60 = 0.65 \text{ ft}^3\text{/min (gas)}$$

$$0.65 \text{ ft}^3\text{/min (gas)} \div 40{,}000 \text{ ft}^3\text{/min (air)} = 0.000016$$

$$0.000016 \times 100 \text{ pct} = 0.0016 \text{ pct gas.}$$

Since the lower explosive level of H_2 is 4 pct, this represents a safety factor of 2,500.

It would not be unreasonable to permit this type of situation. The battery charger would, of course, be deenergized along with the rest of the electrical system in the event of a fan stoppage or other electrical ventilation failure. Also, some provision would have to be made to insure that the station was directly in the mainstream of the ventilating air and not in a small side pocket with no circulation. Possible charger placements are shown in figure 1.

One very important factor that could affect gas mixing to a large degree is the location of the charger. If it were located in the intake airway, the hydrogen would quickly be diluted. However, if the station were located out of the way, in a crosscut, it is conceivable that a pocket of H_2 could accumulate. The latter situation must be avoided, either by placing a curtain or fan to insure airflow through the charging station or by leaving the vehicle parked in the intake airway.

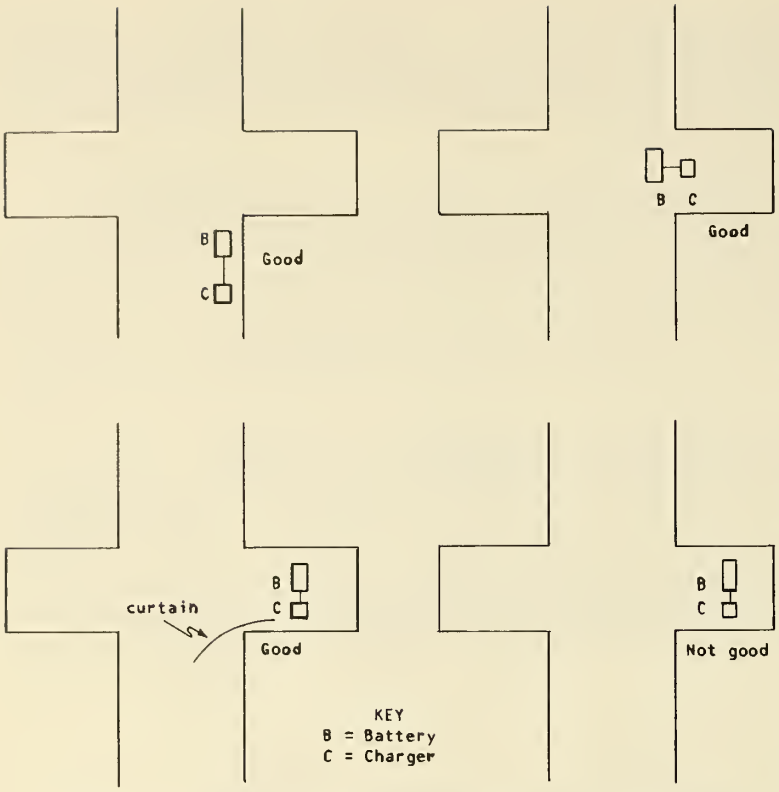

FIGURE 1. - Possible charger placements in an intake entry for a charger not designed to be on a separate split.

Minimum Airflow Quantities

In instances where H_2 evolution calculations and air quantity measurements indicate excessive H_2 concentration, the separate split of air is mandatory. Current Federal regulations do not stipulate any minimum airflow quantities for this split. Without guidelines to insure sufficient airflow over the batteries, many companies may not be providing enough air in their separate splits to dilute the gas before it flows into the return. Since it is simple to estimate airflow, but more expensive to determine hydrogen concentration, some guidelines for dilution requirements are perhaps in order.

From the previously discussed formula for calculating H_2 evolution, batteries in the final stages of charge evolve hydrogen approximately according to the following:

$$(5)\left(\frac{\text{amp-hr}}{100}\right)(\text{number of cells})\ (0.016) = \text{cubic feet of } H_2 \text{ per hour.}$$

Accordingly, dilution requirements could be calculated by--

$$Q(\text{cubic feet per minute}) = \frac{(5)\left(\frac{\text{amp-hr}}{100}\right)(\text{number of cells})\ (0.016)}{(0.008)\ (60)} - \frac{(5)\left(\frac{\text{amp-hr}}{100}\right)(\text{number of cells})\ (0.016)}{60}, \quad (1)$$

where battery stations on a separate air split should have an airflow of at least Q (cubic feet per minute). This quantity of air would be the minimum necessary to dilute the H_2 produced to 0.8 pct hydrogen, not allowing for dilution by room volume. To simplify calculations, it could be assumed that all batteries are 120-cell, 700 amp-hr (the present upper limit in battery size). Then, each battery would require about 140 ft^3/min of air for good

ventilation. Airflow requirements could be estimated from:

(Number of batteries) (140) = cubic feet per minute of ventilating air necessary for an adequate separate split. (2)

The preceding discussion considers the factor of providing enough ventilation to dilute evolved hydrogen gas. However, Federal law requires that all air currents used to ventilate structures or areas enclosing electrical installations shall be coursed directly into a return airway. This presumably is to avoid contamination of intake air with smoke from a possible fire. In view of this regulation, it is recommended here that battery chargers be on a separate splite, even though evidence suggests that to do otherwise would be safe from a hydrogen-dilution standpoint.

The foregoing ventilation statements assume that the battery lids remain open during charging. This is mandatory practice that is sometimes neglected in industry today, especially in low coal. Due to the small volume above the battery top when the lid is closed, dangerous accumulations of hydrogen are likely to accumulate there during charging. An alternative, the use of catalytic battery caps, appears to be an excellent resolution for difficult lid-removal situations.

Catalyst Battery Caps

A catalyst battery cap converts hydrogen and oxygen back into water (2). The caps have the dual function of preventing the escape of any hydrogen from the cells and restraining the loss of any water from the cells.

The safety advantages of catalyst battery caps are considerable. No additional ventilation would be required, either of the tray or of the charging station itself. The battery lids would not have to be opened for charging, a big factor in low coal. The explosion hazard associated with batteries would be eliminated. Since watering of the cells would not be required, no electrolyte would be spilled on top, and the possibility of surface leakage (explained later) would be greatly minimized. Tray corrosion by spilled electrolyte would also be greatly reduced.

These caps have been in use for quite some time in various applications ranging from torpedo batteries to batteries for salt-mine personnel carriers. They have proven to be reliable and effective. Occupational Safety and Health Administration (OSHA) accepts the catalyst battery caps and use in construction and general industry as an alternative to ventilation (2). The only drawback to these devices is their cost (about $4.00 each for small lots and about $2.50 for larger quantities), but this may be easily offset by the advantages.

Battery Surface Leakage and Faults

Since lead-acid traction batteries are quite heavy, often weighing several thousand pounds, the only presently available material which is suitable for tray construction is heavy-gage steel. Steel is a good conductor of

electricity, a disadvantage when used to support an isolated system such as a battery. After a battery has been in operation, coal dust mixed with spilled electrolyte can form a conducting path across the battery top, from the cell terminals to the tray. If these paths are permitted to accumulate, a number of low-resistance paths may form between the various cell terminals and the tray. Since the terminals are at different potentials, currents tend to circulate across the battery top and through the tray, and may cause three problems:

1. Currents circulating in resistive loops cause heating.

2. The presence of paths from the cell terminals to the tray causes a shock hazard for mining personnel.

3. Circulating currents represent wasted battery power and may reduce the amount of time a battery can be used before recharging is necessary. They also tend to increase tray corrosion.

Another potentially hazardous situation that may occur in batteries is the low-resistance-ground fault. A damaged cable in contact with the tray would typify this type of situation. Since the battery is theoretically a floating system, a single such fault would cause no current flow. The effect of surface-leakage paths would cause a certain level of current, depending upon their resistance. However, two simultaneous low-resistance-ground faults would permit extremely high currents to flow. Because of the low internal resistance of lead-acid batteries, currents on the order of 10,000 amp may exist for a short duration, depending on the contact resistance of the fault. A very difficult situation could result because batteries cannot be deenergized: A fire caused by faults would be very difficult to extinguish until the battery was discharged.

Discussion

The surface-leakage problem has been recognized by battery manufacturers for some time. The virtues of keeping battery tops clean have repeatedly been emphasized. However, cleaning is sometimes neglected in the mining industry, especially in low coal. Some alternative way of reducing this problem would be advisable.

Most batteries now in use underground have a thick coating of paint on their trays. This reduces leakage somewhat but is prone to deterioration by chipping, abrasion, and attack by battery acid. Recently, three manufacturers have begun coating their battery boxes inside and out with a tough vinyl compound. This product, known as plastisol, is readily available and can be sprayed onto any properly prepared steel surface. A significant reduction in surface-leakage problems results. Plastisol (or a similar material) is a simple, relatively inexpensive addition to battery safety.

To further increase the safety of batteries, however, exposed intercell connectors must be insulated in some manner. Although this sounds simple, any insulating coating applied to the connectors reduces their heat transfer capabilities. Since batteries release about 80 pct of their heat through the intercell connectors, this can be a serious problem.

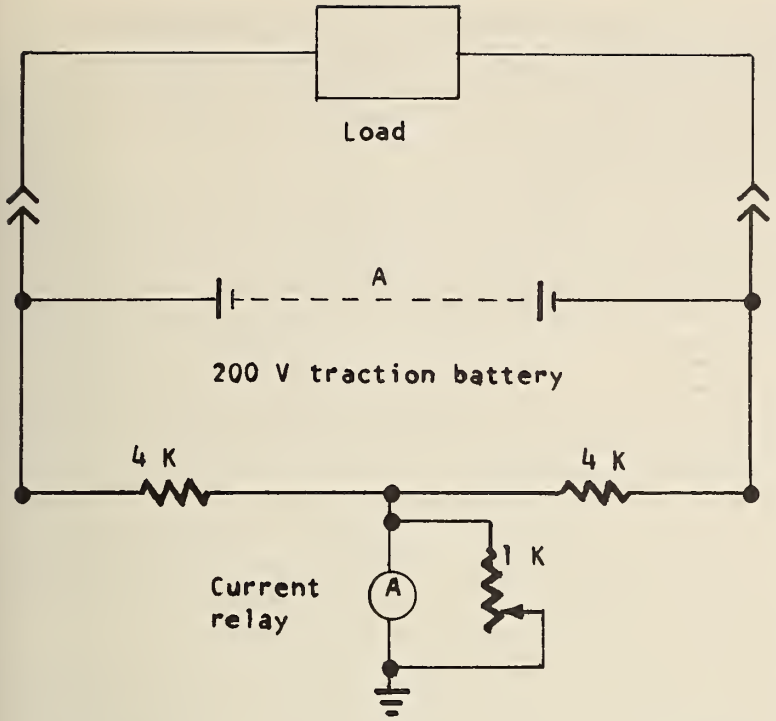

FIGURE 2. - Circuit for detecting faults in batteries, adapted from Statham and Littlewood.

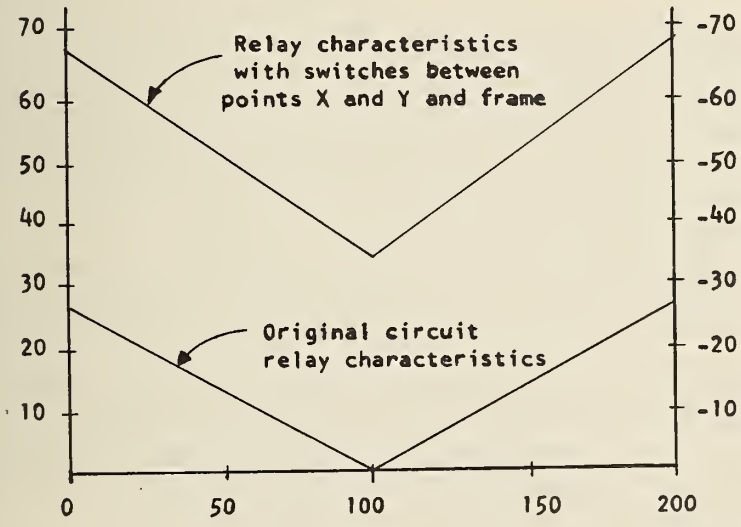

FIGURE 3. - Curve of relay current for various fault positions on battery, from Statham and Littlewood.

Leading battery manufacturers have recently been competing to produce a "dead-top battery," and at least two manufacturers now offer totally insulated intercell connectors as an option on their mining batteries. The system should greatly reduce the possibility of surface leakage and also remove the possibility of dangerous arcing caused by a tool dropped across the battery top.

Statham and Littlewood (6) realized the need for detection and isolation of surface leakage and ground faults in batteries. They developed a fault detection system designed to be fitted to the battery or battery charger. The circuit shown in figure 2 provides a simple method for detecting ground faults that might occur between the battery and its load. One problem with the circuit is that a large portion of the battery itself cannot be protected. For instance, a fault occurring at point A in figure 2 would produce no current flow through the current relay. Figure 3 is a plot of relay current versus fault position on the battery; it is assumed that the current relay shunt is set at 1,000 ohms and that a 200-v traction battery is used.

In order to increase the sensitivity of their circuit to battery surface-leakage faults, Statham and Littlewood proposed installing switches at points

X and Y (fig. 2). These switches would be alternately opened and closed by a mechanical or solid-state device. The dotted line in figure 3 shows the new position sensitivity curve resulting from the modified circuit. The entire battery could be protected in this manner, although sensitivity still varies with fault position for surface leakage faults.

Virr and Pearson (7) devised an electronic ac injection system that would provide sensitivity independent of fault location. They utilized a system of red and green lamps to indicate a "not safe" or "safe" condition. Although Virr and Pearson recommended mounting the device on each battery, this would not be necessary for trackless battery-powered vehicles since a device on the charger would be sufficient to prevent an unsafe battery from being charged. Since the development of surface leakage presumably takes place gradually with accumulation of conducting material on the battery top, continual monitoring of each individual battery is probably unnecessary.

Low-resistance faults to the tray or vehicle frame caused by damage to cables, and so on, represent a different problem. As previously mentioned, no provision is currently available for deenergizing a faulted battery, which would continue to discharge until its stored energy was dissipated.

Some form of circuit breaker between the cells of the battery would provide a way to sectionalize the battery in the event of a fault. In conditions of excessive current flow, the intercell connectors might themselves act as protective fuses, melting down when their current-carrying capacity was exceeded.

Battery Hazards Summary

Evidence suggests that, from a hydrogen dilution standpoint, it would be safe not to isolate charging stations on a separate split of air, coursing used air directly into the returns, as long as a sufficient quantity of air passes over the station. However, Federal regulations pertaining to the ventilation of electrical installations prohibit a change in charging-station ventilation requirements to be made here. It suffices to say that, regardless of the configuration of the charging-station ventilation system, the quantity of airflow should not be less than 140 ft^3/min for each battery on charge.

Proper isolation of the battery electrical system from the mine ground system is a prerequisite to safe battery use. Total electrical safety for any battery installation is, however, a function of charger characteristics as well as battery isolation. Battery chargers will be considered next.

BATTERY-CHARGING HAZARDS

Electrocutions and Grounding

Four battery-related fatalities that occurred in U.S. mines in the last 5 years were electrocutions involving battery chargers (4). A brief review of these accidents will shed some light on the hazards associated with the charging process. It will be seen that, in almost every case, improper grounding was involved.

1. A scoop operator was electrocuted when his body came in contact with the frame of a scoop tractor that was being charged. During the subsequent investigation, it was found that a potential difference of 260 v existed between the tractor frame and mine floor when the charger was energized. The cause of this was a low-resistance surface-leakage fault current between the battery and battery tray which caused the tray, and the tractor frame on which it was resting, to become energized. Faulty insulation between the primary and secondary windings on one arm of the three-phase transformer permitted secondary current to flow in the ground. The glaring error here was the failure of mine personnel to properly ground the steel frame of the tractor while it was being charged.

2. A utility man received a fatal electric shock when his body contacted the frame of a battery charger. A fault existed within the charger that caused 210 vdc and 114 vac to exist between the charger frame and earth. Despite the fact that the primary cause of the electrocution was a worn bushing which failed to insulate the timer circuit from the charger frame, a proper frame ground again could have prevented the fatality.

3. An electrician was fatally injured when he came in contact with a bare conductor on the charging leads of a battery charger while connecting the charger to the vehicle. The electrician was standing in water while attempting to connect the battery. Although the charger switch was in the off position, a primary-to-secondary fault in the charger transformer circumvented the switch (which interrupted only one primary conductor) and caused the charger leads to become energized.

4. A transit man was electrocuted when he contacted the battery ground clamp, which was attached to the charger frame. The charger frame was energized owing to a fault within the charger. The investigation showed the accident to be due to inadequate safety grounds on the frames of all the electrical equipment in the mine.

Transformer Faults

The secondary winding of most traction battery-charger transformers, whether single-phase or three-phase, is isolated from the mine-power-system ground. There are a couple of reasons for this. An isolated system provides protection against electrocution of a person at ground potential who touches a live conductor. A ground would provide an additional path for battery-surface leakage current, which is undesirable.

It is obvious from the preceding section that transformers cannot always be relied upon to maintain secondary isolation. Transient overvoltages and excessive vibration (for example) can cause transformer-winding insulation failures, which can result in a direct connection between the primary and secondary winding. Whether such a connection is direct or through the transformer core, the path permits secondary current to flow in the primary ground. An unisolated secondary does not present an especially hazardous situation unless it occurs with both the following conditions: A fault, which energizes a machine frame such as the battery charger or battery vehicle, and nonexistant

or poor grounding practices. Since both of these conditions are possible in the mine environment, it is necessary to insure that an isolated system remains isolated. This can only be accomplished with improved transformer designs (over those commonly used).

One possible method of insuring electrical isolation between the secondary winding and ground is to install a grounded metallic shield between the primary and secondary windings. Connection between a primary or secondary winding and such a shield would allow excessive ground current to flow, tripping at least a phase-unbalance or ground-overcurrent relay outby the charger. Therefore, the shield method provides a technique for indirectly detecting transformer faults.

Another scheme for insuring secondary isolation is the cast-coil method in which the transformer core and coils are coated with an epoxy material. Casting is achieved by inserting the fully assembled transformer into a cast and then pouring an epoxy material into the cast. After hardening, the epoxy occupies a space between the primary winding and the core and, if desired, the space between the primary and secondary winding. The cast-coil method can be used for preventing primary-to-secondary transformer faults.

The transformer secondary could be deliberately grounded, and ground-check devices could be used to insure that machine frames remain at ground potential. Battery surface leakage to ground could be monitored using one of the methods mentioned previously, with charge being prevented in the case of excessive leakage.

Protective Circuitry

Battery chargers are available with a wide variety of protective devices. Some manufacturers provide little more than overcurrent protection while others include additional protection against problems such as ac transients and exposed live charger plugs. The purpose of this section is to list and discuss various protective devices that might be used in charger design.

Panel Interlocks

Mine battery chargers, designed to accommodate batteries of various voltages, require internal adjustment to change the dc output voltage. Chargers that have fuse-protected outputs also require access to the internal charger circuitry in order to check or change out fuses. Panel interlocks, which interrupt charger input power when access panels are removed, could prevent unauthorized mine personnel from working on dangerous live circuits. This is common practice on practically every other piece of mine power equipment. The technique works by breaking the incoming ground system thereby enabling the outby ground-check monitor to trip its circuit breaker. Often, emergency stop switches are included with external access so anyone at the equipment can quickly trip the power.

Grounding

Failure to properly ground battery chargers and batteries being charged has led to several serious accidents. Federal laws concerning grounding are explicit, and most incidents have resulted from noncompliance rather than any inadequacy in the laws.

It is not uncommon in underground charging stations to find ground conductors absent or disconnected from battery vehicles. These practices firmly indicate that battery-charger ground leads should be monitored. Besides insuring ground continuity, a ground-check circuit would deenergize the charge plug in the case where it is removed from receptacle on the battery box before the charge cycle is complete and prevent an arc from occurring during plug removal.

Protective Coating for Charger Frame

Two of the fatalities mentioned resulted from faults caused by some internal circuitry contacting the charger frame. One charger manufacturer claims that an epoxy compound applied to their charger-cabinet interior effectively insulates it from faults. It is conceivable that the inside and outside of a charger cabinet could be coated with plastisol or some other suitable substances to reduce the possibility of a fault.

Safety Design of Mine Chargers

Considering safe electrical practice as well as the foregoing, the following are suggestions for mine battery-charger designs.

1. The input cable to the charger should contain a monitored ground to insure that the charger frame remains at ground potential.

2. The charger should be equipped with panel interlocks that deenergize the charger at the outby source when access panels are removed.

3. The charger should have an emergency off switch located in a conspicuous place on the charger frame. This switch should not be spring-loaded, thus requiring resetting after use.

4. The charger frame should be coated with an insulating material on the inside and outside. Such a requirement is not absolutely necessary if the frame is connected to a monitored grounding conductor from its power source.

5. The power transformer should be of the cast-core type with epoxy filler between the core the primary coil and between the primary and secondary coils; otherwise, there should be a grounded metallic shield between the primary and secondary windings (the Faraday shielding is preferred).

6. The power transformer should have transient overvoltage protection.

7. The power transformer secondary and all dc components should be isolated from the system ground.

8. The charger should be equipped with a ground-check monitor which insures that the battery box remains at ground potential.

9. The dc connection between the charger and battery box should consist of a single cable with appropriate ground and ground-check conductors.

10. The dc couplers should be of the type that interrupt the ground-check circuit before the charging circuit.

11. Any semiconductor rectifier, charge rate control, or timer circuitry should be protected against transient overvoltages.

12. The power rectifiers should have protective overtemperature relays.

13. The charger should have overcurrent protection on both the input and output.

14. The charger should have a meter or similar device that indicates the state of battery charge.

15. The charger should contain circuitry that prevents a battery of the wrong voltage from being charged; otherwise, keyed battery couplers should be employed.

16. The charger should contain battery surface-leakage detection circuitry that prevents a leaky battery from being charged.

17. The charger time circuitry should operate in a fail-safe manner to prevent battery overcharge.

The inclusion of these devices and techniques in mine chargers should practically eliminate electrocution hazards. Items 6, 11, and 12 are indirectly pointed at personnel protection through equipment protection.

In-Mine Evaluation of a Safe Charger

After investigating chargers made by several manufacturers, it was decided that a modified Kersey Model SSC64-3-180 Dynacharger would meet the needs of the project. All of the charger safety features previously discussed were incorporated in the modified Dynacharger, with the exception of the leakage detector (fig. 4).

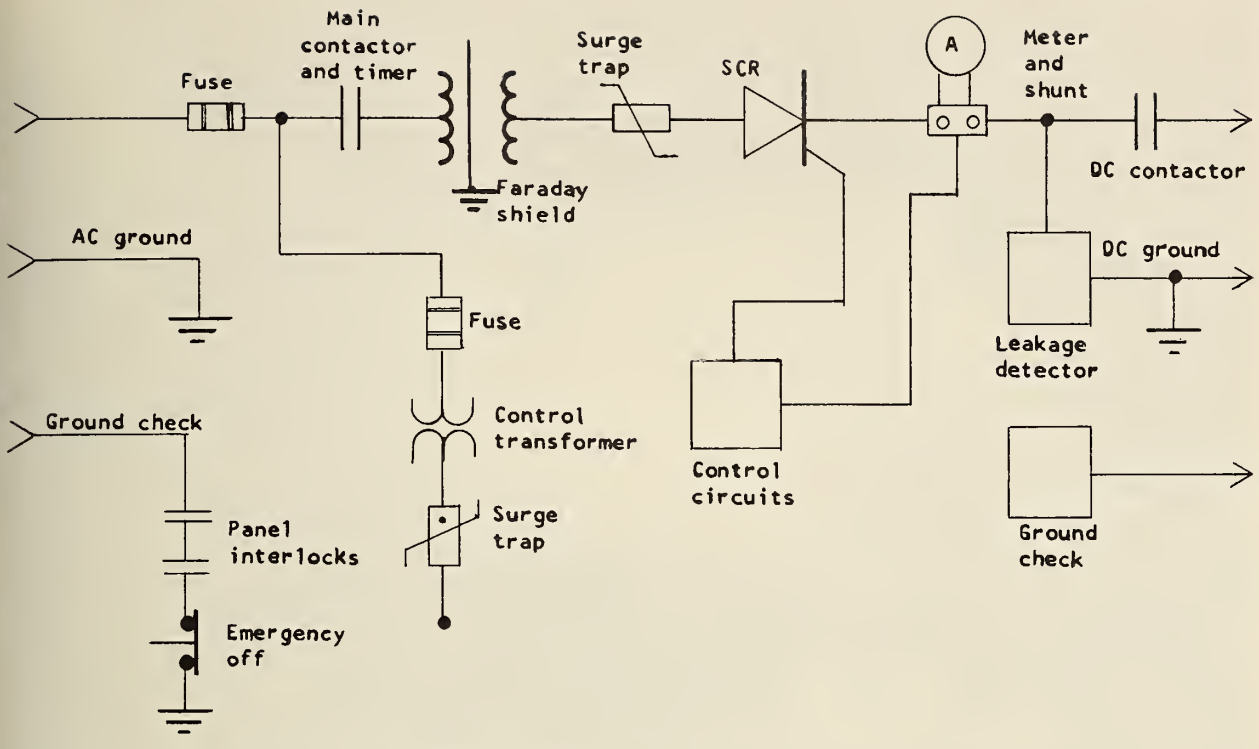

FIGURE 4. - One-line diagram of charger.

Charger Test Site

An Indiana County, Pa., coal mine was selected as the site for testing the safety charger. The mine uses two exceptionally large battery-powered scoops to service a longwall section.

Evaluation Tests

A formal test procedure has been established and implemented. The effort will intensify as soon as the leakage detector is installed in the battery charger. The procedure includes instrumentation for continuously monitoring and recording the frequency of activation of the charger's safety features (that is, ground-check, panel interlocks, etc.). As of this writing, the charger has provided several months of satisfactory service. Mine personnel report no difficulties with the charger, which is very encouraging. Figure 5 provides a photograph of the charger in service.

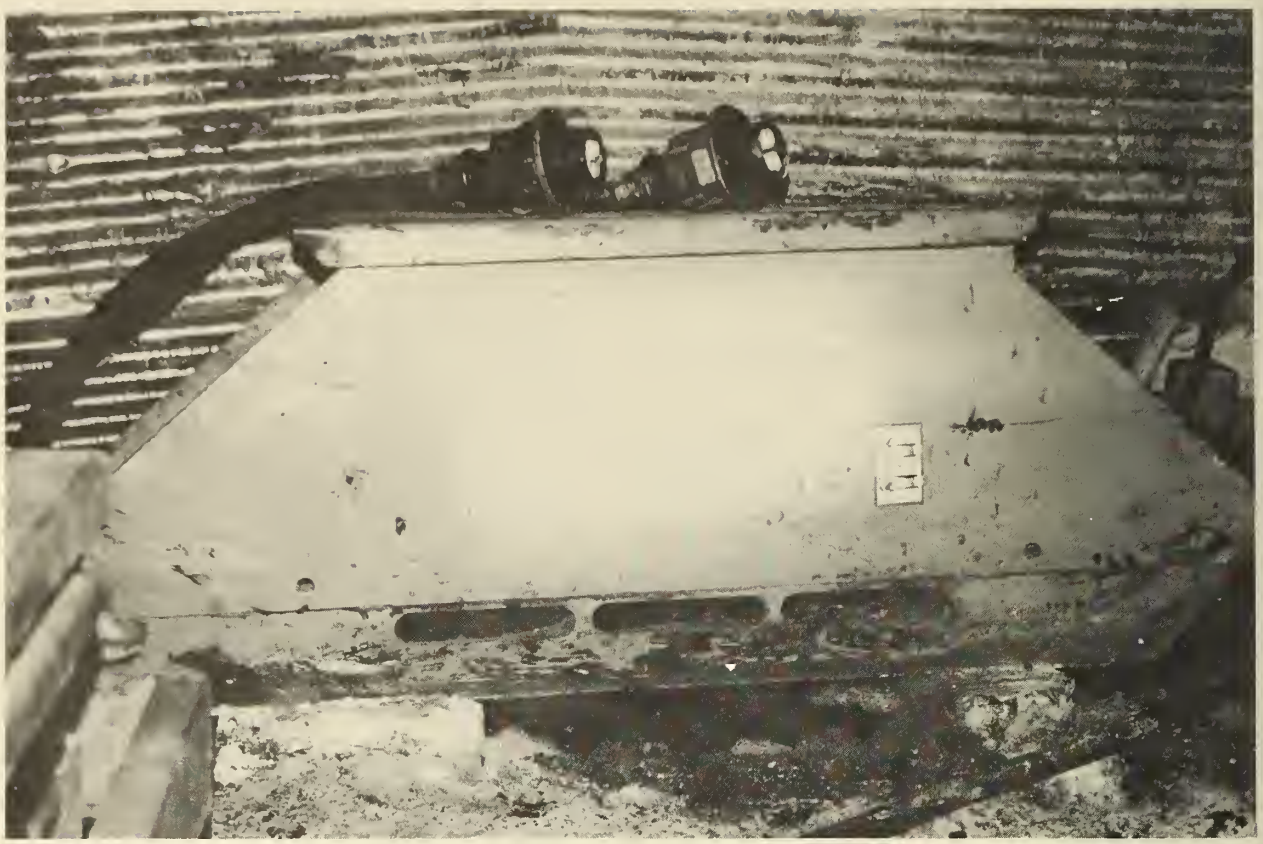

FIGURE 5. - In-mine installation of safety charger.

RECOMMENDATIONS TO REDUCE HAZARDS

Recommendations to reduce the hazards associated with battery use in underground coal mines have been given throughout this paper. The recommendations are briefly summarized below.

Maintenance

A good battery maintenance program is a must for successful battery use. Battery manufacturers usually provide a good program with their products.

Ventilation

Adequate ventilation of a typical small charging station requires little more than common sense. The batteries must be located in the mainstream of airflow during charging and provisions should be made so that 140 ft^3/min of air is available for each battery on charge. Battery lids should be removed during charging. Catalyst battery caps should be considered for a viable alternative to ventilation and lid-removal requirements.

Electrical

Specifications for a safe battery charger will not be repeated here. It suffices to say that safe battery chargers can be made and should be used to provide a larger safety factor in the battery charging and usage process.

CONCLUSIONS

This paper has reviewed the major hazards inherent to underground coal mine battery utilization. Recommendations have been made to significantly improve personnel safety in this area, including minimum ventilation flow rates, battery surface leakage and faults, and a safety design for mine chargers.

REFERENCES

1. Hensler, J. F. The Case for Batteries. Coal Age, March 1965, pp. 90-94.

2. Hydro-Catylator Corp. Hydro-Catylator Sales Bulletin. Hialeah, Fla. 1977, 4 pp.

3. K. W. Battery Co. Service Manual for Motive Power Batteries. Skokie, Ill., 1975.

4. Mining Enforcement and Safety Administration. Reports of Fatal Coal Mine Electrical Accidents. Available for reference at MSHA Health and Safety Analysis Center, Denver, Colo.

5. Morley, L. A., and J. A. Kiefer. Coal Mine Electrical System Evaluation. Volume V. Battery and Battery-Charging Safety. BuMines Open File Rept. 61(5)-78, Feb. 15, 1977, 68 pp.; available for reference at Bureau of Mines facilities in Denver, Colo., Twin Cities, Minn., Bruceton and Pittsburgh, Pa., and Spokane, Wash.; Department of Energy facilities in Carbondale, Ill., and Morgantown, W. Va.; National Mine Health and Safety Academy, Beckley, W. Va.; National Library of Natural Resources, U.S. Department of the Interior, Washington, D.C.; and from National Technical Information Service, Springfield, Va., PB 283 494.

6. Statham, C. D. J., and J. Littlewood. Developments in the Safe Use of Traction Batteries in Coal Mines. IEE Conf. Pub. 74, 1971, pp. 49-53.

7. Virr, L. E., and F. K. Pearson. Fail-Safe Earth-Fault-Detection Device for Battery Supplies. Proc. IEE, v. 121, No. 8, August 1974, pp. 829-830.

FAIL-SAFE ASSESSMENT OF SOLID-STATE PROTECTIVE DEVICES

by

S. S. Venkata,[1] W. T. Crawford,[2] and S. V. R. Kolluri[3]

ABSTRACT

Solid-state protective devices have been introduced in coal mine power systems in the past few years. More and more of these devices will find their way into the mines in the future. They will be required to meet several stringent requirements by Mining Safety and Health Administration (MSHA)--the most important being fail-safe performance. The work reported here describes two techniques, namely, computer simulation and suitable laboratory tests for evaluating the safety of solid-state protective devices. The paper also describes the application of these two techniques to an undervoltage relay and an overcurrent relay. Results and recommendations conclude the paper.

INTRODUCTION

The safety of mine personnel has been one of the primary concerns in the coal mine industry. In order to insure the safety of personnel working in coal mines, it is necessary that faults which could occur in mine electrical power systems be detected and cleared promptly. This implies that each protective device fail in a safe mode if any of the components fail. If this requirement is satisfied the device is said to be fail-safe. The fail-safe analysis is performed to identify the critical components or parameters of the device and to redesign it for perfect fail-safe performance. Before proceeding with the description of the analytical tools and their application to the devices, the term "fail-safe performance" is defined.

DEFINITION OF "FAIL-SAFE PERFORMANCE" (5)[4]

A component failure shall not negate the ability of the device to perform properly its intended function or shall open the circuit interrupting devices.

The use of "redundant components or circuitry" will not be accepted as a method of complying with the requirements of the above definition. This definition should be kept in mind while carrying the fail-safe analysis of solid-state protective devices and in interpreting the results.

---

[1]Associate professor, Department of Electrical Engineering, West Virginia University, Morgantown, W. Va.
[2]Electrical engineer, New River Coal Co., Oakhill, W. Va.
[3]Distribution engineer, Kentucky Power Co., Hazard, Ky.
[4]Underlined numbers in parentheses refer to items in the list of references at the end of this paper.

At present, many solid-state protective devices exist in some coal mines, notable among these are overcurrent relays, undervoltage relays, and ground monitors. In the future more of these devices will be introduced in the mines. The tendency towards using solid-state devices stems from the many advantages these offer over their electromechanical counterparts, the principal advantage being absence of mechanical contacts, which could become a potential source of fire hazards. Also, solid-state devices are fast in response, compact in size, and cheaper. In addition, these overcome problems due to shock, vibrations, and corrosion. However, these devices have the following disadvantages: Breakdown in the components of the device due to high temperature, vulnerability to voltage spikes, and low short time overload capacity.

It is now clear to those concerned with the coal mining industry including the Mine Safety and Health Administration (MSHA) that there is a need to assess the fail-safe performance of solid-state protective devices, both existing and new ones, to be installed in the future. This is because unsafe behavior in solid-state protective devices could jeopardize the safety of the miners.

This paper deals with the safety assessment of solid-state protective devices used in coal mine power distribution systems and discusses two techniques (2-3, 6-7) available for the safety assessment. The first technique involves conducting suitable tests in a laboratory. The second one is a computer simulation technique using standard software packages for circuit analysis such as Electronic Circuit Analysis Program (ECAP) and System of Circuit Analysis Program (SYSCAP).

LABORATORY TESTING OF DEVICES

The laboratory test is performed on the solid-state devices by physically opening and shorting every component in the device. These are also known as open-circuit and short-circuit tests. In the open-circuit test, each component is physically removed from the circuit board. Similarly, every component is shorted in the short-circuit test. By monitoring the level of current in the holding coil or similar component of the device, the decision on the fail-safe performance can be made.

Before performing the destructive open- and short-circuit tests, it is desirable to check the calibration of the device. Also, the device should be subjected to transient voltages of different frequencies to test its dynamic behavior.

Description of Lee-Trip

The Lee-Trip is a solid-state overcurrent relay (OCR). Figure 1 shows the circuit of the device. The Lee-Trip overcurrent relay consists of four main units, namely, power supply, calibration, voltage comparator, and tripping. In the power supply unit 120 vac is applied to a step down transformer. The step down voltage is rectified to 24 vdc and passed into a voltage regulator that puts out 15 vdc and -15 vdc. This output dc voltage is used in the rest of the circuit for the necessary baising.

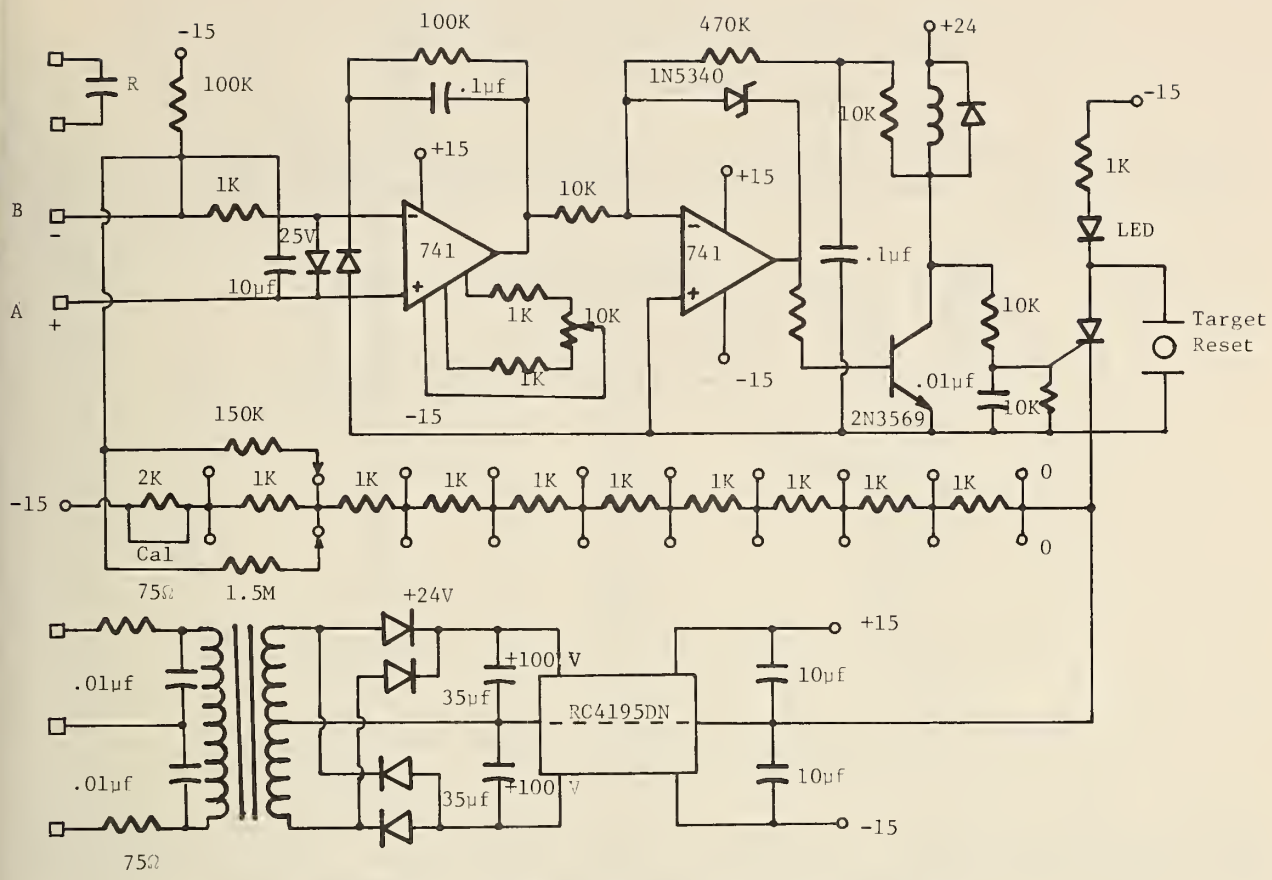

FIGURE 1. - Lee overcurrent relay (solid state).

The calibration unit consists of decade resistor sets that could be varied as desired. The voltage comparator unit consists mainly of two operational amplifiers, while the trip unit has a transistor connected in series with the tripping coil.

The circuit works generally in the following manner: The shunt voltage, which is applied to the terminals A and B, is compared with the reference voltage. The reference voltage, or trip level, is set through the decade resistor. When the shunt voltage is greater than the reference voltage, an indication of overcurrent in power circuit, the operational amplifiers switch off the transistor. This stops current from passing through the tripping coil which opens the normally closed contact R. At this point the silicon-controlled rectifier (SCR) is switched on and the light-emitting diode (LED) lights up indicating that tripping has been accomplished.

Description of Westinghouse Solid-State Undervoltage Relay (UVR) (Seltronic)

This relay was developed by Westinghouse Electric Corp. for use with its Seltronic breakers. The schematic of the solid-state UVR is given in figure 2.

The level of the current through the load coil R_{20} is determined by the regulator action of the zener diode D_4 at the base of transistor Q_4. The

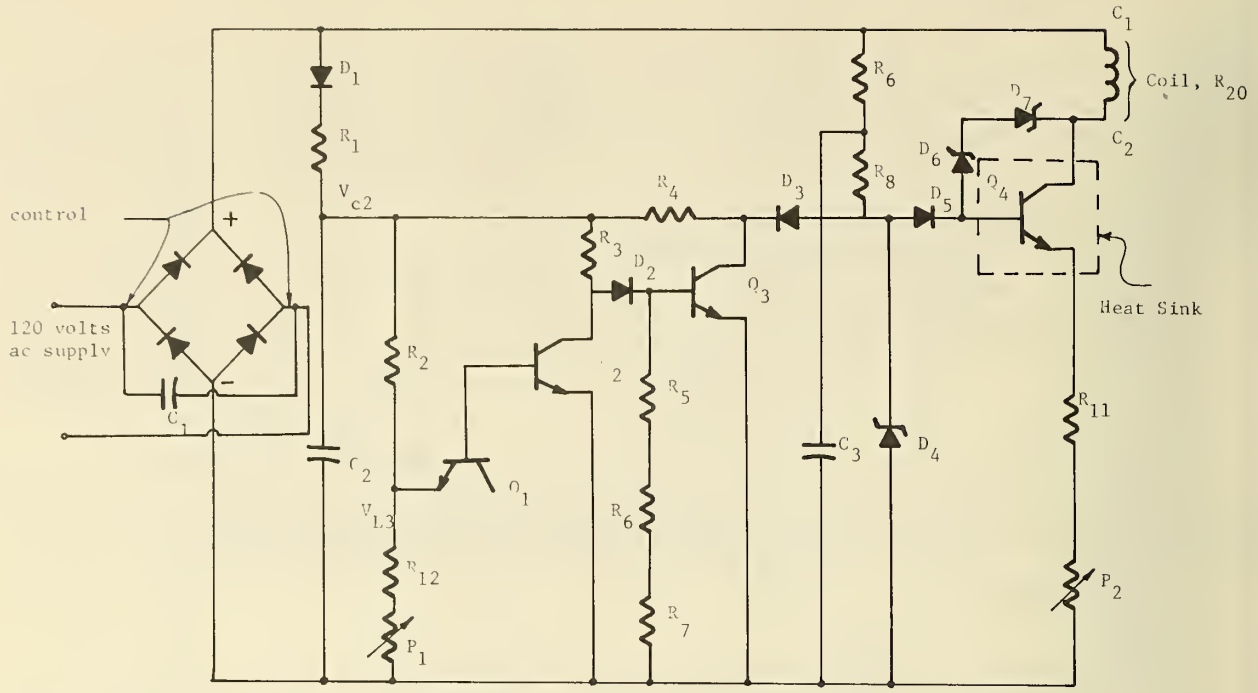

FIGURE 2. - Westinghouse (Seltronic) solid-state undervoltage relay.

voltage across resistance R_{11} and potentiometer P_2 is held at 1.2 v less than the voltage across zener D_4 when the transistor Q_4 is on. Adjusting the resistance R_{11} varies the current for a fixed voltage drop across that resistance.

The load current is turned on and off by respectively opening or shorting zener D_4 to circuit ground through transistor Q_3. Initially, as voltage V_L starts to rise and the voltage across capacitor V_{C2} rises proportionately, transistor Q_2 is biased OFF, which in turn biases transistor Q_3 ON and shorts zener D_4. At the point of pickup, voltage across capacitor V_{C2} causes voltage across R_{12} and P_1, that is, V_{L3}, to rise 0.6 v above the zener voltage of transistor Q_1, which turns transistor Q_2 ON. When Q_2 turns ON, the base bias of transistor Q_3 is shorted which turns transistor Q_3 OFF and causes two effects:

1. Voltage across zener D_4, V_{D4}, rises to the zener voltage D_4 and turns transistor Q_4 and the coil current ON.

2. The resistance path R_4 from C_2 to ground is removed, which causes voltage V_{C2} to jump. This insures a sharp turn-ON and allows a lower dropout level than the pickup level since voltage V_{C2} and V_{C3} are higher with R_4 not connected to circuit ground. If voltage V_L is lowered to the dropout point, the process is reversed. Transistor Q_2 is biased OFF causing transistor Q_3 to be biased ON. This shorts zener D_4, which turns the coil current OFF and also connects capacitor C_2 to circuit ground through resistance R_4 causing voltage V_{C2} to drop sharply and the circuit is returned to its original state.

Results of Laboratory Tests

Lee-Trip Overcurrent Relay

Calibration Test.--The results of the calibration test show that the relay trips with an error of about ±2 pct of the trip setting. The results are given in table 1.

TABLE 1. - Lee-Trip calibration test results

Trip setting voltage, mv	Relay dropout voltage, mv	Relay pull-in voltage, mv
10	10	5.2
15	15	10.2
20	20.1	15.3
25	25.2	20.4
30	29.9	25.2
35	35.0	30.2
40	40.0	35.3
45	45.0	40.3
50	50.0	45.2
55	54.9	50.2
60	60.1	55.1
65	65.6	60.3
70	70.4	65.6
75	75.2	70.6
80	80.6	76.6
85	85.7	81.0
90	92.6	86.5

The setting device or the test equipment might have introduced the error, which is the difference between the trip setting and actual relay dropout voltages.

Transient Voltage Test.--Both triangular and square wave voltages were applied to the relay at two different frequencies, namely 0.1 and 1 Hz. The inputs as well as the contact responses were recorded. The relay did not show any malfunctioning in all the cases, when the output from the strip chart recorders were observed.

Open-Circuit Test.--The relay coil performance was observed by opening one component at a time, while keeping all others in their normal condition. The test was repeated for most of the components. Throughout the tests the trip setting was kept constant at 40 mv. The results are given in table 2.

TABLE 2. - Concise results of open-circuit test on OCR

Opening of components resulted in--					
	Degraded operation			Fail-safe (relay deenergized immediately as the component was opened)	Fail unsafe (relay remained energized from the instant of opening the component)
Normal operation	Component	Dropout voltage, mv	Pull-in voltage, mv		
R_1	R_8	43.0	37.8	Dual decade switch	R_7
R_2	R_{10}	43.5	39.1	R_4	
R_3	R_{11}	42.0	36.7	R_9	
R_{12}	R_{13}	34.4	33.7	R_{16}	
R_{14}		Vibration		R_{17}	
	D_1	of contacts			
		at 34.0 and	33.8		
	D_2	dropout at			
		35.0			
R_{15}				Transformer	
C_1				Transistor	
C_2				Relay coil	
C_3					
C_4	D_3	39.5	34.2		
C_5	D_4	39.5	34.2		
C_6					
C_7					
C_8					
C_9					
C_{10}					
SCR					
LED					
D_5					
D_6					
D_7					
D_8					

It was not certain whether the components that did not affect the normal operation of the relay would not have done so if left open for a longer time.

Short-Circuit Tests.--This test was similar to the open-circuit test. All components were shorted one at a time. The detailed results are shown in table 3.

TABLE 3. - Concise results of short-circuit test on OCR

Shorting of components resulted in--					
Normal operation	Degraded operation			Fail-safe (relay deenergized immediately as the component was shorted)	Fail unsafe (relay remained energized from the instant of shorting the component)
	Component	Dropout voltage, mv	Pull-in voltage, mv		
R_3	R_{10}	38.8	34.3	R_1	R_2
R_4				R_7	R_5
R_9				R_8	R_6
R_{10}				R_{12}	R_{14}
R_{13}				C_5	C_6
R_{15}				C_8	C_7
R_{16}				D_1	D_3
R_{17}				D_2	D_4
C_1				D_5	D_7
C_2				D_6	D_8
C_9				Transformer	Transistor
C_{10}				Relay coil	

Westinghouse Solid-State UVR (Seltronic)

The failure of each of the components was simulated in the laboratory. Each component was physically opened and shorted and device performance was observed for each of the failures. For the device to be fail-safe, it is expected to drop out at the dropout value of 48 v ±5 pct, where ±5 pct is the tolerance value. That means if the device drops out between 46 v and 50 v for each failure condition, it is considered to be fail-safe. The detailed results of the tests performed on the UVR are tabulated in table 4.

TABLE 4. - Concise results of practical fail-safe analysis on Westinghouse UVR (Seltronic)

Components that totally failed unsafe	Components that totally failed safe	Components that failed safe in open mode and unsafe in short mode	Components that failed safe in short mode and unsafe in open mode
None	R_1	R_2	D_4
	R_3		
	R_4		
	R_5		
	R_6		
	R_7	R_8	
	R_9	R_{11}	
		R_{12}	
	Q_2, Q_3		
	D_6		
	D_7		
	Q_1 or D_8		
	D_1		
	D_2	D_3	
	D_5	Q_4	
	C_2		
	C_3		
	C_4		

Interpretation of the Laboratory Test Results

Lee-Trip Overcurrent Relay

From the results it is observed that resistor R_7 failed unsafe in the open mode of failure (table 2) and resistors R_2, R_5, R_6, R_{14}, capacitors C_6, C_7, and diodes D_3, D_4, D_7, D_8, failed unsafe in the short mode (table 3). These components are therefore critical components.

Westinghouse Solid-State UVR (Seltronic)

From the laboratory test results it is observed that diode D_4 failed unsafe in the open mode and resistors R_2, R_8, R_{11}, R_{12}, diode D_3 and transistor Q_4 failed unsafe in the short mode (table 4). These components are therefore the critical components.

COMPUTER SIMULATION TECHNIQUES FOR SAFETY

Two well-known and standard software programs that could be used for the fail-safe assessment of solid-state devices are (1) Electronic Circuit Analysis Program (ECAP) (4) and (2) System of Circuit Analysis Program (SYSCAP) (1).

In each of the programs, the opening and shorting of each component of the device can be simulated along with the proper input operating conditions. By monitoring the current level in the component that determines the successful operation of the device (for example, coil in a relay), the critical and unsafe components could be identified in each mode of operation.

Description of ECAP (4)

ECAP is a set of computer programs that have been integrated to form a system capable of analyzing an electronic circuit from a description of its topology. Three forms of analysis are possible with ECAP. They are a direct current (dc) analysis, an alternating current (ac) analysis, and a transient (TR) analysis. Each of these analysis programs will recognize the standard linear circuit elements with some few exceptions. The most outstanding feature of ECAP is its ability, in the transient mode of analysis, to handle nonlinear elements in a piecewise linear fashion through the use of switches.

Alternating Current Analysis

This program provides the steady-state solution for linear circuits that contain resistors, fixed voltage sources, fixed current sources, and dependent current sources. Circuit parameters can be modified in this analysis very simply by just inserting a modify statement and the intended modifications.

Direct Current Analysis

This program provides dynamic solution for linear circuits subject to sinusoidal excitation at a fixed frequency. The circuits may be composed of the following elements: Resistors, capacitors, inductors, voltage and current sources, dependent current sources, and mutually coupled inductors. In addition to modifying parameters as in the dc analysis, frequency may also be changed to provide ac analysis at any frequency.

Transient Analysis

The transient analysis program provides the time response of a circuit subject to user-specified driving functions. The circuits may consist of resistors, capacitors, inductors, fixed or time-dependent voltage and current sources, dependent current sources and switches. There are two possible responses from the program. The transient response provides the node voltages, element currents, and switch actuation times as outputs. The voltage and currents are computed at the start of a transient solution and at uniform intervals of time until the solution is reached. The equilibrium response provides a final dc steady-state solution with capacitors automatically open circuited and inductors short circuited.

In all of these analyses, each element can be opened and shorted within the program. Input voltages can be applied to the devices to simulate their operating conditions, complete with fluctuations and transients. The transient analysis program was used exclusively in this study, since it met all requirements.

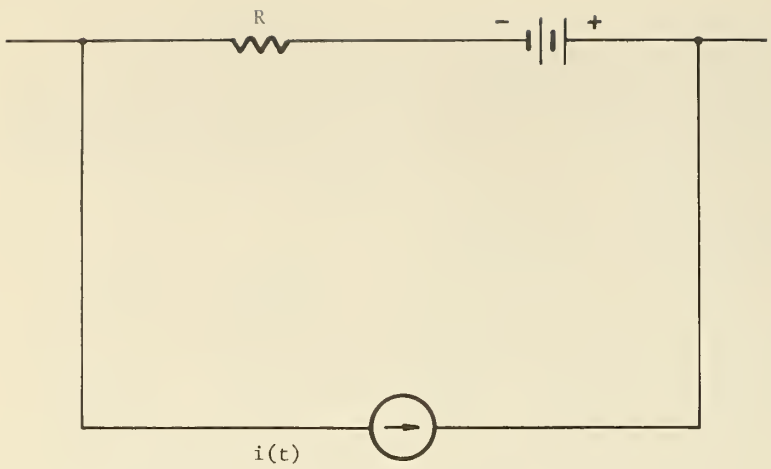

FIGURE 3. - Switch circuit to replace diode.

Modeling of Components

Any solid-state device usually contains resistors, inductors, capacitors, diodes, transistors, operational amplifiers, etc. Although it is obvious how to model the first three passive components, it is not clear how to model the active and nonlinear elements or subsystems. This section deals with the modeling of diodes, transistors, and operational amplifiers of the solid-state devices.

Diodes

Diodes can be handled as switches. The switches are current-sensitive branches in the circuit. Figure 3 shows the diode model used for the fail-safe assessment of solid-state overcurrent relays. Any branch can be assigned as a switch. The branches so designated have their current monitored throughout the transient solution. The switch is considered "on" when the current is positive and "off" when it is negative. Thus when the current changes sign, the sense of the switch changes accordingly. Each element can have two values entered in its input data. Then the actuation of a switch can cause these circuits elements to change values. This can therefore be used to simulate the forward conduction and voltage drop and the reverse resistance of a diode. Zener diodes can also be modeled in the same way.

Transistors

A transistor is modeled by the use of an expanded ECAP known as PRECAP (7), which extends the ECAP language to include complex multi-element models for electronic components. There are several models in the form of subprograms available on storage that may be called upon within the ECAP program. One, two, and three region transistor models are available with default parameters already stored. The transistor model may be called using these default parameters or specifying new ones. The transistor pin-node numbers must be user specified. The computer then inserts the model, creating additonal nodes as needed.

Operational Amplifiers

Operational amplifiers (OP AMP's) present the worst modeling problem encountered so far. These chips contain a multitude of elements in themselves (fig. 4). ECAP is limited to a circuit size of 20 nodes and 60 branches. It is also limited in its number of particular elements. For example, the common 741 OP AMP chip has 20 transistors and 23 nodes. Obviously, this cannot be

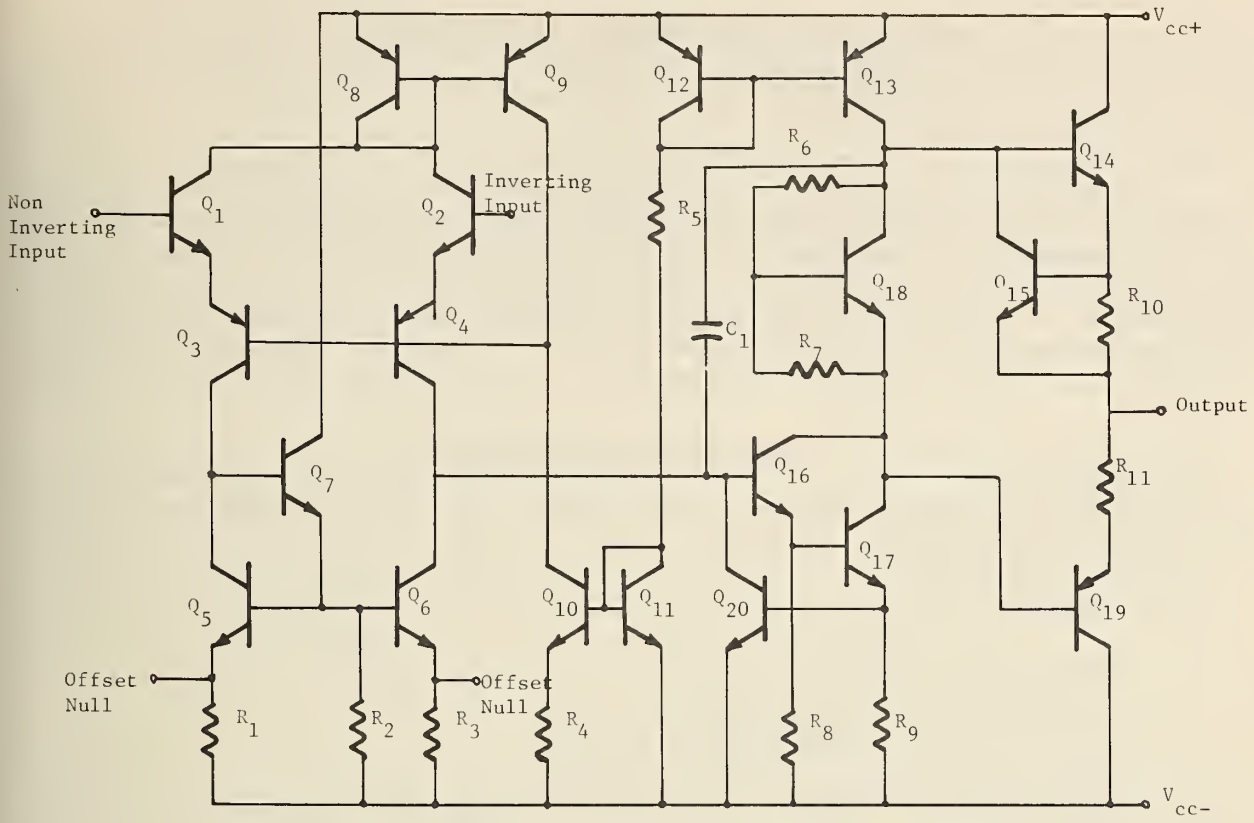
Non Inverting Input
Inverting Input
Offset Null
Offset Null
Output
V_{cc+}
V_{cc-}
Q_1 Q_2 Q_3 Q_4 Q_5 Q_6 Q_7 Q_8 Q_9 Q_{10} Q_{11} Q_{12} Q_{13} Q_{14} Q_{15} Q_{16} Q_{17} Q_{18} Q_{19} Q_{20}
R_1 R_2 R_3 R_4 R_5 R_6 R_7 R_8 R_9 R_{10} R_{11}
C_1

FIGURE 4. - Schematic diagram of LM741C OP AMP chip.

simulated in its entirety. Instead the effect of the OP AMP is modeled very simply. This involved only the inverting and noninverting pins and the output pin. A dependent current is inserted and the effects of the OP AMP are observed. Figure 5 depicts the model of the OP AMP adopted in this paper.

This does not allow proper testing of opening and shorting each and every pin with the others to see how it affects the operation. This is a serious drawback, but this is the only way to model such a device on ECAP.

Description of SYSCAP

SYSCAP (1) is a system of computer programs that performs static-dynamic and linear-nonlinear analysis of electronic circuits. Basically, an electronic circuit is simulated by creating a mathematical model of the circuit topology. The model usually consists of a series of nodes that are interconnected by circuit elements and devices and are driven by signal

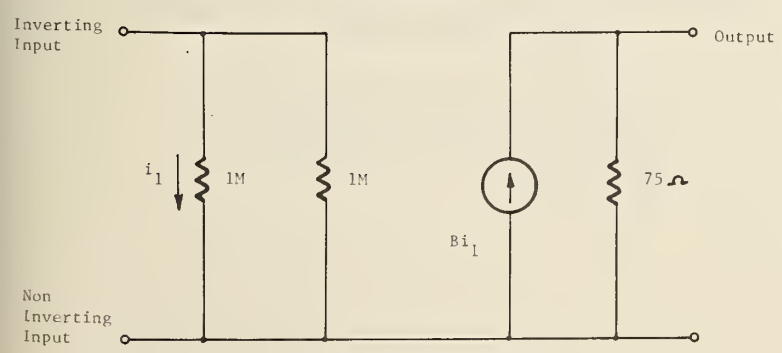

FIGURE 5. - Basic model for LM741C OP AMP.
$B = -1.33 \times 10^9$.

sources and power supplies. The topology of the circuit is coded into a form compatible with the SYSCAP system. The system also includes a built-in semiconductor device parameter data base (Data Bank), which simplifies the semiconductor coding for the user.

This input data is then submitted to one (or more) of the SYSCAP systems analysis programs; ALCAP, DICAP, and TRACAP write the model equations for the circuit and perform linear ac, dc, and transient analyses, respectively, on the user's circuit. From the user point of view this program is simpler than ECAP. Also, it can handle larger size of systems and the entire fail-safe performance results can be obtained with one computer run, whereas ECAP requires one run for each mode of failure.

Direct Current Analysis

SYSCAP's dc analysis program, called DICAP, performs the following types of static or dc analysis:

1. Nominal analysis.
2. Parameter variation.
3. Circuit failure simulation.
4. Worst case analysis.
5. Power supply turn-on simulation.
6. Sensitivity analysis.

Accordingly, the user tests a circuit by mathematically simulating the voltages or currents. This information is submitted to DICAP for analysis. The DICAP simulates the effect of these factors and calculates steady-state voltages and currents.

Out of the six types of dc analysis, circuit failure simulation (CFS) is best suited for the purpose. By specifying the CFS option in the program control entry, the user can simulate single catastrophic failures of circuit components. The following kinds of catastrophic failures are simulated:

Elements	Simulated failures
Transistors.....	Base emitter (B-E) open/base collector (B-C) open-open.
Do.....	B-E short/B-C short-short.
Diodes.....	Open/short.
Resistors.....	Do.
Voltage sources.....	Do.

Results of Computer Simulation Techniques

Lee-Trip Overcurrent Relay

The two operational amplifiers were broken down to their simplest linear form and modeled with resistors and voltage sources. The transistor was modeled using a different software package called PRECAP (7), which is compatible with ECAP. All diodes were represented as switches. Two portions of the device's circuit were not modeled--the power supply including transformer and a thyristor resetting circuit--since these play secondary roles in the successful operation of the device. All other elements (linear and passive) were modeled without much difficulty.

The device was systematically tested, element by element, to determine theoretically if the device was fail-safe. This was done by simulating the shorting and opening of all the important components, keeping the trip setting constant at 40 mv. The results are shown in concise form in tables 5 and 6, which show four different types of responses of the relay: Normal operation, degraded operation (that is relay operates successfully, but above or below 40 mv), fail-safe operation, and fail unsafe operations.

TABLE 5. - Concise results of theoretical analysis of OCR (opening of components)

Opening of components resulted in--				
Normal operation	Degraded operation		Fail-safe (relay deenergized	Failed unsafe (relay does not deenergize
	Component	Dropout voltage, mv		
R_3	R_8	68	R_9	R_7
R_{14}			R_6	
R_2			R_4	
R_5				
R_{12}				
R_{15}				
C_7				
C_8				
C_9				
C_{10}				
D_6				
D_5				

TABLE 6. - Concise results of theoretical analysis of OCR (shorting of components)

Shorting of components resulted in--				
Normal operation	Degraded operation		Fail-safe (relay deenergized)	Failed unsafe (relay does not deenergize)
	Component	Dropout voltage		
R_3	None	None	R_7	R_2
			R_{12}	R_6
R_9			R_5	
R_4			R_{14}	
R_{15}			R_8	
C_9				
D_6			C_7	
C_{10}			C_8	

Westinghouse Solid-State UVR (Seltronic)

The computer simulation was done for this relay using the SYSCAP program. The undervoltage relay was modeled following a standard format as outlined in SYSCAP II manual. All the parameters in the circuit except for the bridge rectifier were modeled to simplify the analysis. The transistor Q_1 was modeled as a zener diode. All the desired component failure were simulated in both the open and short mode using the DICAP and its circuit failure simulation (CFS) option.

It is assumed in the analysis that no simultaneous or sequential failures occur. The current through the coil (R_{20}) was monitored, since this is the key component upon which the successful operation of the UVR depends.

For the UVR to be fail-safe whenever a component fails the current through coil R_{20} must decrease from several milliamperes to the microampere level and deenergize the coil. If not, the component has failed unsafe. The results of the test are presented in table 7.

TABLE 7. - Concise results of theoretical fail-safe analysis on Westinghouse UVR (Seltronic)

Components that totally failed unsafe	Components that totally failed safe	Components that failed safe in open mode and unsafe in short mode	Components that failed safe in short mode and unsafe in open mode
None	R_1	Q_4	D_4
	R_2	R_{11}	
	R_3		
	R_4		
	R_5		
	R_6		
	R_7		
	R_8		
	R_9		
	R_{12}		
	Q_2, Q_3		
	D_6		
	D_7		
	D_8 or Q_1		
	D_1		
	D_2		
	D_3		
	D_5		
	C_2		
	C_3		
	C_4		

Interpretation of Computer Simulation Techniques' Results

Lee-Trip Overcurrent Relay

Close observation of tables 5 and 6 reveal that resistor R_7 failed unsafe in the open mode and resistors R_2 and R_6 failed unsafe in short mode. The remaining components failed safe in both the modes of failure. The above components are therefore the critical components in the device.

Westinghouse Solid-State UVR (Seltronic)

From table 7 it is observed that zener diode D_4 failed unsafe in the open mode, while the resistor R_{11} and transistor Q_4 failed unsafe in the short mode. Therefore these are the critical components in the device.

SUMMARY, CONCLUSIONS, AND RECOMMENDATIONS

This paper describes the techniques available for the safety analysis of solid-state protective devices. The theoretical assessment of any solid-state device could be made by feeding its structure into one of the two standard

software programs ECAP and SYSCAP. The latter one is more versatile and easy to use. The safety of any solid-state device could be practically investigated by performing suitable laboratory tests outlined briefly in the paper. It is suggested that both the theoretical and practical approaches be followed for solid-state device since one can verify the results of the other and thereby the final results could be made more reliable and dependable.

Conclusions Related to Safety Assessment on Solid-State Devices

Lee-Trip Overcurrent Relay

From tables 2, 3, 5, and 6 it is seen that the laboratory results on the OCR were 87 pct consistent with the computer results. Although the entire circuit was tested in the laboratory, the power supply system shown in the bottom part of figure 1 of the circuit could not be modeled in the theoretical analysis due to the dimensional limitations of the ECAP software. This is one of the two reasons for the 13 pct inconsistency. Another reason for the disagreement in both the results could be due to the differences in parameter values used in theoretical analysis and their actual values when the laboratory tests were done.

From the results of the two investigations it was observed that the resistor R_7 failed unsafe in the open mode of failure and the resistor R_2 and R_6 failed unsafe in the shorted mode. These components are therefore the critical ones. The other nine components that failed unsafe in the short-circuit test should be examined closely. If the Lee Trip were to be perfect fail-safe device, considerable modification in the circuitry would be required.

Westinghouse Solid-State UVR (Seltronic)

The laboratory test on the UVR was done using suitable techniques and computer simulation analysis was done using SYSCAP software program. From the tables 4 and 7 it is seen that the following components failed safe: Resistors R_1, R_3, R_4, R_5, R_6, R_7, R_9, capacitors C_2, C_3, C_4, diodes D_1, D_2, D_5, D_6, D_7, D_8, and transistors Q_2, Q_3. The zener diode D_4 failed unsafe in the open mode for practical as well as computer simulation analysis. The results of other components did not agree between theoretical and practical approaches. Some of the possible reasons are (1) the bridge rectifier was not included in the computer simulation analysis, whereas it was present when the laboratory test was done on the UVR and (2) the inadequacy of modeling the active components of the device.

In order to make the UVR totally fail-safe the device needs to be redesigned with respect to the components that failed safe in one mode or other. These components are D_4, R_{11}, and Q_4.

Recommendations

The safety performance of a solid-state device depends on how adequately the components of the device have been modeled. In the future, efforts should be made to improve the models of diodes, transistors, rectifiers, and operational amplifiers. Also, prior to laboratory testing, the device should be subjected to environmental conditioning, so that the results obtained are more realistic.

REFERENCES

1. Control Data Corp. Cybernet Services, User Information Manual. Data Services Publications, Minneapolis, Minn., 1975, Chapters 1-7.

2. Crawford, W. T., E. U. Ibok, and S. S. Venkata. Fail-Safe Assessment of Solid-State Overcurrent Relays Using Computer Simulation Technique. Proc. 7th Ann., Pittsburgh Conf., on Modeling and Simulation, v. 7, pt. 1, April 1976, pp. 43-46.

3. Ibok, E. U., W. T. Crawford, S. V. R. Kolluri, and S. S. Venkata. Safety and Reliability Assessment of Solid-State Protective Devices Used in Coal Mine Power Systems. Conf. Rec., 11th Ann. Meeting, IEEE, Ind. Appl. Soc., October 1976, pp. 85-90.

4. International Business Machines. 1620 Electronic Circuit Analysis Program. User's Manual, Program No. 1620-EE-02x, April 1970.

5. Mining Enforcement and Safety Administration. Guidelines for Evaluation of Metered Relays and Solid-State dc Overcurrent Devices for Protecting dc Trolley Feeder Wires. Available from MSHA Technical Support, Beckley Mining Academy, Beckley, W. Va. 25801.

6. Stanek, E. K. Digital Computation of Transients and Safety Testing of Mine Electrical Power Systems. BuMines Open File Rept. 52-78, July 1977, 200 pp.; available for reference at Bureau of Mines facilities in Denver, Colo., Twin Cities, Minn., Bruceton and Pittsburgh, Pa., and Spokane, Wash.; Department of Energy facilities in Carbondale, Ill., and Morgantown, W. Va.; National Mine Health and Safety Academy, Beckley, W. Va.; National Library of Natural Resources, U.S. Department of the Interior, Washington, D.C.; and from National Technical Information Service, Springfield, Va., PB 283 400.

7. _____. Digital Computation of Transients and Safety Testing of Mine Electrical Power Systems. 1975-76 Annual Report. BuMines Open File Rept Rept. 41-77, July 1976, 184 pp.; available for reference at Bureau of Mines facilities in Denver, Colo., Twin Cities, Minn., Bruceton and Pittsburgh, Pa., and Spokane, Wash.; Department of Energy facilities at Carbondale, Ill., and Morgantown, W. Va.; National Library of Natural Resources, U.S. Department of the Interior, Washington, D.C.; and from National Technical Information Service, Springfield, Va., PB 265 074.

AN INTERACTIVE MINE POWER SYSTEM SIMULATION

by

Frederick C. Trutt,[1] Richard A. Rivell,[2] and Lloyd A. Morley[1]

ABSTRACT

For increased safety and production, it is essential that the behavior of mine electrical power systems be clearly understood during normal operating conditions as well as in severe fault situations. As a result, the Bureau of Mines and the Pennsylvania State University have developed a combined alternating current-direct current (ac-dc) interactive mine power system simulation capable of predicting electrical characteristics in these cases. The model utilizes a load-flow approach for determination of system voltages, power flows, and currents under normal or balanced fault operating conditions. Typical loading characteristics, as well as standard cable parameters, are available within the model for ease of system construction. Configuration and parameter modifications may also be made interactively so the results of design changes may be easily determined.

INTRODUCTION

Load-flow and fault studies, which determine voltage, power, and current at various points in an electrical network under specified loading and input conditions, are essential for achieving safe and reliable power system designs. Manual computation in all but the most trivial problems is prohibitively time consuming. As a result of the increasing need for economic and safety studies and their computational complexity, various computer programs have been developed (1-2, 6).[3]

Computer programs for power system studies often utilize an iterative algorithm for the solution of bus voltages and a node basis for establishing a mathematical description of the network. Input data are expressed in percent or per unit, the latter being more convenient. Computation proceeds until prescribed conditions are satisfied to some predetermined degree of precision. After the iterative procedure has converged to the appropriate voltages, bus information and line flows are displayed. Voltage levels, line-power and current flows, and power factor are examined, and appropriate modifications are made to transformer taps, system scheduling, or design. The modified parameters are reevaluated, and the process continues until satisfactory results are obtained. The accepted solution is called a base solution or

[1]Associate professor.
[2]Research assistant.
All of the authors are with the Pennsylvania State University, University Park, Pa.
[3]Underlined numbers in parentheses refer to items in the list of references at the end of this paper.

base case for the prescribed network. Data from the base may be utilized to speed up further studies in which each successive change represents a small deviation from the preceding one. Programs that are iterative have appreciably decreased turnaround time, increased throughput, and simplified network modifications.

The APL load-flow program described herein is typical of predecessor utility-oriented programs. Differences include the availability of default impedance data for common transmission cables in underground mining, default average real and reactive power (loads) for common underground mining equipment, and a capability for analysis of combined alternating current-direct current (ac-dc) systems. Also, interactive modifications include changing transformer taps; adding and/or deleting surge or power correction capacitors; adding and/or deleting transmission cables; adding and/or deleting loads; and adding buses, transformers, and constant voltage buses (5).

Adaptions to the conventional algorithm are greatly facilitated by the APL language, thereby allowing increased computation speed, decreased storage requirements, and flexibility in network configuration. Optimal use of the APL language has been evaluated against clarity, ease of "debugging," and program modification flexibility. Design and execution of the APL load-flow program has been carried out on the IBM 370/168 computer at the Pennsylvania State University under the APLSV processor. However, the capabilities of APLSV (APL shared variable), which allow reading and writing of variables to auxiliary storage, have not been utilized since implementation is not standard. No attempt has been made to contain program size to previously traditional (that is, APL/360) workspace limits, 32,000 bytes. Instead, the full 64,000-byte workspace in APLSV is made available. In its present form, the program occupies approximately 40,000 bytes for problems of the magnitude presented in the examples but could be condensed to fit on a 32,000-byte system simply by using less descriptive variable names.

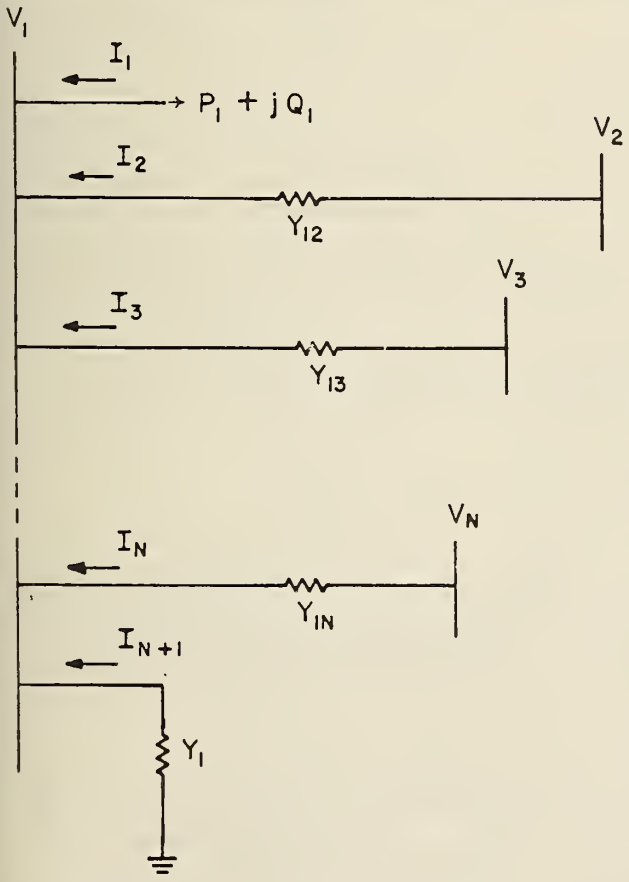

FIGURE 1. - One-line diagram corresponding to bus 1.

THEORETICAL DEVELOPMENT

Model development is formulated around the determination of a corrected voltage at a bus from given line admittances, scheduled real and reactive powers, and initially assigned voltages. Node equations are developed from a one-line power-system diagram with the neutral bus omitted but used as the reference for specification of node or bus voltages.

Figure 1 shows a one-line diagram of a power system segment corresponding to lines terminating on bus 1. The variables are--

V_N = voltage at bus N with respect to ground, per unit,

$Y_{1N} = \frac{1}{Z_{1N}}$, $Z_{1N} = R_{1N} + jX_{1N}$, admittance between bus 1 and bus N, per unit,

Y_1 = total admittance from bus 1 to ground, per unit,

P_1 = real power flowing out of bus 1, per unit,

and Q_1 = reactive power flowing out of bus 1, per unit.

The equations for current entering the network at bus 1 are

$$I_1 = \frac{-(P_1 - jQ_1)}{V_1^*},$$

$$I_2 = Y_{12}(V_2 - V_1),$$

$$I_3 = Y_{13}(V_3 - V_1),$$

$$I_N = Y_{1N}(V_N - V_1),$$

$$I_{N+1} = -Y_1 V_1.$$

Using Kirchoff's current law, substituting and solving for V_1:

$$V_1 = \frac{1}{Y_{11} + Y_1}\left[\frac{-(P_1 - jQ_1)}{V_1^*} + Y_{12}V_2 + Y_{13}V_3 + \ldots + Y_{1N}V_N\right]$$

where $Y_{11} = Y_{12} + Y_{13} + Y_{1N}$ = sum of all admittances connected between bus 1 and the other N buses. For the Kth bus the general equation is

$$V_K = \frac{1}{Y_{KK} + Y_K}\left[\frac{-(P_K - jQ_K)}{V_1^*} + \sum_{n=1}^{N} Y_{KN}V_N\right] \quad n \neq k \qquad (1)$$

Equation 1 determines the corrected value for V_K based on scheduled power P_K and Q_K plus initial voltage estimates. The voltage V_K thus calculated and the estimated value for V_K^* will not agree. Substitution of the conjugate of the calculated value V_K for V_K^* in equation 1 to calculate another value of V_K will bring V_K and V_K^* closer to agreement.

Equation 1 applies at buses where real and reactive power loading (or no connected load) are specified. For the sake of generality, provision for handling controlled generator buses has been included. Here, voltage magnitude rather than reactive power is specified, and the voltage for each iteration is found by computing a value for reactive power and substituting it in equation 1. Reactive power may be determined from equation 1 by rearranging terms and solving for Q_K.

$$Q_K = IM\left[((V_K \times (Y_{KK} + Y_K)) - \sum_{n=1}^{N} Y_{Kn}V_n)\ V_K^*\right]$$

where $n \neq k$ and IM means "imaginary part of." After substitution in equation 1, the new complex V_K is then multiplied by the ratio of the specified constant magnitude of V_K to the magnitude of the computed V_K, yielding the corrected complex voltage of specified magnitude with corrected phase angle.

The corrected complex voltage is found accordingly at each load or generator bus and is used in calculating the corrected voltage at the next. The usual convention is to designate bus 1 as the "swing bus" corresponding to the utility source; that is, no real or reactive power is specified, only voltage magnitude and an assumed voltage-reference angle. Generators at this bus will supply the difference between the specified real and reactive power into the system and the total system output plus losses. Therefore, the process is repeated from bus 2 through the last bus (n) to complete the first iteration. The process is carried out through a number of iterations until the amount of correction in voltage at every bus is less than some predetermined precision index.

Small incremental changes in bus voltage increase the number of iterations required to bring the solution to within an acceptable precision index. Convergence may be accelerated by multiplying the amount of correction in voltage by an appropriate constant. Such constants or multipliers are called acceleration factors. Thus, during calculation of a corrected voltage, the difference between the new value and the previous value is multiplied by the acceleration factor and added to the previous voltage yielding an improved new voltage. Acceleration factors between 1.0 and 1.6 for both real and imaginary components have produced good results depending upon problem type. Determination of the best acceleration factor for a particular problem is difficult, however, and is primarily a matter of judgment. Experience thus far has indicated that factors as high as 1.6, which are often used for utility problems with loop systems, may not be ideal for radial-type mining configurations. In this latter case, values in the range from 1.2 to 1.4 have been found to work best in the majority of problems.

Component representation for determination of the admittances in figure 1 follows standard procedures. Transformers are represented by their π equivalent circuits (6) as shown in figure 2. Here, N is the off-nominal turns ratio for transformer taps set at other than unity, and Y is the reciprocal of the transformer-leakage impedance in per unit. When N = 1, corresponding to a nominal system transformer, this equivalent circuit reduces to the transformer leakage admittance connected between the system buses. Construction of the equivalent circuit is accomplished by the APL load-flow program. The user simply indicates the transformer leakage impedance, off-nominal turns-ratio N, and the bus number associated with the tap side.

Line charging as a result of the capacitance of cables or transmission lines may be handled in two ways. One method allows capacitive reactance to be lumped on buses at the line terminals. If handled in this manner, reactive-power flow through this capacitance will be calculated and displayed in the output. Surge and power-factor-correction capacitors may be handled similarly.

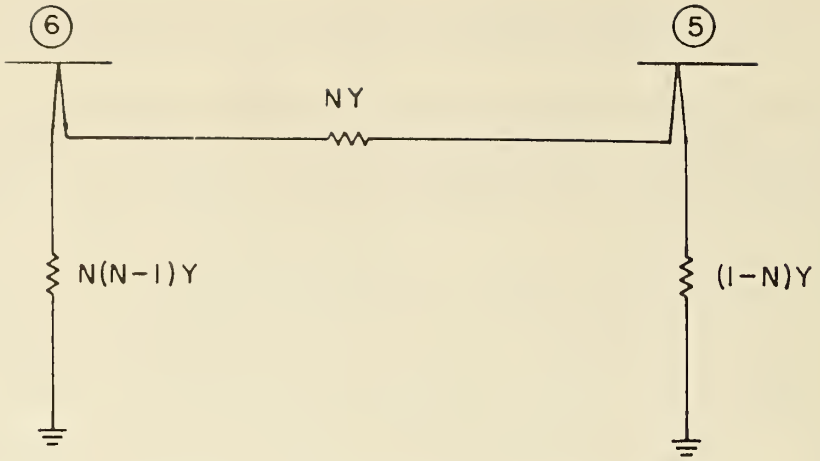

FIGURE 2. - Transformer equivalent circuit.

The alternative to specifying capacitive reactance is to specify capacitive reactance along with the resistance and inductive reactance of the cable or transmission line. Reactive-power flow associated with line charging is then added to the reactive-power flow in the line and displayed as a total for the line. The program utilizes the equivalent circuit in figure 3 for lumping the computed capacitive reactance on the line terminals. The requested input R, X_L, and X_C are in per unit. These quantities are totals for the given size, rating, insulation, and length of the particular cable used.

To facilitate transmission-cable selection and evaluation, a table of per-unit length impedance values for standard cables used in underground mining has been constructed (4) and is stored within the model. As an alternative to resistance, inductive reactance, and capacitive reactance input, standard impedance values may thus be selected by specification of cable size, rating, insulation, and length. To convert stored impedance values to per-unit values, two base values are required. The two chosen here are kilovolt-ampere base and kilovolt base.

Scheduled power loads may be input as one complex number (P + jQ) representing the algebraic sum of loads on a given bus or as a series of loads. Again, to facilitate load selection and evaluation, average (default) load values for various mining equipment have been tabulated (4) and stored. A listing of these load values is given in table 1. To further enhance studies, a mixed input of loads (P + jQ) and equipment numbers (default load values) is permitted. Values greater than or equal to 20 in absolute value are interpreted as equipment default selections.

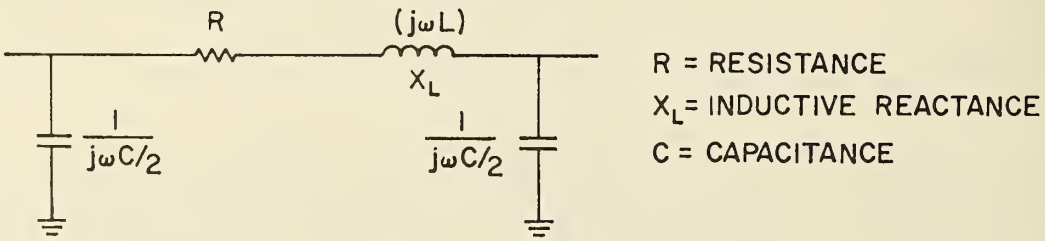

FIGURE 3. - Equivalent π circuit for a cable or transmission line.

TABLE 1. - Equipment default power values

Number	Identification	Current	Hp	V	P, kw	Q, kva	Number	Identification	Current	Hp	V	P, kw	Q, kva
CONTINUOUS MINERS (CUTTING AND LOADING)							BELT DRIVES (ALL MAKES)						
20	CM11	-	525	550	181	359.0	70	-	ac	75	550	39	39.7
21	CM11	-	525	440	181	359.3	71	-	ac	75	440	39	39.7
22	CM26	-	400	550	130	257.7	72	-	dc	75	550	39	0
23	CM26	-	400	440	130	257.9	73	-	dc	75	250	39	0
24	CM28	-	200	550	90	119.6	74	-	ac	100	550	52	53.0
25	CM28	-	200	440	90	120.1	75	-	ac	100	440	52	53.0
26	CM35	-	225	550	120	122.4	76	-	dc	100	550	52	0
27	CM35	-	225	440	120	122.4	77	-	dc	100	250	52	0
28	CM45	-	500	550	175	302.7	78	-	ac	125	550	65	66.3
29	CM45	-	500	440	175	302.9	79	-	ac	125	440	65	66.2
30	CM60	-	500	550	175	302.7	80	-	dc	125	550	65	0
31	CM60	-	500	440	175	302.9	81	-	dc	125	250	65	0
32	CM100	-	525	550	181	359.0	82	-	ac	150	550	78	79.5
33	CM100	-	525	440	181	359.3	83	-	ac	150	440	78	79.5
34	CM245	-	290	550	151	153.7	84	-	dc	150	550	78	0
35	CM245	-	290	440	151	154.0	85	-	dc	150	250	78	0
36	HH105	-	450	550	150	297.7	86	-	ac	175	550	91	92.8
37	HH105	-	450	440	150	297.4	87	-	ac	175	440	91	92.8
38	HH115	-	450	550	150	297.7	88	-	dc	175	550	91	0
39	HH115	-	450	440	150	297.4	89	-	dc	175	250	91	0
40	HH265	-	300	550	157	159.8	90	-	ac	200	550	104	106.1
41	HH265	-	300	440	157	160.0	91	-	ac	200	440	104	106.1
42	HH455	-	450	550	150	297.7	92	-	dc	200	550	104	0
43	HH455	-	450	440	150	297.4	93	-	dc	200	250	104	0
44	HH605	-	450	550	150	297.7	94	-	ac	225	550	117	119.3
45	HH605	-	450	440	150	297.4	95	-	ac	225	440	117	119.3
46	ICM	ac	405	550	181	241.3	96	-	dc	225	550	117	0
47	ICM	ac	405	440	181	241.3	97	-	dc	225	250	117	0
48	ICM	dc	405	550	171	0	98	-	ac	250	550	130	132.6
49	ICM	dc	405	250	181	0	99	-	ac	250	440	130	132.6
50	ICM	ac	475	550	177	306.5	100	-	dc	250	550	130	0
51	ICM	ac	475	440	177	306.5	101	-	dc	250	250	130	0
52	ICM	dc	475	550	177	0	102	-	ac	275	550	143	145.8
53	ICM	dc	475	250	177	0	103	-	ac	275	440	143	145.9
54	8CM	ac	350	550	147	291.7	104	-	dc	275	550	143	0
55	8CM	ac	350	440	147	291.6	105	-	dc	275	250	143	0
56	9CM	ac	395	550	120	160.0	106	-	ac	300	550	156	159.1
57	9CM	ac	395	440	120	159.9	107	-	ac	300	440	156	159.1
58	10CM	ac	535	950	181	359.2	108	-	dc	300	550	156	0
59	10CM	ac	535	550	181	359.1	109	-	dc	300	250	156	0
60	10CM	ac	535	440	181	359.2	FEEDERS-BREAKERS (ALL MAKES)						
61	12CM	ac	385	950	172	229.3	110	-	ac	100	550	60	44.9
62	12CM	ac	385	550	172	229.3	111	-	ac	100	440	60	51.4
63	12CM	ac	385	440	172	229.3	112	-	ac	125	550	65	66.3
64	12CM	ac	530	950	214	285.3	113	-	ac	125	440	65	66.2
65	12CM	ac	530	550	214	285.3	114	-	ac	150	550	75	76.5
66	12CM	ac	530	440	214	285.3	115	-	ac	150	440	75	76.1
67	14CM	ac	350	950	170	226.6	116	-	ac	175	550	78.3	104.4
68	14CM	ac	350	550	170	226.6	117	-	ac	175	440	78.3	104.3
69	14CM	ac	350	440	170	226.6	118	-	ac	200	550	81.2	108.2

TABLE 1. - Equipment default power values--Continued

Number	Identification	Current	Hp	V	P, kw	Q, kva
FEEDERS-BREAKERS (ALL MAKES)--Continued						
119	-	ac	200	440	81.2	108.2
120	-	ac	225	550	83.9	145.2
121	-	ac	225	440	83.9	145.3
FEEDERS (ALL MAKES)						
122	-	ac	50	550	26	26.5
123	-	ac	50	440	26	26.5
124	-	dc	50	550	26	0
125	-	dc	50	250	26	0
126	-	ac	75	550	33.6	44.8
127	-	ac	75	440	33.6	44.8
128	-	dc	75	550	33.6	0
129	-	dc	75	250	33.6	0
130	-	ac	100	550	37.3	64.5
131	-	ac	100	440	37.3	64.6
132	-	dc	100	550	37.3	0
133	-	dc	100	440	37.3	0
ROOF BOLTERS						
134	Single boom.	ac	40	550	15	19.9
135		ac	40	440	15	19.9
136		dc	40	550	15	0
137		dc	40	250	15	0
138	Double boom.	ac	80	550	30	40.0
139		ac	80	440	30	39.9
140		dc	80	550	30	0
141		dc	80	250	30	0
142	Single boom.	ac	30	550	10.5	14.0
143		ac	30	440	10.5	14.0
144		dc	30	550	10.5	0
145		dc	30	250	10.5	0
SECTION FANS						
146	-	ac	50	550	22.4	29.8
147	-	ac	50	440	22.4	29.8
148	-	ac	40	550	18	24.0
149	-	ac	40	440	18	24.0
150	-	ac	25	550	11.2	14.9
151	-	ac	25	440	11.2	14.9
SHUTTLE CARS						
152	10SC	ac	95	550	13	13.2
153	10SC	ac	95	440	13	13.2
154	10SC	dc	60	550	13	0
155	10SC	dc	60	250	13	0
156	10SC	ac	135	550	15	19.9
157	10SC	ac	135	440	15	19.9
158	10SC	dc	105	550	15	0
159	10SC	dc	105	250	15	0
160	15SC	ac	160	550	20	26
161	15SC	ac	160	440	20	26
162	16SC	ac	90	550	10	13
163	16SC	ac	90	440	10	13
164	16SC	dc	55	550	10	0
165	16SC	dc	55	250	10	0
166	18SC	ac	57.5	550	9	9.18
167	18SC	ac	57.5	440	9	9.19
168	18SC	dc	45	550	9	0
169	18SC	dc	45	250	9	0
170	40	ac	40	550	15	15.3
171	40	ac	40	440	15	15.2
172	40	dc	40	550	15	0
173	40	dc	40	250	15	0
174	48	ac	60	550	18	31.1
175	48	ac	60	440	18	31.1
176	48	dc	60	550	18	0
177	48	dc	60	250	18	0

Synchronous machines and generators, at other than the swing bus, require specification of real-power and constant-voltage magnitude. Fixed-voltage buses may also be utilized as an aid in performing fault computations. In this case, a constant complex voltage is specified.

Finally, a check has been incorporated for comparing the current flows in cables and transformers with rated values. This procedure utilizes stored cable ampacities and component ratings. Should these be exceeded, a message to that effect is printed.

SIMULATION USE AND EXAMPLES

Simulation operation is entirely interactive between the user, situated at an appropriate terminal, and the connected computer. The terminal-computer connection may be hard-wired or can easily be established over a standard telephone link. The following three examples will show user-computer dialog during interactive operation of the model. The first two demonstrations illustrate use of the simulation for load-flow computations of mixed ac-dc as well as ac systems, while the final example shows modification and fault computation capabilities.

The first case study is a mixed ac-dc system corresponding to rail haulage in an underground coal mine as shown in figure 4 (5). The connections between buses 1, 2, 3, 4, 5, and 6 represent the cables and transformers of the ac portion of the system, while the connections between buses 5, 6, 7, 8, 9, and 10 represent the dc cable and rectifier resistances. The rectifiers are, of course, situated at buses 5 and 6. The load on bus 4 represents an induction motor ac load while the loads on buses 7 to 10 represent dc haulage loading for a specified position of the locomotive on its track.

The conversation between computer and user for input of this example was as given in table 2. In all cases, computer responses are given in italics while user input is shown in standard type. First, a simulation run is initiated by user input of the word "loadflow." The computer responds with a reminder to use per-unit values and request a run name. Further dialog indicates that load and cable default values will not be utilized in the run (all parameters will be input as their actual per-unit impedances or powers), that the exceeding of the transformer or cable capacities will not be checked, that a voltage precision index of 0.0001 has been selected, and that this is a 10-bus problem with a reference voltage on the swing bus of 1.0 + j0.0. The computer then requests pure ac or pure dc cable input which is supplied as the bus pair connected plus the cable resistance, inductive reactance, and capacitive reactance (an infinite value of shunt capacitive reactance is represented by a zero). In this example, transformer leakage impedances are also supplied as if they were cable connections since all transformers are set at nominal taps. The end of this data is then signified by a zero, and the computer requests data on ac-dc connections. This is given as the bus pair and resistance with a zero input to signify the termination of data. Loading is then requested, and this information is supplied as per-unit real and reactive load power. This problem has no capacitators, generators, voltage sources, or transformers set at off-nominal taps, and no errors in input requiring modification have been made. An offer to display line currents of connecting elements in the output is declined, and the computer informs the user that simulation execution has begun. Upon completion of computations, the user is told that convergence has been achieved after 97 iterations, and the system bus voltages and line power flows are displayed (line currents were refused during input). Finally, a request for modifications is made which would allow the user to reconfigure the system and initiate a new run using these base-case bus voltages as a starting point in the iteration procedure. The negative response terminates execution, and the example is completed.

TABLE 2. - AC-DC rail haulage example

```
     LOADFLOW
          LOADFLOW 7 13 1977 - INPUT/OUTPUT IN PER UNIT
          RUN NAME:  AC-DC HAULAGE EXAMPLE

WILL LOAD OR CABLE DEFAULT VALUES BE USED THIS RUN?  YES OR NO
NO
ARE CABLE AND TRANSFORMER AMPACITIES TO BE CHECKED?  YES OR NO
NO
INPUT:  CONVERGENCE TOLERANCE (1E-3, 1E-6, ETC.)
     1E-4
INPUT:  TOTAL NUMBER OF BUSES
     10
INPUT:  VOLTAGE AT SWING BUS (BUS NUMBER 1)
     1.0  0.0

                FOR ALL (NON AC TO DC) CABLES
INPUT:  BUS PAIR, CABLE IMPEDANCE (R XL XC)

INDICATE END OF CABLE DATA BY ZERO
     1 2 .00145  .05051 0
INPUT NEXT CABLE
     2 3 .00580 .001999 0
INPUT NEXT CABLE
     3 4 .22105 .19100 0
INPUT NEXT CABLE
     2 5 .00370 .160997 0
INPUT NEXT CABLE
     3 6 .00370 .16099 0
INPUT NEXT CABLE
     10 9 .43196 0 0
INPUT NEXT CABLE
     0

                FOR ALL AC TO DC CONNECTIONS
INPUT:  AC BUS, DC BUS, RESISTANCE
     5 9 .215982
     5 8 .431965
     6 8 .215982
     6 7 .215982
     0

                FOR ALL SCHEDULED LOADS
INPUT:  BUS NUMBER, POWER VALUES (+P +Q)
INDICATE END OF LOAD DATA BY ZERO
     4 .133 .177
     7 .133 0
     8 .133 0
     9 .133 0
     10 .133 0
     0
ARE TRANSFORMERS, CAPACITORS, GENERATORS, OR VOLTAGE SOURCES REQUIRED INITIALLY?
NO
```

TABLE 2. - AC-DC rail haulage example--Continued

```
ARE MODIFICATIONS DESIRED?  YES OR NO
NO
SHOULD LINE CURRENTS BE DISPLAYED?  YES OR NO
NO
EXECUTING

CONVERGENCE TO WITHIN A TOLERANCE OF 0.0001 REAL 0.0001 IMAGINARY REACHED
AFTER 97 ITERATIONS

BUS VOLTAGES
```

	XY COORDINATES		POLAR COORDINATES	
BUS	REAL	IMAGINARY	VOLTAGE MAG	ANGLE(DEGREES)
1	1.0000000000	.0000000000	1.0000000000	.0000000000
2	.9864767189	-.0358439658	.9871277054	-2.0809460903
3	.9839242532	-.0353413172	.9845587563	-2.0571077168
4	.9152003486	-.0913299763	.9153960145	-1.1846726773
5	.9800167495	-.0913299763	.9842631731	-5.3241457075
6	.9804435405	-.0715518695	.9830509682	-4.1739937292
7	.9529056594	.0000000000	.9529056594	.0000000000
8	.9644059423	.0000000000	.9644059423	.0000000000
9	.9192740609	.0000000000	.9192740609	.0000000000
10	.8518300131	.0000000000	.8518300131	.0000000000

LINE FLOWS

BUS		POWER FLOW			REVERSE POWER FLOW		
FROM	TOWARD	P	Q	PF	P	Q	PF
1	2	.71674	.24716	.95	-.71590	-.21813	.96
2	3	.36933	.19701	.88	-.36829	-.19665	.88
3	4	.14593	.18817	.61	-.13300	-.17700	.60
2	5	.34186	.01937	1.00	-.34142	.00000	1.00
3	6	.22226	.00822	1.00	-.22207	.00000	1.00
10	9	-.13300	.00000	1.00	.14353	.00000	1.00
5	9	.29617	.00000	1.00	-.27661	.00000	1.00
5	8	.04525	.00000	1.00	-.04433	.00000	1.00
6	8	.08486	.00000	1.00	-.08325	.00000	1.00
6	7	.13721	.00000	1.00	-.13300	.00000	1.00

```
ARE MODIFICATIONS DESIRED?  YES OR NO
NO
```

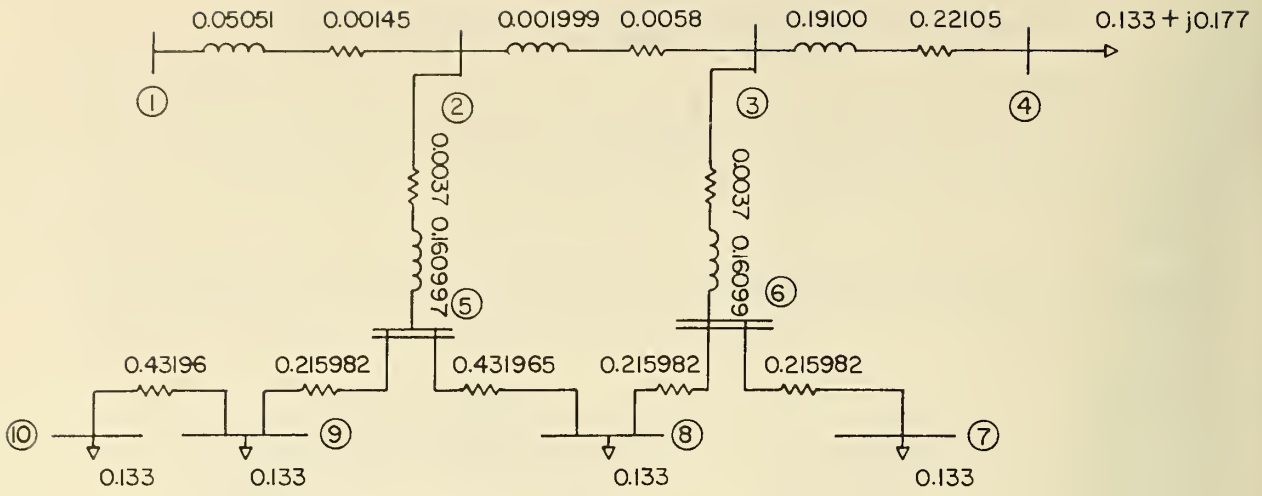

FIGURE 4. - Underground coal mine rail haulage example.

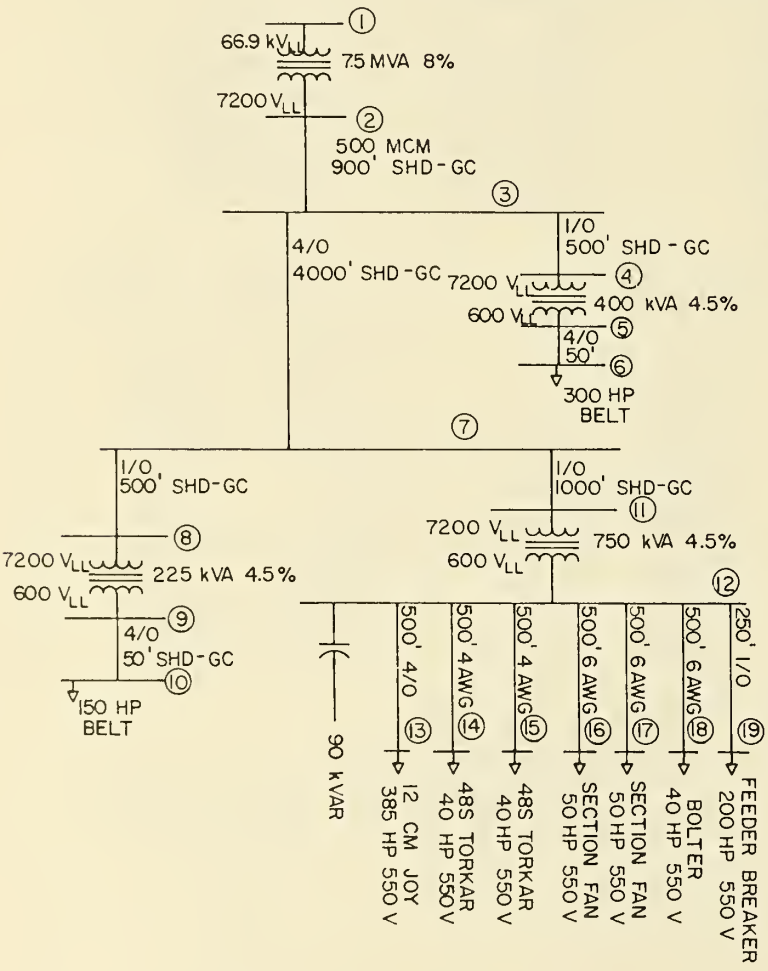

FIGURE 5. - Typical underground coal mine section.

A second example depicting one section of a purely ac underground coal mine is shown in figure 5. Here, the swing bus (bus 1) represents the utility connection at the main-mine transformer and all loads, cables, and transformers are as indicated. Transformer leakage reactances are in percent on the transformer rating.

For this situation, the user-computer conversation proceeds (table 3) as before except that now load or cable default values may be utilized and ampacity checks are requested. As a result, the problem power vase is also requested as input. The use of cable defaults now allows for these inputs in terms of cable size and length as shown. In addition, information on voltage ratings, whether shielded or unshielded, insulation type, and the line-to-line voltage base at the cable are required by the program in order to select the proper

impedances from the default table and convert them to per-unit values. Next, scheduled loads are requested and input as default values from table 1, with the exception of the 90-kvar (kilovolt-amper reactive) capacitor on bus 12. This load is presented as per-unit real and reactive power as shown in the previous example. This reactive power is negative since the capacitance supplies reactive power to the system. No fixed-voltage sources, shunt capacitors, or constant-voltage buses are required initially, and all transformers leadage impedances are specified in per unit. Transformer taps are set at nominal and kilovolt-ampere ratings are required for ampacity checking. No input errors were found that required modification, and it is not required that line currents be displayed. After interpretation of the user response to the line-current question, the computer initiates execution and presents output information for this run in the form of rectangular and polar-form bus voltages plus all line power flows and power factors. A request for system modification is the issued.

As a final example (table 4) showing the capabilities of system modification and fault analysis, the question is answered in the affirmative, the run is named, and the list of possible modifications is viewed. To simulate the fault situation, modify loads, add cables, and add capacitor modifications are selected. This will allow reconfiguration of the system into a form for standard fault analysis (3). Such a computation requires that all default induction-machinery loads be removed and that these machines be replaced by their transient reactances connected in series with a unit-voltage source. Thus, the fault is simulated by a small resistance (10^{-15} per unit) connected between bus 12 and ground, and all default loads are removed. Replacement of these loads is then accomplished by connecting simulated cables with a reactance equal to the machine transient reactances from all load buses to the swing bus. The computer then resumes execution, and upon convergence the bus voltages, line power flows and currents are output. The bus-to-ground current from bus 12 of 73.6 per unit corresponds to an actual fault current of 15.9 ka.

TABLE 3. - AC system case study

```
LOADFLOW
     LOADFLOW 7 13 1977 - INPUT/OUTPUT IN PER UNIT
     RUN NAME:  UNDERGROUND MINING SECTION

WILL LOAD OR CABLE DEFAULT VALUES BE USED THIS RUN?  YES OR NO
YES
ARE CABLE AND TRANSFORMER AMPACITIES TO BE CHECKED?  YES OR NO
YES
INPUT:  POWER BASE (THREE PHASE IN KVA)
     225
INPUT:  CONVERGENCE TOLERANCE (1E-3, 1E-6, ETC.)
     1E-2
INPUT:  TOTAL NUMBER OF BUSES
     19
INPUT:  VOLTAGE AT SWING BUS (BUS NUMBER 1)
     1.0  0.0

                FOR ALL (NON AC TO DC) CABLES
INPUT:  BUS PAIR, CABLE IMPEDANCE (R XL XC)

(TO UTILIZE CABLE DEFAULT VALUES IN PLACE OF CABLE IMPEDANCES:  USE CABLE SIZE
FOLLOWED BY LENGTH (FT)
SELECT 1 AWG USING 1, 1/0 AWG USING 10, 250 MCM USING 250, ETC.)
INDICATE END OF CABLE DATA BY ZERO
     2 3 500 900
INPUT:  VOLTAGE RATING, INSULATION TYPE (2KVSHD EPR, ETC.)
     8KVSHD EPR
INPUT:  KVBASE (LINE-TO-LINE) FOR THIS CABLE
     7.2
INPUT NEXT CABLE
     3 7 40 4000
INPUT:  VOLTAGE RATING, INSULATION TYPE (2KVSHD EPR, ETC.)
     8KVSHD EPR
INPUT:  KVBASE (LINE-TO-LINE) FOR THIS CABLE
     7.2
INPUT NEXT CABLE
     7 8 10 500
INPUT:  VOLTAGE RATING, INSULATION TYPE (2KVSHD EPR, ETC.)
     8KVSHD EPR
INPUT:  KVBASE (LINE-TO-LINE) FOR THIS CABLE
     7.2
INPUT NEXT CABLE
     9 10 40 50
INPUT:  VOLTAGE RATING, INSULATION TYPE (2KVSHD EPR, ETC.)
     2KVSHD EPR
INPUT:  KVBASE (LINE-TO-LINE) FOR THIS CABLE
     .6
INPUT NEXT CABLE
     7 11 10 1000
INPUT:  VOLTAGE RATING, INSULATION TYPE (2KVSHD EPR, ETC.)
     8KVSHD EPR
INPUT:  KVBASE (LINE-TO-LINE) FOR THIS CABLE
     7.2
```

TABLE 3. - AC system case study--Continued

```
INPUT NEXT CABLE
     12 13 40 500
INPUT:  VOLTAGE RATING, INSULATION TYPE (2KVSHD EPR, ETC.)
     2KVSHD EPR
INPUT:  KVBASE (LINE-TO-LINE) FOR THIS CABLE
     .6
INPUT NEXT CABLE
     12 14 4 500
INPUT:  VOLTAGE RATING, INSULATION TYPE (2KVSHD EPR, ETC.)
     2KVSHD EPR
INPUT:  KVBASE (LINE-TO-LINE) FOR THIS CABLE
     .6
INPUT NEXT CABLE
     12 15 4 500
INPUT:  VOLTAGE RATING, INSULATION TYPE (2KVSHD EPR, ETC.)
     2VKSHD EPR
INPUT:  KVBASE (LINE-TO-LINE) FOR THIS CABLE
     .6
INPUT NEXT CABLE
     12 16 6 500
INPUT:  VOLTAGE RATING, INSULATION TYPE (2KVSHD EPR, ETC.)
     2KVSHD EPR
INPUT:  KVBASE (LINE-TO-LINE) FOR THIS CABLE
     .6
INPUT NEXT CABLE
     12 17 6 500
INPUT:  VOLTAGE RATING, INSULATION TYPE (2KVSHD EPR, ETC.)
     2KVSHD EPR
INPUT:  KVBASE (LINE-TO-LINE) FOR THS CABLE
     .6
INPUT NEXT CABLE
     12 18 6 500
INPUT:  VOLTAGE RATING, INSULATION TYPE (2KVSHD EPR, ETC.)
     2KVSHD EPR
INPUT:  KVBASE (LINE-TO-LINE) FOR THIS CABLE
     .6
INPUT NEXT CABLE
     12 19 10 250
INPUT:  VOLTAGE RATING, INSULATION TYPE (2KVSHD EPR, ETC.)
     2KVSHD EPR
INPUT:  KVBASE (LINE-TO-LINE) FOR THIS CABLE
     .6
INPUT NEXT CABLE
     3 4 10 500
INPUT:  VOLTAGE RATING, INSULATION TYPE (2KVSHD EPR, ETC.)
     8KVSHD EPR
INPUT:  KVBASE (LINE TO LINE) FOR THIS CABLE
     7.2
INPUT NEXT CABLE
     5 6 40 50
INPUT:  VOLTAGE RATING, INSULATION TYPE (2KVSHD EPR, ETC.)
     2KVSHD EPR
INPUT:  KVBASE (LINE-TO-LINE) FOR THIS CABLE
     .6
INPUT NEXT CABLE
     0
```

TABLE 3. - AC system case study--Continued

```
                FOR ALL AC TO DC CONNECTIONS
INPUT:  AC BUS, DC BUS, RESISTANCE
     0

                FOR ALL SCHEDULED LOADS
INPUT:  BUS NUMBER, POWER VALUES (+P +Q) AND DEFAULT NUMBERS
INDICATE END OF LOAD DATA BY ZERO
     6 106
     10 82
     12 0 -.4
     13 62
     14 170
     15 170
     16 146
     17 146
     18 134
     19 118
      0
ARE TRANSFORMERS, CAPACITORS, GENERATORS, OR VOLTAGE SOURCES REQUIRED INITIALLY?
YES
                FOR ALL FIXED VOLTAGE SOURCES
INPUT:  BUS, FIXED VOLTAGE
INDICATE END BY ZERO
     0

                FOR ALL CAPACITORS
INPUT:  BUS NUMBER, IMPEDANCE (R X)
INDICATE END OF CAPACITOR DATA BY ZERO
     0

                FOR ALL CONSTANT VOLTAGE BUSES
INPUT:  BUS NUMBER, REAL POWER, VOLTAGE MAGNITUDE
INDICATE END OF CONSTANT VOLTAGE DATA BY ZERO
     0

                FOR ALL TRANSFORMERS
INPUT:  BUS PAIR (TAP SIDE FIRST), IMPEDANCE (R X), RATIO, KVA RATING
INDICATE END OF TRANSFORMER DATA BY ZERO
     1 2 .00015 .0024 1.0 7500
     8 9 .01 .045 1.0 225
     11 12 .003 .0135 1.0 750
     4 5 .005625 .025312 1.0 400
     0
ARE MODIFICATIONS DESIRED?  YES OR NO
NO
SHOULD LINE CURRENTS BE DISPLAYED?  YES OR NO
NO
EXECUTING
```

TABLE 3. - AC system case study--Continued

CONVERGENCE TO WITHIN A TOLERANCE OF 0.01 REAL 0.01 IMAGINARY REACHED AFTER 165 ITERATIONS

BUS VOLTAGES

BUS	XY COORDINATES REAL	XY COORDINATES IMAGINARY	POLAR COORDINATES VOLTAGE MAG	POLAR COORDINATES ANGLE(DEGREES)
1	1.0000000000	.0000000000	1.0000000000	.0000000000
2	.9918527016	-.0065477011	.9918743137	-.3782317555
3	.9911694322	-.0065402549	.9911910100	-.3780620649
4	.9909008887	-.0063768004	.9909214070	-.3687136743
5	.9676619503	-.0201833844	.9678724188	-1.1948956801
6	.9654910354	-.0192343672	.9656826085	-1.1412869331
7	.9873953811	-.0051502755	.9874088130	-.2988533056
8	.9872577031	-.0050649400	.9872706954	-.2939426417
9	.9658486105	-.0175504007	.9660080512	-1.0410050037
10	.9647613723	-.0170782617	.9649125206	-1.0141472846
11	.9861761496	-.0044107366	.9861860132	-.2562573691
12	.9580845817	-.0211535726	.9583180783	-1.2648293958
13	.9307982812	-.0051769837	.9308126779	-.3186686815
14	.9497951509	-.0140325026	.9498988050	-.8464400777
15	.9497951509	-.0140325026	.9498988050	-.8464400777
16	.9380479885	.001959523	.9380500352	.1196882698
17	.9380479885	.001959523	.9380500352	.1196882699
18	.9448920066	-.0057118496	.9449092705	-.3463474102
19	.9476869360	-.0122891553	.9477666126	-.7429428860

LINE FLOWS

BUS FROM	BUS TOWARD	POWER FLOW P	POWER FLOW Q	PF	REVERSE POWER FLOW P	REVERSE POWER FLOW Q	PF
2	3	2.87723	2.99792	.69	-2.87524	-3.00432	.69
3	7	2.08262	2.17101	.69	-2.07165	-2.19818	.69
7	8	.36205	.38568	.68	-.36197	-.38887	.68
9	10	.34723	.35370	.70	-.34667	-.35346	.70
7	11	1.61003	1.68608	.69	-1.60678	-1.69161	.69
12	13	.80425	1.03614	.61	-.76445	-1.01919	.60
12	14	.06776	.06813	.71	-.06667	-.06803	.70
12	15	.06776	.06813	.71	-.06667	-.06803	.70
12	16	.10495	.13313	.62	-.09956	-.13278	.60
12	17	.10495	.13313	.62	-.09956	-.13278	.60
12	18	.06905	.08889	.61	-.06667	-.08874	.60
12	19	.36932	.48332	.61	-.36089	-.48131	.60
3	4	.71250	.74620	.69	-.71219	-.74935	.69
5	6	.69557	.70817	.70	-.69333	-.70722	.70
1	2	2.92894	3.21165	.67	-2.92610	-3.16631	.68
8	9	.36249	.38774	.68	-.35960	-.37473	.69
11	12	1.60766	1.68936	.69	-1.59088	-1.61387	.70
4	5	.71254	.74791	.69	-.70643	-.72040	.70

ARE MODIFICATIONS DESIRED? YES OR NO

TABLE 4. - Fault example

```
ARE MODIFICATIONS DESIRED?  YES OR NO
YES
     DESCRIPTION:
WOULD YOU LIKE TO SEE THE LIST OF MODIFICATION OPTIONS?  YES OR NO
YES
```

MODIFICATION	OPTION NAME
INCREASE NUMBER OF BUSES	ADD BUSES
CHANGE TAPS ON TRANSFORMERS CURRENTLY IN THE SYSTEM	CHANGE TAPS
ADDITION AND/OR DELETION OF LOADS ON BUSES CURRENTLY IN THE SYSTEM	MODIFY LOADS
ADDITION AND/OR DELETION OF SURGE AND/OR POWER FACTOR CORRECTION CAPACITORS ON BUSES CURRENTLY IN THE SYSTEM	ADD CAPACITORS OR DELETE CAPACITORS OR ADD/DELETE CAPACITORS
ADDITION AND/OR DELETION OF TRANSMISSION LINES ON BUSES CURRENTLY IN THE SYSTEM	ADD CABLES OR DELETE CABLES OR ADD/DELETE CABLES
ADDITION OF TRANSFORMERS BETWEEN BUSES CURRENTLY IN THE SYSTEM	ADD TRANSFORMERS
ADDITION OF CONSTANT VOLTAGE REQUIREMENTS ON BUSES CURRENTLY IN THE SYSTEM	ADD FIXED VOLTS
ADDITION OF VOLTAGE SOURCES	ADD VOLTAGE SOURCES

```
INPUT:    LIST OF OPTION NAMES DESIRED

MODIFY LOADS ADD CAPACITORS ADD CABLES

                CAPACITOR MODIFICATIONS
                     ADDITIONS (ONE AT A TIME)
 INPUT:  BUS NUMBER, IMPEDANCE (R X)
 INDICATE END OF CAPACITOR BY ZERO
      12 1E-15 0

      0
```

TABLE 4. - Fault example--Continued

```
                FOR ALL SCHEDULED LOADS
INPUT:  BUS NUMBER, POWER VALUES (+P +Q) TO BE ADDED AND DEFAULT NUMBERS
[NOTE:  TO DELETE USE NEGATIVE VALUES]
INDICATE END OF LOAD DATA BY ZERO
     6 -106
    10 -82
    12 0 .4
    13 -62
    14 -170
    15 -170
    16 -146
    17 -146
    18 -134
    19 -118
     0

              TRANSMISSION CABLE MODIFICATIONS
              ADDITIONS (ONE AT A TIME)
INPUT:  BUS PAIR, CABLE IMPEDANCE (R XL XC)
     1 6 0 .15 0
INPUT:  EQUIVALENT CABLESIZE FOR AMPACITY CHECK
     500
INPUT:  KVBASE (LINE-TO-LINE) TO BE USED FOR AMPACITY CHECK
     .6
INPUT NEXT CABLE
     1 10 0 .3 0
INPUT:  EQUIVALENT CABLESIZE FOR AMPACITY CHECK
     500
INPUT:  KVBASE (LINE-TO-LINE) TO BE USED FOR AMPACITY CHECK
     .6
INPUT NEXT CABLE
     1 19 0 .225 0
INPUT:  EQUIVALENT CABLE SIZE FOR AMPACITY CHECK
     500
INPUT:  KVBASE (LINE-TO-LINE) TO BE USED FOR AMPACITY CHECK
     .6
INPUT NEXT CABLE
     1 18 0 1.25 0
INPUT:  EQUIVALENT CABLESIZE FOR AMPACITY CHECK
     500
INPUT:  KVBASE (LINE-TO-LINE) TO BE USED FOR AMPACITY CHECK
     .6
INPUT NEXT CABLE
     1 17 0 .9 0
INPUT:  EQUIVALENT CABLESIZE FOR AMPACITY CHECK
     500
INPUT:  KVBASE (LINE-TO-LINE) TO BE USED FOR AMPACITY CHECK
     .6
INPUT NEXT CABLE
     1 16 0 .9 0
INPUT:  EQUIVALENT CABLESIZE FOR AMPACITY CHECK
     500
INPUT:  KVBASE (LINE-TO-LINE) TO BE USED FOR AMPACITY CHECK
     .6
INPUT NEXT CABLE
     15   0 1.125 0
```

TABLE 4. - Fault example--Continued

```
INPUT:  EQUIVALENT CABLESIZE FOR AMPACITY CHECK
     500
INPUT:  KVBASE (LINE-TO-LINE) TO BE USED FOR AMPACITY CHECK
     .6
INPUT NEXT CABLE
     1 14 0 1.125 0
INPUT:  EQUIVALENT CABLESIZE FOR AMPACITY CHECK
     500
INPUT:  KVBASE (LINE-TO-LINE) TO BE USED FOR AMPACITY CHECK
     .6
INPUT NEXT CABLE
     1 13 0 .116883 0
INPUT:  EQUIVALENT CABLESIZE FOR AMPACITY CHECK
     500
INPUT:  KVBASE (LINE-TO-LINE) TO BE USED FOR AMPACITY CHECK
     .6
INPUT NEXT CABLE
     0
SHOULD LINE CURRENTS BE DISPLAYED?  YES OR NO
YES
EXECUTING RESUMED

CONVERGENCE TO WITHIN A TOLERANCE OF 0.01 REAL 0.01 IMAGINARY REACHED AFTER
 197 ITERATIONS

BUS VOLTAGES
```

	XY COORDINATES		POLAR COORDINATES	
BUS	REAL	IMAGINARY	VOLTAGE MAG	ANGLE(DEGREES)
1	1.0000000000	.0000000000	1.0000000000	.0000000000
2	.8637305919	-.0369752598	.8645216627	-2.4512662167
3	.8553151342	-.0329237888	.8559485701	-2.2044076994
4	.8554127427	-.0331325781	.8560541619	-2.2181203559
5	.8754483565	-.0341596058	.8761145493	-2.2345222751
6	.8766989203	-.0356907420	.8774251113	-2.3312453669
7	.8026505894	.0214919043	.8029382733	1.5337947381
8	.8026298237	.0213373513	.8029133929	1.5228094729
9	.8224227427	.0074085601	.8224561109	.5161186841
10	.8229142293	.0061356655	.8229371028	.4271905973
11	.7846448350	.0506895512	.7862804511	3.6962801992
12	.0000000000	.0000000000	.0000000000	-75.6298215895
13	.0976437240	-.1522489974	.1808702685	-57.3262294445
14	.0185720611	-.0936879163	.0955109790	-78.7874339000
15	.0185720611	-.0936879163	.0955109790	-78.7874339000
16	.0471216920	-.1802566918	.1863140596	-75.3499030862
17	.0471216920	-.1802566918	.1863140596	-75.3499030862
18	.0327144851	-.1467679452	.1503697685	-77.4342247063
19	.0297792793	-.0883217286	.0932069376	-71.3675290982

TABLE 4. - Fault example--Continued

LINE FLOWS

BUS FROM	BUS TOWARD	POWER P	POWER Q	PF	CURRENT MAG	CURRENT ANGLE
2	3	17.57001	46.31691	.35	57.30044	288.32264
3	7	16.55629	46.22149	.34	57.36001	287.50285
7	8	.17292	-.37837	.42	.51812	66.97277
9	10	.02119	-.48531	.04	.59064	88.01562
7	11	11.57774	44.15517	.25	56.85096	286.22633
12	13	.00000	.00000	1.00	7.82928	99.57695
12	14	.00000	.00000	.99	.87635	95.45293
12	15	.00000	.00000	.99	.87635	95.45293
12	16	.00000	.00000	1.00	1.07753	100.71204
12	17	.00000	.00000	1.00	1.07753	100.71204
12	18	.00000	.00000	.99	.86965	98.62771
12	19	.00000	.00000	.99	4.32992	95.20144
3	4	-.13400	-.64126	.20	.76536	99.59843
5	6	-.23638	-.71150	.32	.85575	106.14357
1	2	18.88129	55.59884	.32	58.71741	288.75741
8	9	.17233	.38472	.41	.52503	67.39376
11	12	9.69783	43.64026	.22	56.85606	286.22509
4	5	-.13558	-.64830	.20	.77370	99.59439
1	6	.23794	.82201	.28	.85575	286.14362
1	10	-.02045	.59029	.03	.59064	268.01561
1	19	.39254	4.31209	.09	4.32992	275.20145
1	18	.13046	.85981	.15	.86965	278.62778
1	17	.20029	1.05875	.19	1.07753	280.71210
1	16	.20029	1.05875	.19	1.07753	280.71210
1	15	.08328	.87238	.10	.87635	275.45298
1	14	.08328	.87238	.10	.87635	275.45298
1	13	1.30258	7.72017	.17	7.82928	279.57696
3	2	-17.19803	-45.93846	.35	57.30737	108.32003
8	7	-.17284	.37627	.42	.51571	246.85041
10	9	-.02045	.48563	.04	.59064	268.01561
11	7	-9.69783	-43.64026	.22	56.85606	106.22509
13	12	1.30258	.55551	.92	7.82928	279.57696
14	12	.08328	.00840	.99	.87635	275.45298
15	12	.08328	.00840	.99	.87635	275.45298
16	12	.20029	.01379	1.00	1.07753	280.71210
17	12	.20029	.01379	1.00	1.07753	280.71210
18	12	.13046	.00898	1.00	.86965	278.62778
19	12	.39254	.09374	.97	4.32992	275.20145
4	3	.13417	.63889	.21	.76260	279.64188
6	5	.23794	.71216	.32	.85575	286.14362
2	1	-18.36413	-47.32428	.36	58.71741	108.75741
9	8	-.16957	.39713	.39	.52503	247.39376
12	11	.00000	.00000	1.00	56.85606	106.22509
5	4	.13895	.66345	.20	.77370	279.59439
6	1	-.23794	-.71216	.32	.85575	106.14362
10	1	.02045	-.48563	.04	.59064	88.01561
19	1	-.39254	-.09374	.97	4.32992	95.20145
18	1	-.13046	-.00898	1.00	.86965	98.62778
17	1	-.20029	-.01379	1.00	1.07753	100.71210
16	1	-.20029	-.01379	1.00	1.07753	100.71210
15	1	-.08328	-.00840	.99	.87635	95.45298
14	1	-.08328	-.00840	.99	.87635	85.45298
13	1	-1.30258	-.55551	.92	7.82828	99.57695

TABLE 4. - Fault example--Continued

FROM BUS	TO GROUND	P	Q	MAG	ANGLE
12	0	.00000	.00000	73.65024	284.37018

CURRENT RATING EXCEEDED IN TRANSFORMERS

ON BUS	ACTUAL CURRENT (P U)	RATED CURRENT (P U)
1	58.717	33.333
11	56.856	3.333

CURRENT RATING EXCEEDED IN CABLES

FROM BUS	TO BUS	ACTUAL AMPS	RATED AMPS
2	3	1034	536
3	7	1035	321
7	11	1026	211
12	13	1695	321
12	14	190	122
12	15	190	122
12	16	233	93
12	17	233	93
12	18	188	93
12	19	937	211
1	19	937	536
1	13	1695	536

ARE MODIFICATIONS DESIRED? YES OR NO
NO

CONCLUSIONS

It has been demonstrated that the interactive mine power system simulation may be used to predict mine power system behavior under typical operating conditions as well as in fault situations. Such simulations may be effectively utilized by personnel in the mining industry for system design as well as for locating problem areas of existing networks. Interactive conversation greatly enhances and speeds up analysis. Further, construction of a systematic method for the sizing of circuit breakers, fuses, transformers, cables, and other components is facilitated by the ease with which system modifications may be made. All of these should lead to the design of safer and more reliable mine power systems.

REFERENCES

1. Consolidation Coal Co. Program Final for Power System Analysis--Users Guide. Midwestern Region, Evansville, Ind., 1975, 10 pp.

2. Coombe, L. W., and D. G. Lewis. Digital Calculation of Short-Circuit Currents in Large Complex-Impedance Networks. Trans. AIEE, v. 75, pt. 3, 1956, pp. 1394-1397.

3. Elgard, O. I. Electrical Energy Systems Theory. McGraw-Hill Book Co., Inc., New York, 1971, 564 pp.

4. Morley, L. A., F. C. Trutt, and R. A. Rivell. Coal Mine Electrical System Evaluation. Extended APL Mine Electrical System Load-Flow Program. BuMines Open File Rept. 55-78, Sept. 30, 1977, 100 pp.; available for reference at the Bureau of Mines facilities in Denver, Colo., Twin Cities, Minn., Bruceton and Pittsburgh, Pa., and Spokane, Wash.; Department of Energy facilities in Carbondale, Ill., and Morgantown, W. Va.; National Mine Health and Safety Academy, Beckley, W. Va.; National Library of Natural Resources, U.S. Department of the Interior, Washington, D.C.; and from National Technical Information Service, Springfield, Va., PB 283 497.

5. Stanek, E. K. Digital Computation of Transients and Safety Testing of Mine Electrical Power Systems. BuMines Open File Rept. 52-78, July 1977, 200 pp.; available for reference at Bureau of Mines facilities in Denver, Colo., Twin Cities, Minn., Bruceton and Pittsburgh, Pa., and Spokane, Wash.; Department of Energy facilities in Carbondale, Ill., and Morgantown, W. Va.; National Mine Health and Safety Academy, Beckley, W. Va.; and National Library of Natural Resources, U.S. Department of the Interior, Washington, D.C.; and from National Technical Information Service, Springfield, Va., PB 283 400.

6. Ward, J. B., and H. W. Hale. Digital Computer Solution of Power Flow Problems. Trans. AIEE, v. 75, pt. 3, 1956, pp. 398-404.

REMOTE ENERGIZING-DEENERGIZING OF TROLLEY WIRE

by

D. S. Kimmel[1]

ABSTRACT

The Bureau of Mines sponsored development of a system to remotely energize and deenergize the trolley wire in a section, in response to demands from vehicles as they enter and leave the controlled section. The scheme developed utilizes a detector/actuator that controls a direct current (dc) contactor located at the outby end of the section. The detector/actuator responds to signals from a 3-kHz oscillator located either at the inby end of the section or on a trolley-powered vehicle. If the oscillator is on the vehicle, the system provides automatic deenergizing of the trolley wire when the vehicle's pole is removed or the vehicle leaves the section. Prototype equipment has been built and tested at the Bureau's Bruceton, Pa., trolley track site, and has demonstrated the ability to also provide load discrimination for faults of 300 amp or more.

ACKNOWLEDGMENTS

The helpful assistance of E. L. Litchfield, G. J. Conroy, and J. N. Murphy of the Bureau of Mines is gratefully acknowledged. Thanks is also due to D. A. Paice and A. B. Shimp, Westinghouse Research colleagues, and T. L. Gardner, Westinghouse technician, who built and tested the prototype equipment.

INTRODUCTION

Because of roof conditions in the northern West Virginia coalfields, the Mine Safety and Health Administration (MSHA) has permitted coal operators to operate with only three entries on a section. This requires that trolley vehicles be operated in the entry used for intake air to the section. MSHA has granted permission for this variance provided the trolley wire is deenergized when it is not actually in use.

At present, one method for handling this problem is to manually connect and disconnect the trolley wire to an insulated feeder cable by means of a fused trolley nip at the inby end. Instances may arise when the vehicle remains parked at the inby end of the section for several hours with no convenient means of deenergizing the trolley wire. In any event, the manual procedure is not only inconvenient and sometimes dependent upon trolley phone communications, it does not insure that the disconnect will occur when it should.

[1]Senior engineer, Power Electronics Laboratory, Design and Development Center, Westinghouse Electric Corp., Pittsburgh, Pa.

A better solution to the problem would be to provide an automatic system to connect and disconnect the trolley wire based upon the need for power in a particular section. MSHA asked the Bureau of Mines Pittsburgh Mining and Safety Research Center (PMSRC) to develop such an automatic system. The result was contract H0166157, for which the following tasks were established:

1. Evaluation of specific system requirements, identification of the potential application problems, and development of the detailed performance specifications to be met by the system.

2. Identification and evaluation of various techniques to achieve the automatic connect/disconnect, and selection of the candidate approach that appears most suitable.

3. Design and development of the required circuits and analysis of failure modes to verify the fail-safe features of the design.

4. Construction and testing of a breadboard model to verify the concept.

5. Construction and testing of a prototype, including the installation of the system in a suitable mine agreed upon by the Bureau technical project officer.

6. Reporting on the results of testing and the establishment of recommendations in a final project report.

PERFORMANCE GOALS

After consultation and discussion with Bureau of Mines personnel, various individuals in the coal mining industry, and based upon our experience in previous coal mining applications projects, we established system goals:

1. The system should be as fail-safe as practical (failure of components should deenergize the trolley wire).

2. Nothing should be permanently added to or mounted on the vehicles, if possible.

3. No extra wires should be strung along the haulageway.

4. Ground fault protection should be provided when the trolley wire is energized.

5. It would be desirable for the trolley wire to be deenergized automatically when it is not needed.

6. It would be desirable to control power to the trolley wire from any location in the section, including the vehicle.

To implement such a scheme, the power must be controlled by an electrically operated switch, such as a contactor. The contactor coil must be actuated

by an electronic circuit that detects commands to energize and deenergize the trolley wire. The electronic control circuit requires some means of differentiating between a legitimate load, such as vehicle, and an illegitimate load.

Because the primary purpose of installing an automatic energizing-deenergizing system was to reduce the hazards associated with faults on energized trolley wires, any failures in the control system were to be such as to render the trolley wire disconnected. A high degree of fail-safe operation was to be provided inherently by the judicious choice of a system concept. In addition, the electronic control for the contactor and the means of energizing the contactor were also to be designed so that the expected failure mode of any component would not cause the contactor to be energized. Another means of achieving reliability was to apply conservative safety factors to the required ratings of all components utilized in the system.

EVALUATION OF ALTERNATIVE SYSTEMS

One method to enable the contactor controlling circuit to discern a legitimate load such as a vehicle is to provide all such equipment with a vehicle signature device, either temporarily or permanently, when it enters the controlled section. This device must indicate to the control circuit that a vehicle is in the section and that power is required. If the vehicle leaves the section, or its trolley pole is removed, power could then be removed. Power could then be reapplied when the vehicle reenters the section or its trolley pole is returned to the line. Several possible schemes were considered:

1. A relatively low current diode could be inserted across the vehicle to produce a low level rectified current when an alternating current (ac) signal was applied. However, the presence of such a diode could not be detected once the direct current (dc) voltage was applied. Although the contactor could be held in by reason of vehicle load current, it would also be held in by low level ground faults, and this scheme was rejected.

2. Resonant filters to provide identifiable impedances at several discrete frequencies could be attached across each vehicle load. This characteristic would then be detected by the contactor electronic control circuit and acted upon accordingly. However, the influence cable inductance complicates this method.

3. A small, low-power transmitter, located on each vehicle, whose output would be coupled to the trolley wire. An auxiliary power source, such as a battery, would be required to initially provide the signal to energize the trolley wire. Another possible power source would be a low voltage (12 v or less) ac that is current-limited and continuously applied to the trolley wire.

Prior experience with electronic equipment in coal mining applications has shown that any scheme requiring equipment permanently mounted on all vehicles, requires regular maintenance schedules and detracts from vehicle availability. To avoid this, the scheme finally chosen can be utilized with or without equipment on the vehicles, depending on the operator's preference.

All the system goals can be achieved either by providing an oscillator to be picked up at the entry by a vehicle using the section or by mounting oscillators on those vehicles that will operate in the section.

SYSTEM DEVELOPMENT AND ANALYSIS

The scheme chosen from the trolley wire energizing-deenergizing system is shown in figure 1. The basic idea is to apply an ac signal of 3 kHz at the inby end of the trolley wire and detect the current that flows through a series resonant circuit at the outby end. If less than a minimum current is received for any reason, such as a fault on the line, an equipment failure, or after a given time interval, power is automatically removed from the trolley wire.

The operation of the system is as follows: The trolley wire is normally deenergized and the oscillator is turned off. If a vehicle approaches the section from the outby end, the operator must stop and depress the ON button before entering the section. The ON button causes the detector-actuator to energize the contactor coil CX and thus close the contactor. This energizes the trolley wire in the controlled section and also turns on the oscillator at the inby end via the normally closed inby OFF button. When the detector-actuator determines that 3-kHz ac current is flowing, it holds in the contactor. This permits the operator to release the ON button and proceed into the section. Of course, the trolley wire can be deenergized at any time by depressing the OFF button.

At the inby end of the trolley wire can be energized by depressing the ON button, which momentarily causes the oscillator to be powered from the feeder. If the feeder is not available at the inby end, an auxiliary power source is utilized to supply the oscillator momentarily. Once the oscillator is on, 3-kHz current is detected by the trolley wire. When the trolley wire is energized, the oscillator recives power from it and the ON button can be released. To deenergize the trolley wire from the inby end, the OFF button is depressed, which turns off the oscillator. This causes the outby detector-actuator to see no ac current and, therefore, drops out the contactor.

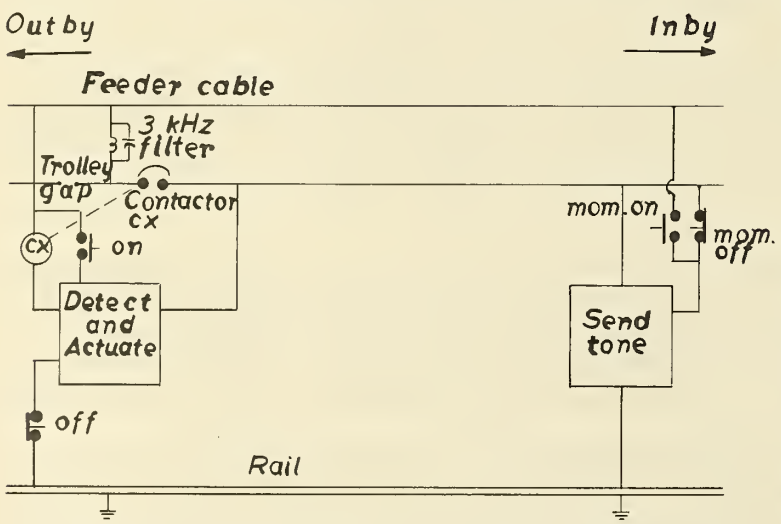

FIGURE 1. - Remote energizing trolley wire system.

During the time the trolley wire is energized, some protection against ground faults is provided because a fault will shunt a portion of the 3-kHz current, and the contactor will drop out when the detector senses less than a minimum value of 3-kHz current.

In order to design an automatic energizing-deenergizing system, it was necessary to make some assumptions concerning the limits on the trolley wire section parameters. From previous work[2] it was determined that the trolley wire can be represented by a lumped parameter series inductor and resistor, whose values increase fairly linearly with trolley wire length. The inductance is approximately 0.35 mh per 1,000 ft and the resistance approximately 14 mohms per 1,000 ft.

For the purpose of evaluating the effects of varying the oscillator and detector impedances, frequency, and sensitivity, it was decided to assume the controlled section would have a minimum length of 1,000 ft and a maximum length of 5,000 ft.

An investigation was made to determine a convenient operating frequency for the system. Since the basic function of the system was to permit energizing of the trolley wire from a remote location, it was felt imperative that noise signal be prevented from falsely causing the trolley wire to remain energized. Detection of illegitimate loads on the system was only a secondary goal.

To minimize sensitivity to noise, it was determined the frequencies above approximately 2 kHz and below 50 kHz were desirable.

Another factor that was considered was the inductive nature of the trolley wire, which means that as the frequency increases, the current at the receiving end decreases owing to the increasing trolley wire impedance. If a given magnitude of current is required at the receiving end to overcome noise sensitivity problems, then increasing the operating frequency requires an increase in the oscillator power output.

For these reasons, the choice of 3 kHz was reasonable. It would have been possible, however, to use other frequencies in the range of 2 to 5 kHz and obtain satisfactory results.

A computer simulation of the automatic trolley wire energizing system was devised to investigate the trade offs in vehicle size, length of trolley in the section, and sensitivity of ground fault protection. Figure 2 shows the circuit that was used to generate the computer program. Some simplifying assumptions were made concerning the computer simulation, algebraic expressions I_1 and I_2 were written in terms of the circuit parameters of interest, and then a BASIC program was run with many various combinations of values for load, line length, oscillator and detector impedances, etc.

---

[2]Paice, D. A., A. B. Shimp, and R. P. Putkovich. Circuit Breaker Development and Application. Phase I. BuMines Open File Rept. 103(1)-75, Mar. 12, 1974, 165 pp.; available for reference at Bureau of Mines facilities in Denver, Colo., Twin Cities, Minn., Pittsburgh, Pa., Spokane, Wash.; Department of Energy facility at Morgantown, W. Va.; National Library of Natural Resources, U.S. Department of the Interior, Washington, D.C.; and from National Technical Information Service, Springfield, Va., PB 248 310.

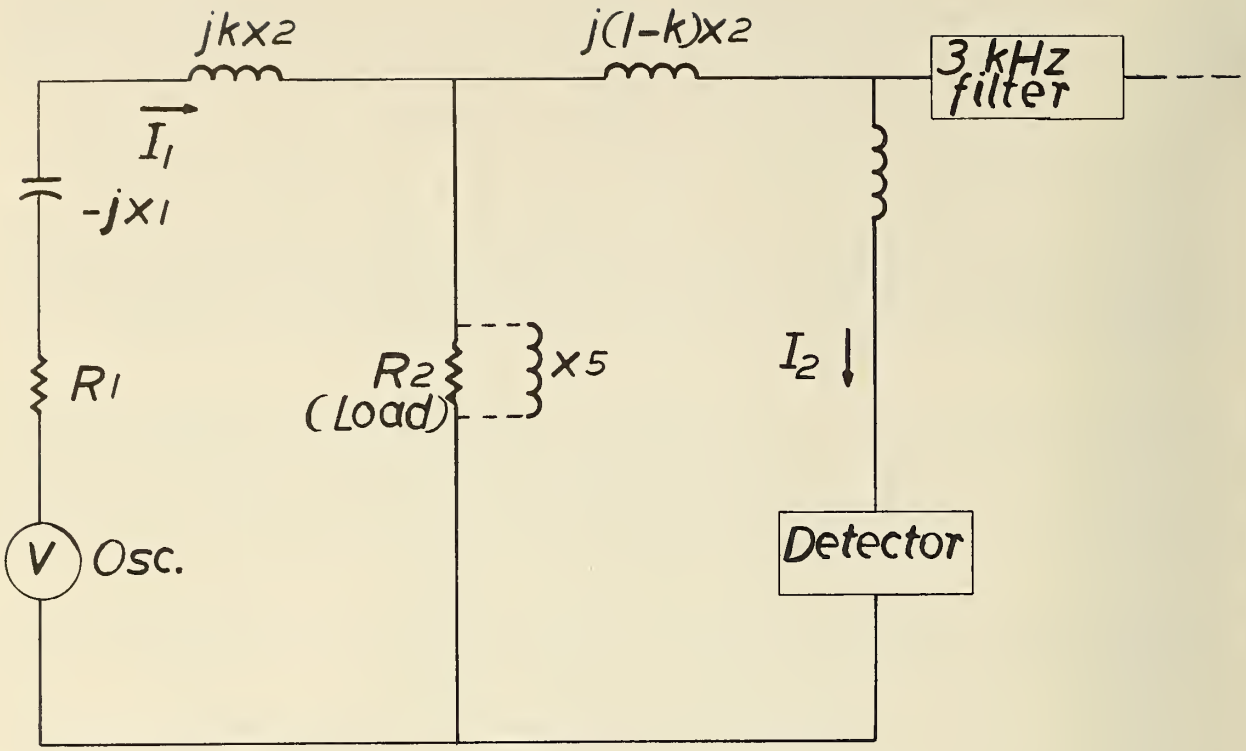

FIGURE 2. - Computer model of trolley system.

The computer results were used to help design the oscillator and detector-actuator circuits. An analysis of the data also shows that it is possible to obtain more sensitive load discrimination by a control system that measures both the oscillator output current I_1 and the outby current I_2.

For the sake of simplicity and reliability, it was decided to build the prototype system with a single detector located at the outby end as shown in figure 1. This system results in less sensitivity to faults than could be achieved with two detectors but gives good performance and provides cost, size, and simplicity advantages.

Figure 3 is a graph that illustrates the different currents caused by a 2-Ohm resistive load and a 15-ton locomotive load. The equivalent circuit for a 15-ton locomotive was derived from information in the report by Paice, Shimp, and Putkovich. These curves show that the system can discriminate between a 15-ton locomotive and a 2-ohm fault, except if the fault occurs within 53 ft of the detector. (Subsequent field tests with the prototype at Bruceton, Pa., have demonstrated the capability of the system to discriminate between a locomotive and a 1-ohm fault located anywhere on the trolley section.)

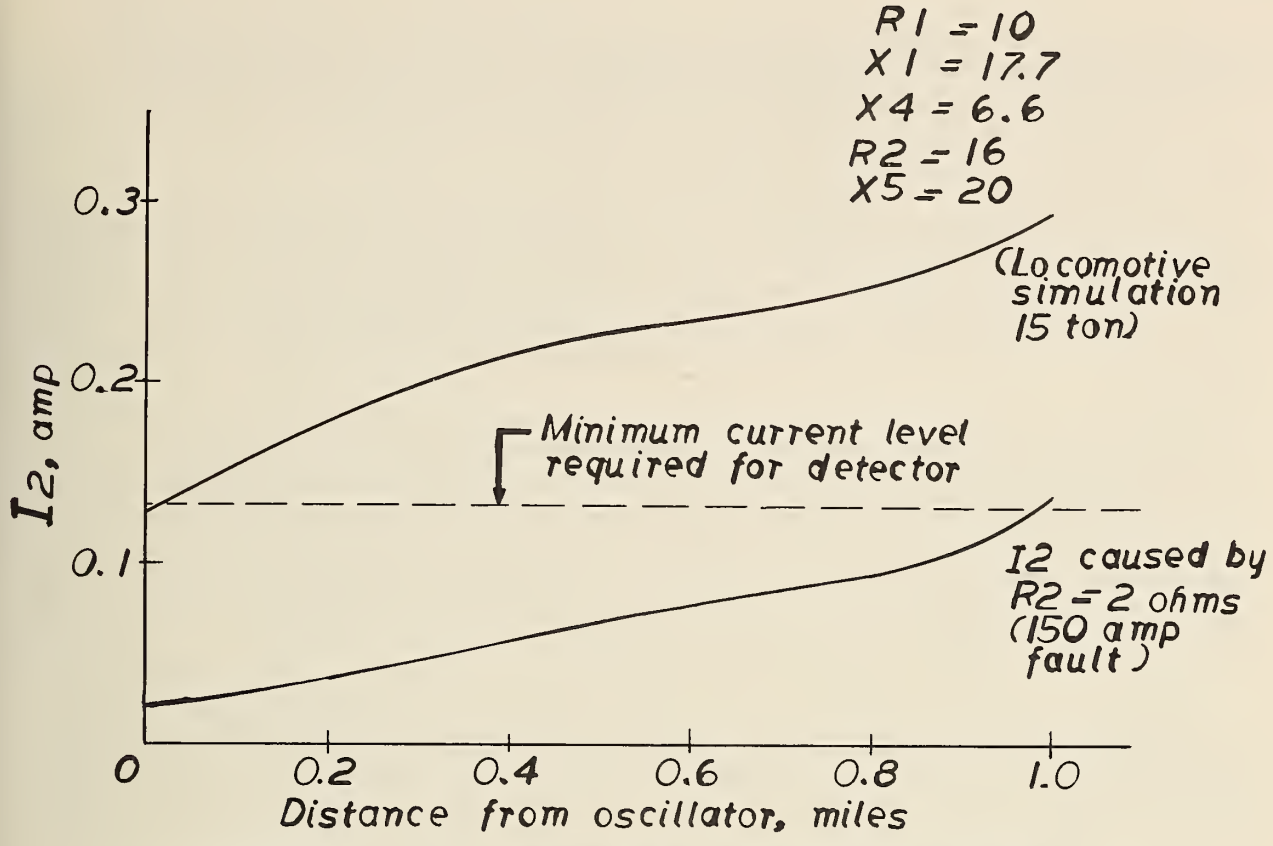

FIGURE 3. - Variation between 2-ohm load and 15-ton locomotive.

PROTOTYPE DEVELOPMENT

The oscillator circuit originally developed for the Discriminating Circuit Breaker Systems (footnote 2) was modified to provide a 10-volt rms output signal at a frequency of 3 kHz. Supply voltage is normally provided to the oscillator via the trolley wire and is stepped down through a power resistor.

When the trolley line is deenergized, some auxiliary source of power is required for the oscillator until the outby detector has sensed the 3-kHz signal and actuated the contactor. Several alternative auxiliary power schemes were investigated and from the standpoint of reliability, the most judicious choice might be a hand-cranked generator. The most convenient and readily available source was rechargeable nickel-cadium batteries, which were utilized for the prototype, and they have performed exceptionally well to date.

The batteries are trickle-charged from the trolley line and are capable of retaining about 80 pct of their charge for periods up to several months between charges. When fully charged, they should deliver at least 200 2-second duration starts while still retaining up to 50 pct of charge.

The oscillator circuitry, nickel-cadmium cells, and ON-OFF buttons were housed in a Westinghouse ac Magnetic Starter NEMA 1 enclosure, whose outside dimensions are 6-3/4 inches wide, 11-1/8 inches high, and 5-1/2 inches deep.

The power resistor was located on one side, outside the enclosure, in a guarded partially open area to allow free-air cooling. Figure 4 is a photograph of the oscillator unit, mounted on one of the outside trolley wire support columns at Bruceton. The batteries are located in the lid of the enclosure, which is shown to the left of the unit.

The outby detector-contactor actuator was designed specifically for this project. The 3-kHz signal that appears on the trolley line whenever power is requested passes through a tuned circuit and into a level detector. If there is a sufficient level of signal present, then the output is delayed to help prevent both nuisance tripping and undesired pickup of power due to noise and transients.

The ON button at the detector-actuator controls the contactor coil directly through an output transistor. Thus, an operator can manually hold the contactor at this unit, even though the inby oscillator is malfunctioning or a large illegitimate load is present. However, as soon as the operator releases the ON button, the contactor will not hold in unless sufficient 3-kHz signal is present. The OFF button is directly in series with the contactor coil, and thus overrides all other controls.

Automatic deenergization of the trolley wire is accomplished by means of a time-delay relay. After the pre-set delay (variable from 3 to 30 min) has occurred, the normally closed contacts of the relay, which are in series with the contactor coil and OFF button, open and thus deenergize the trolley wire.

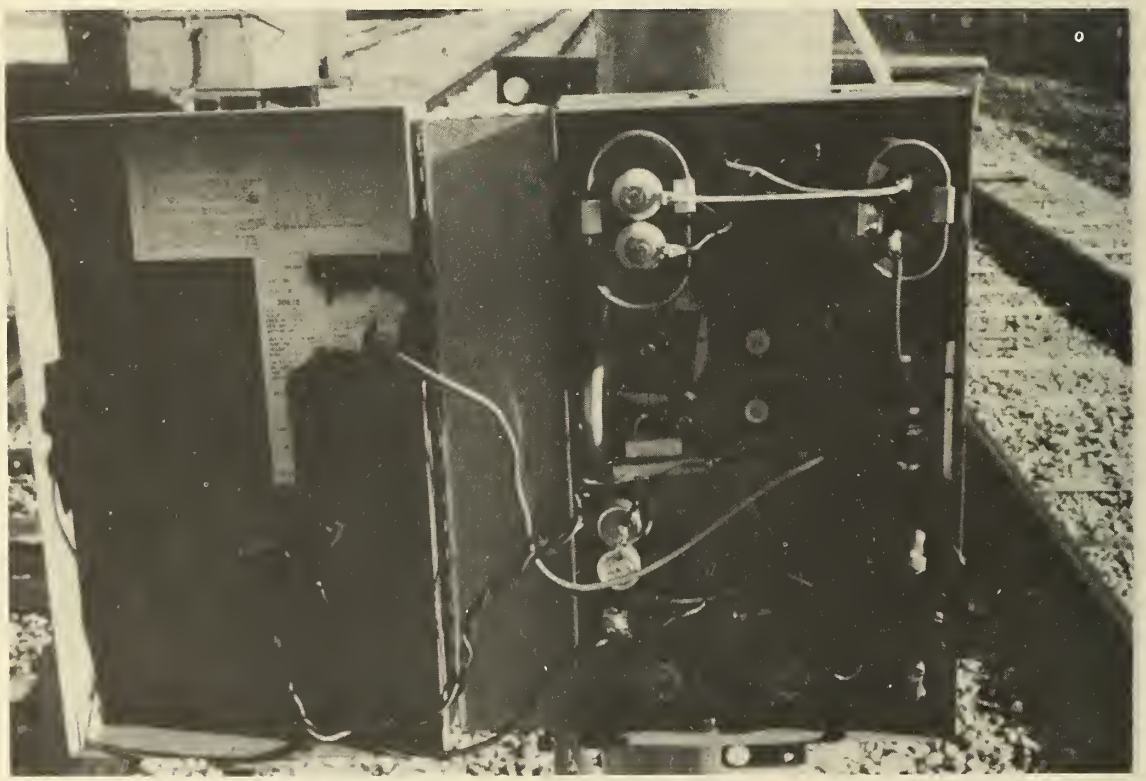

FIGURE 4. - Prototype oscillator unit.

The detector-actuator circuit was housed in the same type of enclosure as the oscillator unit described in the previous section; and a photo of the unit, mounted on the side of a safety switch enclosure at Bruceton, is shown in figure 5.

Also shown in figure 5 is the 3-kHz filter circuit, which is a necessary part of the system for some installations. The filter, consisting of a parallel resonant choke and capacitor, prevents the external dc power distribution system from interaction with the 3-kHz signal present in the controlled section, while at the same time permitting the 88-kHz trolley phone signals to pass in and out of the section unimpeded.

The 3-kHz filter circuit and the contactor were mounted inside the safety switch enclosure that was available at the Bruceton site. They are shown in figure 6. The filter choke and capacitor are located in the lower center of the photo, and the contactor is located above and to the left, on the side of the enclosure. The locomotive operating at the test track draws currents in excess of 600 amp when it negotiates a tight S-curve, and the prototype did not spuriously trip out on this load. Another successful test was the remote opening and closing of the contactor while the locomotive was set in the full-forward mode with the brakes locked on.

The equipment was installed, tested, and operated in environmental conditions more severe than that likely to be encountered at an inmine installation, because the test site was aboveground and exposed to the winter weather.

FIGURE 5. - Prototype detector-actuator unit.

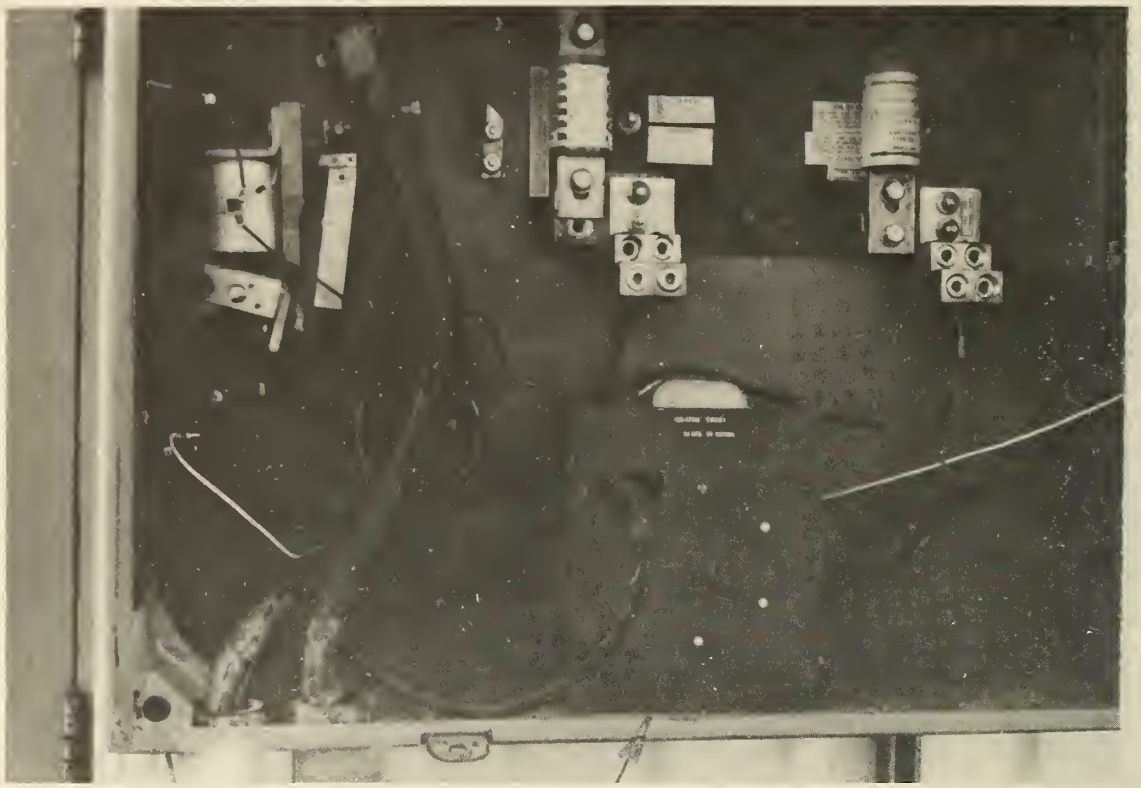

FIGURE 6. - 3-kHz filter circuit and contactor (inside safety switch enclosure).

SUMMARY

The automatic system developed for the Bureau of Mines provides for remote control of power to the trolley wire in a controlled section of the mine. The prototype equipment that was installed and tested at the Bureau's Bruceton facility enables deenergizing the trolley wire by means of an operator-actuated button or an automatic time-delay dropout. One feature of that system was that no modifications or additions were required for any vehicles or trolley operated equipment. In addition, the system demonstrated load discrimination for current of 300 amp or more.

Plans are presently underway to modify the system so that the trolley wire can be energized and deenergized from a vehicle, by placing the oscillator unit on the vehicle. This provides automatic deenergizing when the vehicle leaves the section or the vehicle's trolley pole is removed. The presence of an operator on the seat of the vehicle can be a necessary condition for trolley wire energization by connecting a "dead man's switch" on the seat in series with the oscillator's power supply. The production of sufficient numbers of oscillator units and several detector-actuators can be carried out by a vendor with experience in building production equipment suitable for a coal mine environment.

PORTABLE REMOTE CONTROL OF TROLLEY CIRCUIT BREAKERS

by

Harry M. Dushac[1]

ABSTRACT

The movement of off-track mining equipment in a mine entry under energized trolley or feeder lines is a hazardous procedure when there is less than 12 inches clearance between the mining equipment and the trolley. A portable remote-control system has been developed under a Bureau of Mines research contract that is capable of controlling the overcurrent trip level setting of a direct current (dc) trolley circuit breaker. The system also has the capability of providing for the immediate shutdown of the trolley power by a member of the moving crew if the piece of mining equipment to be moved contacts the trolley wire or feeder.

BACKGROUND OF THE PROBLEM

Whenever off-track mining equipment is moved in an entry when energized trolley or feeder lines exist, there is danger that this equipment could come in contact with the trolley or feeder line, possibly causing serious damage by fire. To minimize this hazard, on October 31, 1973, Mine Safety and Health Administration (MSHA) promulgated Section 75.1003-2, Title 30, Code of Federal Regualtions (CFR). This new regulation became effective on January 1, 1974.

Section 75.1003-2 lists the precautions that must be taken every time off-track mining equipment is moved in areas where energized trolley wires are present. It also lists additional precautions that must be taken when there is less than 12 inches of vertical clearance between the off-track equipment and the energized trolley wire. Some of these additional precautions are--

1. No person shall be permitted to be inby the equipment being moved in the ventilating air current that is passing over the equipment.

2. The settings of all circuit breakers providing short-circuit protection for the trolley wire shall be reduced to not more than 50 pct of the short-circuit current that would flow if the equipment contacted the trolley wire.

3. A miner shall be stationed at the first circuit breaker outby the equipment being moved at all times. The miner must be in direct communication with the miners actually moving the equipment. In fact, he or she shall have two independent means of establishing two-way voice communications.

---

[1]Electrical engineer, Lee Engineering Div., Consolidation Coal Co., McMurray, Pa.

The moving of off-track equipment in the presence of energized trolley lines creates a hazard to personnel, equipment, and even the mine itself. This hazard has a direct bearing on productivity and the well-being of all personnel in the area.

The successful development of a system for the remote control of circuit breakers should increase the probability of automatically tripping the circuit breaker in case of an accident. It should also substantially reduce the time required to manually trip the circuit breaker if necessary.

The objective of this contract was to design and demonstrate a reliable system to remotely control trolley line circuit breakers from a location close to the off-track mining equipment that is being moved in the vicinity of energized trolley or feeder lines and incorporate the additional voice communication devices required by Section 75.1003-2, Title 30 CFR into the system.

Information was obtained from several operating mines on the details involved in the movement of off-track equipment in the mine. Supervisory, production, and maintenance personnel from each of the selected mines were interviewed in order to answer questions such as--

1. What vehicles are used during an equipment move?

2. What safety equipment is used?

3. How many persons are required, along with their particular job functions?

4. What is the procedure once the move is started?

The answers to these questions made it possible to determine the necessary control functions required for the remote-control system, along with the individual that should be in command of the system.

Preliminary field tests were necessary to determine the appropriate method of transmitting and receiving control information from the piece of mining equipment being moved to the trolley circuit breaker location. The tests determined that the carrier frequency range (60 kHz to 180 kHz) would be the most appropriate frequency for the transmission of control information.

A preliminary prototype remote-control system[2] was designed and fabricated in accordance with the information obtained from the field test data. The prototype equipment was successfully tested at the Shoemaker mine of Consolidation Coal Co. during four equipment moves. The overcurrent trip setting of the controlled circuit breaker was considerably lower than the normal settings of the circuit breakers during a regular operating shift. Trip settings were reduced to 300 amp during most of the equipment moves instead of trip levels near 3,000 amp as during normal mine operation (300 vdc trolley).

---

[2]Lee Engineering Div., Consolidation Coal Co. Develop Remote Control of Circuit Breakers. Contract No. H03660290.

Because the preliminary field test program was successful, it was decided that the final prototype systems should be designed and fabricated as production prototypes.

DESCRIPTION OF SYSTEM

The remote control system consists of three major subparts:

1. Transmitter control unit and ultrahigh frequency (uhf) "emergency trip" radio.

2. Receiver unit, overcurrent relay.

3. Circuit breaker unit.

The system will be used according to figure 1 for pulling a piece of off-track mining equipment into the mine. The reverse procedure applies to pulling a piece of equipment out of the mine.

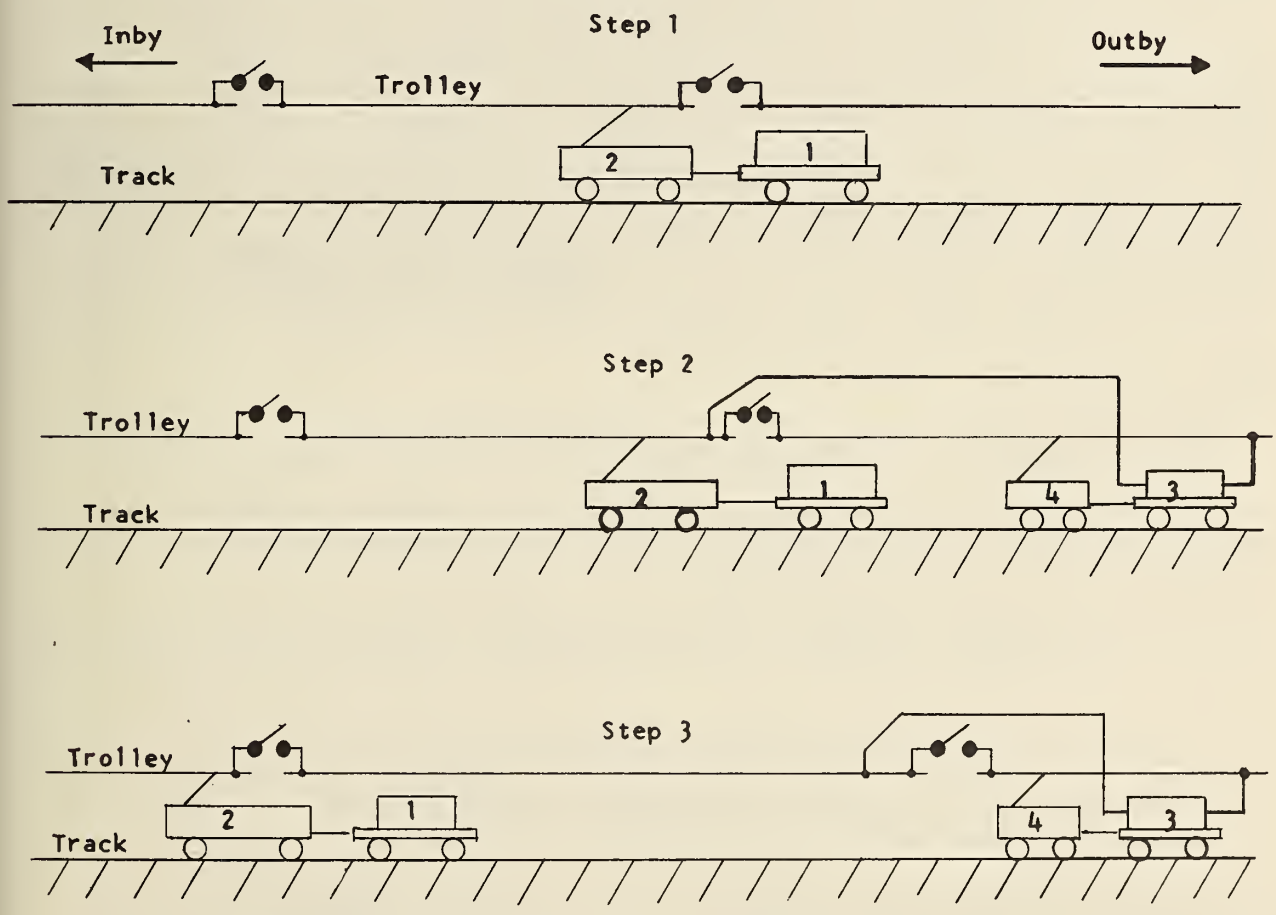

FIGURE 1. - Pulling a piece of off-track mining equipment into the mine.

EQUIPMENT LIST

1. Off-track mining equipment mounted on a flat car.

2. Locomotive with the transmitter control unit.

3. Circuit breaker and the receiver unit mounted on a flat car.

4. Small utility jeep.

The locomotive operator advances the locomotive until the locomotive trolley pole is on the inby side of the dead-block. The off-track mining equipment being moved is still on the outby side of the dead-block. At this point, the locomotive operator gives permission to the operator on the jeep (4 in fig. 1) to advance the circuit breaker.

The operator of the jeep (4 in fig. 1), a certified electrician, disconnects the circuit breaker and advances toward the locomotive. He then connects the circuit breaker around the disconnect switch at the locomotive.

The locomotive operator selects one of the eight possible settings for the solid-state overcurrent relay, located at the receiver unit, and then closes the reset switch. The circuit breaker closes and the setting of the solid-state overcurrent relay is determined. The locomotive can now pull the off-track mining equipment toward the next inby disconnect switch. During this move, the energized trolley wire above the equipment is protected by a circuit breaker, which has reduced overcurrent setting and can be opened by the locomotive operator. If the receiver unit fails to receive the signal from the transmitter control unit, the circuit breaker will open and it will not reclose until a reset signal is received. Figures 2 and 3 show the transmitter control unit and the receiver unit with solid-state overcurrent relay, respectively.

The remote control system has the following capabilities:

1. The system will be able to trip the power circuit breaker automatically in the event the mining machinery has come in contact with the trolley line. Other ways to trip power are--

   a. If contact between the machinery and the trolley line is made and the current flow exceeds the trip setting, the breaker will open.

   b. The operator can depress the red pushbutton located on the transmitter control unit. This will transmit a signal to the receiver unit, which will open the power circuit breaker supplying power to the trolley line. The pushbutton is labeled "Emergency Trip."

   c. The transmitter control unit also has the capability of an emergency trip by means of a portable, remotely carried uhf radio. This uhf radio can be used by an individual walking alongside the equipment move in the event that low coal conditions exist and clearances are minimal

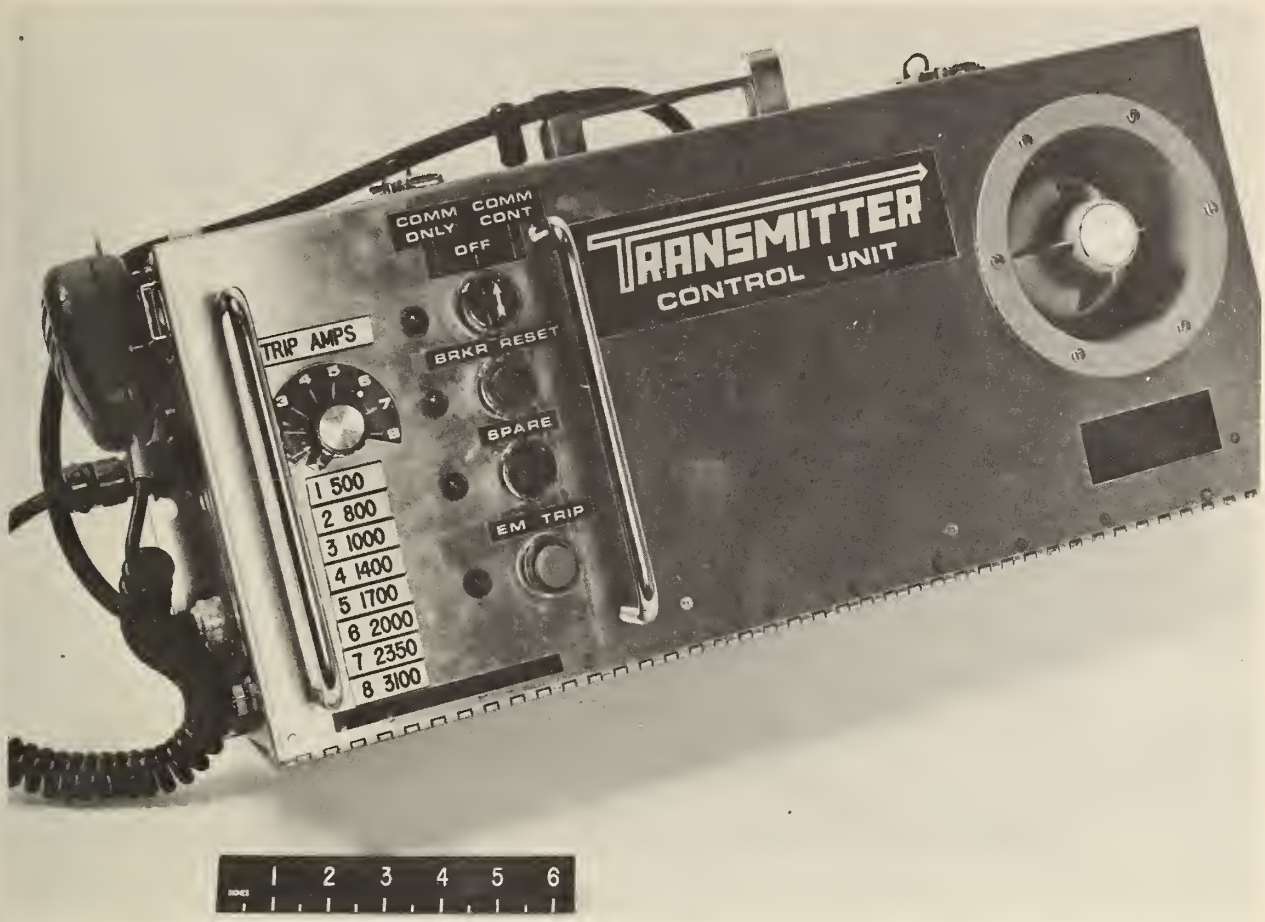

FIGURE 2. - Production prototype transmitter control unit.

between the mining machinery and the trolley line. When the uhf emergency trip signal is detected by the transmitter control unit as discussed above, a trip message is transmitted to the receiver unit.

An individual carrying a uhf transmitter will normally be within 50 to 100 ft of the equipment that is being transported. The transmitting distance for the uhf radio under most mining conditions should be in the range of at least a few hundred feet, which is more than adequate for this application.

d. Loss of carrier frequency signal from the transmitter control unit after a predetermined adjustable time delay will result in the tripping of the circuit breaker. This feature will monitor the integrity of the system.

2. The transmitter control unit will have the capability of resetting the circuit breaker unit in the event that the power was tripped unintentionally or because the trip setting of the circuit breaker was initially set too low.

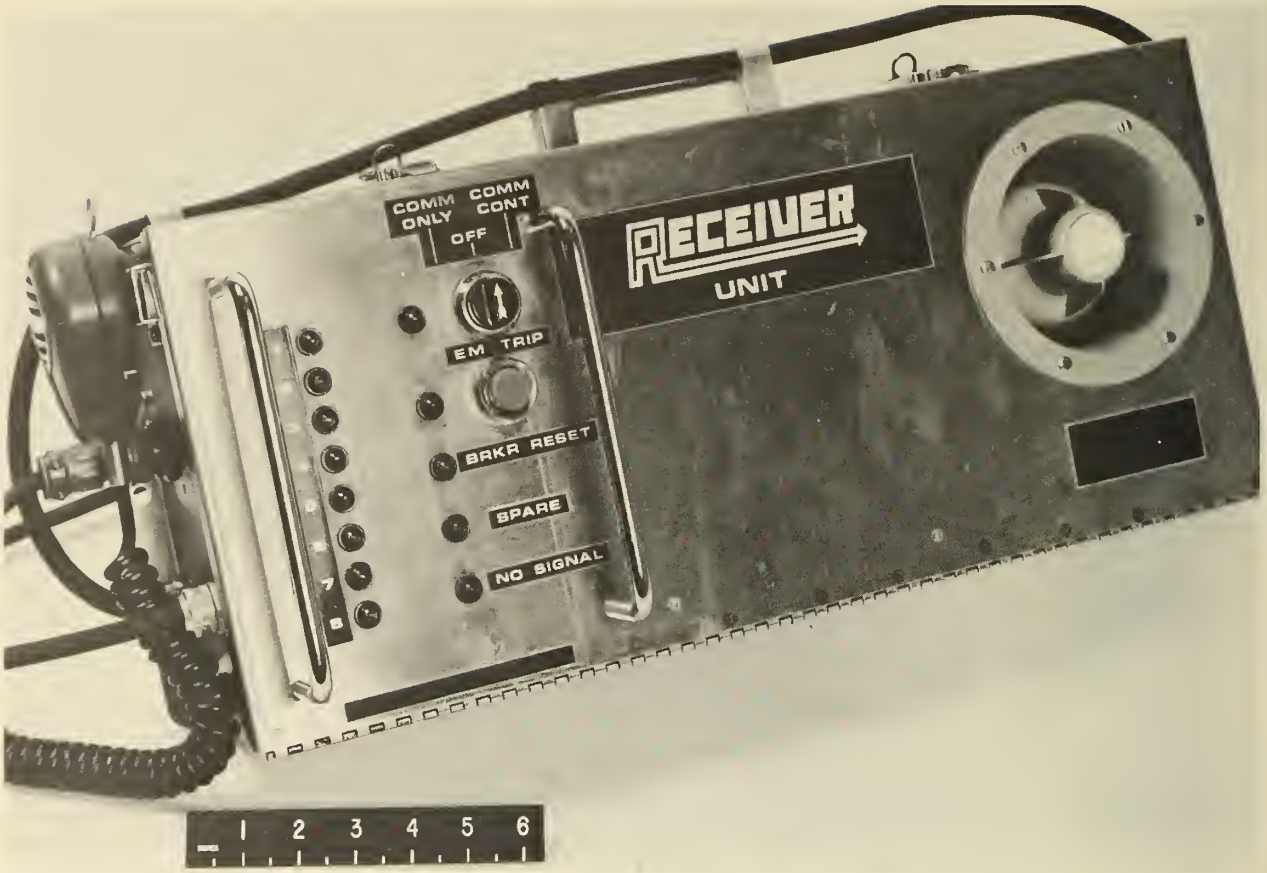

FIGURE 3. - Production prototype receiver unit.

3. The transmitter control unit will be able to adjust the overcurrent trip setting of the circuit breaker to one of eight fixed predetermined current levels. The eight overcurrent trip levels can be selected as shown on the front panel of the transmitter control unit. A spare function switch has also been located on the front panel of the unit. This switch can be used to operate any desired control function necessary during the move as required. The spare function may operate a light, buzzer, bell, or some other device to indicate a particular function.

The transmission of control data is based on a three-tone multicode concept. The tone code groups are in the audio frequency range (300 to 3,000 Hz). The appropriate tone groups are used to select the eight different overcurrent trip settings of the circuit breaker and also the "emergency trip," "breaker reset," and "spare" function controls.

The transmitter control unit also has the capability of two-way voice communication with the receiver unit. The operating frequencies of the system can be selected appropriately from 60 kHz to 190 kHz.

The receiver unit will receive the control data and convert this information to the overcurrent trip level settings of the circuit breaker and also the various control functions: Emergency trip, breaker reset, and the spare. The control information from the receiver unit is interfaced to the circuit breaker unit through optical isolators which provide up to 2,500 v of electrical isolation between the trolley circuit breaker and the 12-vdc receiver circuitry. The receiver will remember the last correctly received message and will not change status until another legitimate message is received or a loss of carrier frequency signal is indicated. Light-emitting diodes (LED) are used to continually display the status of the remote control system. Two-way voice communication with the transmitter control unit is also included.

The circuit breaker unit is the third major part of the system and it consists of the following items: Power circuit breaker, electrical shunt, solid-state overcurrent relay, and insulated power cable with insulated heavy-duty clamps. A wiring diagram of the circuit breaker unit is illustrated in figure 4.

The physical size of the circuit breaker unit enclosure will depend upon the type and size of the dc circuit breaker to be used. The gage of the insulated power cable depends upon the amperage requirements expected during an equipment move. Figure 5 illustrates the receiver unit and the circuit breaker unit mounted on a vehicle during the equipment move.

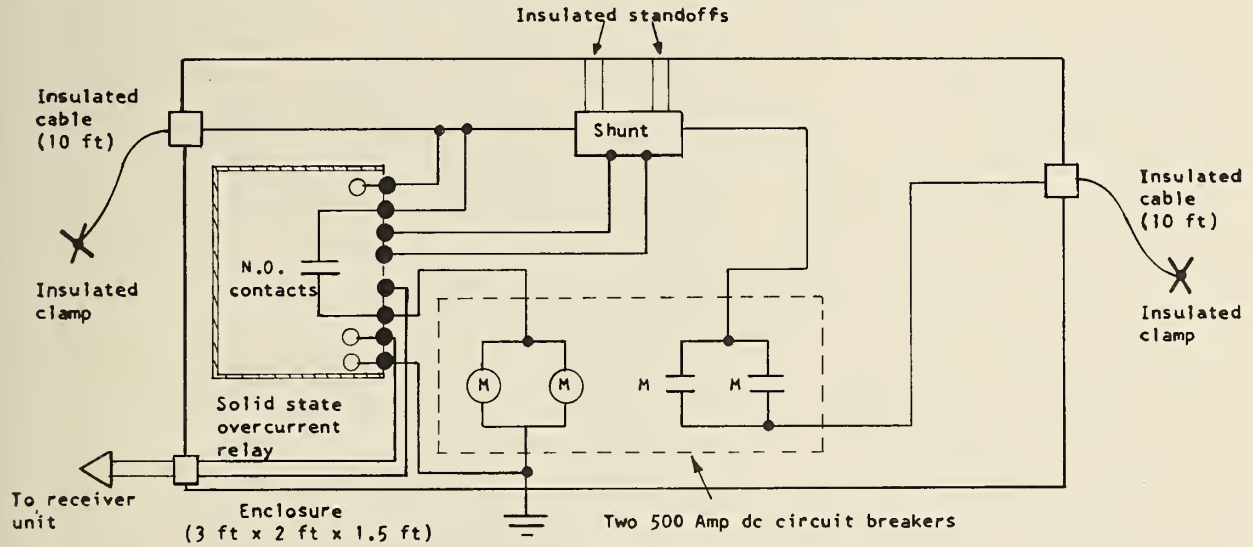

FIGURE 4. - Wiring diagram of the circuit breaker unit.

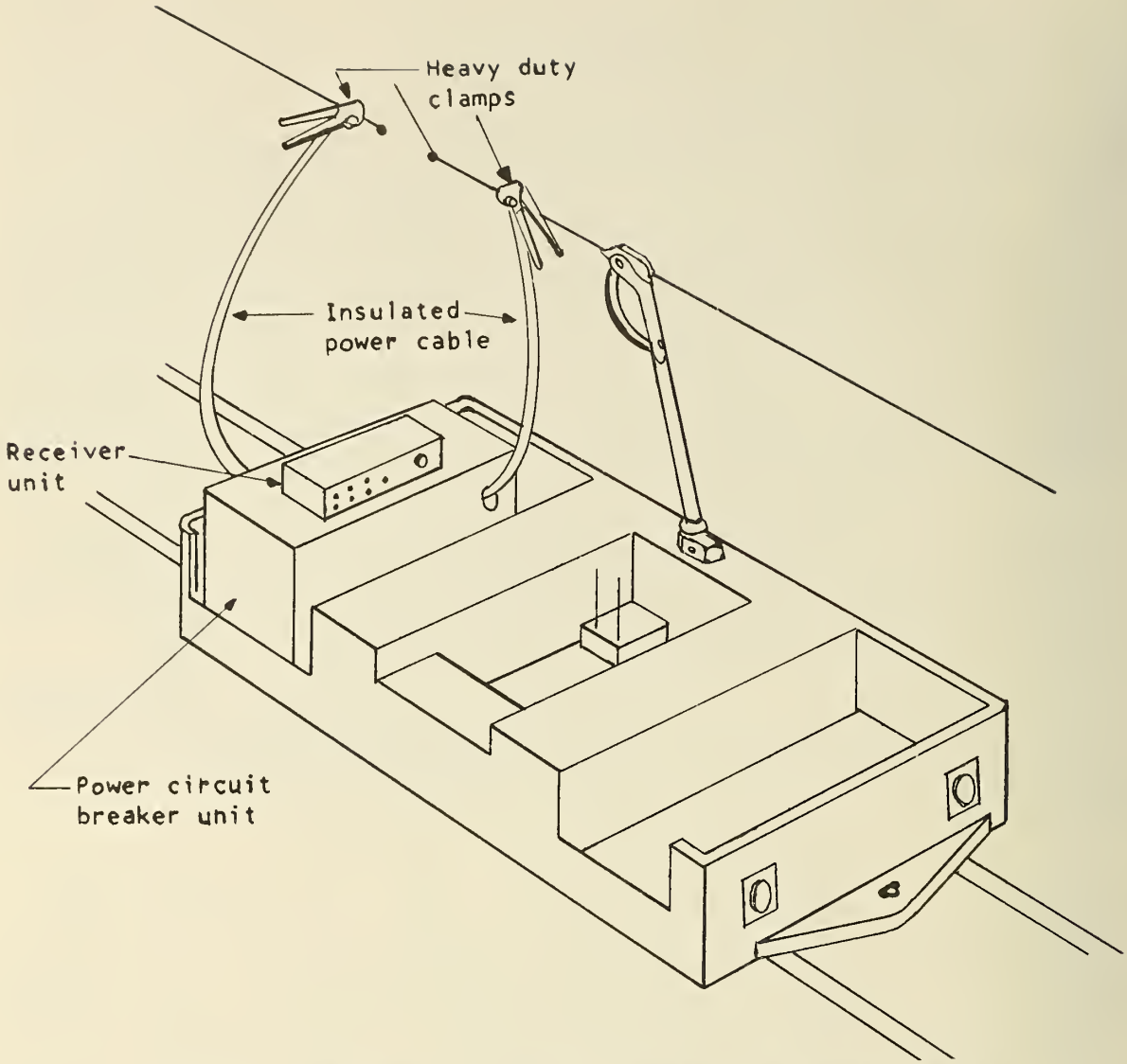

FIGURE 5. - Receiver unit and circuit breaker unit mounted on vehicle.

CONCLUSION

Two prototype remote control systems have been designed, fabricated, and successfully bench tested. Both systems are expected to be placed in operation in different coal mines during the summer of 1978. The systems will be used to control the dc circuit breaker overcurrent trip setting and also will be able to trip and reset the circuit breaker remotely during equipment moves.

☆U.S. GOVERNMENT PRINTING OFFICE: 1979-603-002/48

INT.-BU.OF MINES,PGH.,PA. 23888

H 33 80

DEC 19
N. MANCHESTER,
INDIANA 46962

LIBRARY OF CONGRESS
0 002 960 004 1